NASA

MEMORANDUM

LONGITUDINAL AND LATERAL STABILITY AND

CONTROL CHARACTERISTICS OF VARIOUS COMBINATIONS OF THE

COMPONENTS OF TWO CANARD AIRPLANE CONFIGURATIONS

MACH NUMBERS OF 1.41 AND 2.01

By Cornelius Driver

Langley Research Center
Langley Field, Va.

NATIONAL AERONAUTICS AND
SPACE ADMINISTRATION
WASHINGTON
October 1958
Declassified May 29, 1961
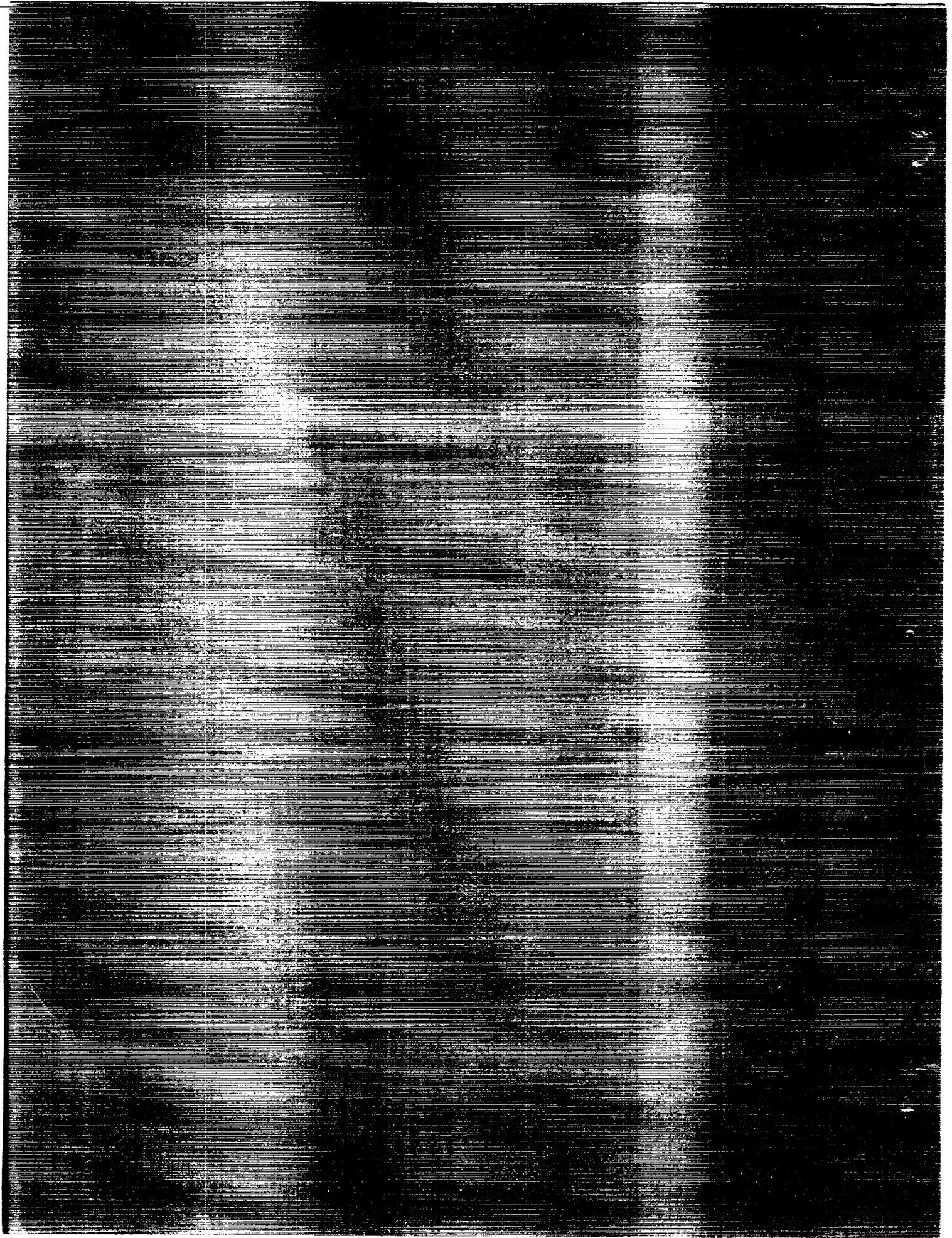
NATIONAL AERONAUTICS AND SPACE ADMINISTRATION

NASA MEMO 10-1-58L

LONGITUDINAL AND LATERAL STABILITY AND

CONTROL CHARACTERISTICS OF VARIOUS COMBINATIONS OF THE

COMPONENT PARTS OF TWO CANARD AIRPLANE CONFIGURATIONS

AT MACH NUMBERS OF 1.41 AND 2.01

By Cornelius Driver

SUMMARY

An investigation has been conducted in the Langley 4- by 4-foot supersonic pressure tunnel to determine the aerodynamic characteristics in pitch and sideslip of a generalized canard airplane model. Two wings of equal area but differing in plan form were investigated. The model was equipped with a trapezoidal canard surface with an area 12 percent of the wing area, a low-aspect-ratio vertical tail, and twin ventral fins.

The interference effects of the canard wake on the wing result in little or no gain in the total lift at a Mach number of 1.41 but at a Mach number of 2.01 a substantial portion of the canard lift is retained with a resultant increase in total lift. Because these interference effects of the canard wake appear to be concentrated near the leading edge of the wing, the proper location of the wing leading edge with respect to the center of moments may result in a substantial increase in the moment increment provided by a canard surface even though the total lift provided by the canard is small. For these configurations the trapezoidal wing retained the most lift and had the largest favorable moment increment produced by the canards.

The canard configurations have the same characteristic decrease in directional stability with angle of attack as most conventional high-fineness-ratio supersonic configurations. Although the presence of the canard surface caused a small increase in the directional stability at a Mach number of 1.41 for the delta-wing configuration, the presence of the canards resulted in small decreases in the directional-stability level at a Mach number of 2.01 for both wing configurations. A canard deflection of 15° provides an increase in the positive effective dihedral approximately as large as that provided by the presence of the vertical tail. This effect of canard deflection might complicate the lateral-control problem in the case of a rolling pull-up maneuver.

INTRODUCTION

The initial results of a research program at the Langley 4- by
4-foot supersonic pressure tunnel to determine the aerodynamic charac-
teristics of generalized canard airplane configurations at supersonic
speeds are reported in reference 1. Results at high subsonic speeds
are reported in reference 2. Some effects of canard size on the aero-
dynamic characteristics at supersonic speeds are reported in reference 3.
A comparison of the stability and control characteristics of a delta-
wing configuration with combinations of trailing-edge flaps and canard
controls is presented in reference 4. The present report presents the
results for two complete models and various combinations of their com-
ponent parts at combined angles of attack and sideslip at Mach numbers
of 1.41 and 2.01.

SYMBOLS

The results are presented as force and moment coefficients with
lift, drag, and pitching moment referred to the stability axis system
and rolling moment, yawing moment, and side force referred to the body
axis system. (See fig. 1.) The reference center of moments was at
body station 25 which corresponds to a location 17.8 percent ahead of
the leading edge of the wing mean geometric chord for the trapezoidal
wing and to a point 7.75 percent behind the leading edge of the wing
mean geometric chord for the delta wing.

C_L lift coefficient, $\dfrac{F_L}{qS}$

C_D' approximate drag coefficient equal to C_D at zero sideslip, $\dfrac{F_D'}{qS}$

C_m pitching-moment coefficient, $\dfrac{M_{Ys}}{qS\bar{c}}$

C_l rolling-moment coefficient, $\dfrac{M_X}{qSb}$

C_n yawing-moment coefficient, $\dfrac{M_Z}{qSb}$

C_Y side-force coefficient, $\dfrac{F_Y}{qS}$

F_L lift force

F_D' drag force

M_{Ys} moment about y-axis

M_X moment about x-axis

M_Z moment about z-axis

F_Y side force

L/D lift-drag ratio

q free-stream dynamic pressure

S wing area including fuselage intercept

b span

$\bar{c}$ wing mean geometric chord

M_∞ free-stream Mach number

α angle of attack of fuselage reference line, deg

β angle of sideslip of fuselage reference line, deg

δ_c deflection angle of canard with respect to the fuselage reference line, positive when trailing edge is down, deg

C_{n_β} directional stability parameter, $\dfrac{\partial C_n}{\partial \beta}$

C_{l_β} effective dihedral parameter, $\dfrac{\partial C_l}{\partial \beta}$

C_{Y_β} side-force parameter, $\dfrac{\partial C_Y}{\partial \beta}$

4

C_{L_α} variation of lift coefficient with angle of attack

C_{m_α} variation of pitching-moment coefficient with angle of
          attack

Subscripts:

s   denotes stability axis system

max   denotes maximum

Configurations:

B_1 body shown in figure 2; body coordinates given in table II

W_1 trapezoidal wing shown in figure 2(b); geometric character-
          istics given in table I

W_2 delta wing shown in figure 2(b); geometric characteristics
          given in table I

C_4 canard surface shown in figure 2(c); geometric characteris-
          tics given in table I

V_1 vertical tail shown in figure 2(c); geometric characteristics
          given in table I

U_1 ventral fins shown in figure 2(c); geometric characteristics
          given in table I

MODELS AND APPARATUS

The model details are shown in figure 2 and the geometric charac-
teristics are presented in tables I and II. The body of the model had
a fineness ratio of 10.57 and consisted of a parabolic nose faired into
the frustum of a cone which was followed by a cylindrical section. Coor-
dinates of the body are given in table II. The delta and trapezoidal
wings (fig. 2(b)) had hexagonal sections and aspect ratios of 2.31 and
3.00, respectively. The canard surface (fig. 2(c)) also had hexagonal
sections and the ratio of total canard area to total wing area was 0.12.
The canard deflections were set by remote control. The model was
equipped with a low-aspect-ratio vertical tail and twin ventral fins.
(See fig. 2(c).) Photographs of the models are presented in figure 3.

Force measurements were made through the use of a six-component internal strain-gage balance. The model was mounted in the tunnel on a remotely controllable rotary-type sting. The sting-angle range was varied from -4° to about 28° at various roll angles from 0° to 90°.

TEST CONDITIONS

The test conditions are summarized in the following table:

Mach number 1.41   2.01
Stagnation temperature, °F   100   100
Stagnation pressure, lb/sq ft absolute   1,440   1,440
Reynolds number based on $\bar{c}$ of delta wing . . . 3.24×10^6 2.68×10^6
Reynolds number based on $\bar{c}$ of trapezoidal
  wing . . . . 2.54×10^6 2.10×10^6

The stagnation dewpoint was maintained sufficiently low (-25° F or less) so that no condensation effects were encountered in the test section. The angle of incidence was corrected for the deflection of the balance and sting under load. The Mach number variation in the test section was approximately ±0.01 and the flow-angle variation in the vertical and horizontal planes did not exceed about ±0.1°. The base pressure was measured and the chord force was adjusted to a base pressure equal to the free-stream static pressure.

The estimated maximum variations in the individual measured quantities are as follows:

C_L . . . .   ±0.0003
C_D' . . . .   ±0.001
C_m . . . .   ±0.0004
C_l . . . .   ±0.0004
C_n . . . .   ±0.0001
C_Y . . . .   ±0.0015
α, deg . . . .   ±0.2
β, deg . . . .   ±0.2
δ_c, deg . . . .   ±0.1

<center>RESULTS AND DISCUSSION</center>

The order of presentation of the results is as follows:

<center>Longitudinal Characteristics</center>

The complete breakdown data for the trapezoidal-wing configuration
are presented in figures 4 and 5 and for the delta-wing configuration in
figures 6 and 7 for Mach numbers of 1.41 and 2.01, respectively. The
reference center of moments for both configurations is on the fuselage
center line at body station 25. It is recognized that this location
gives an undesirably high level of static longitudinal stability at
supersonic speeds. This position was chosen, however, as a compromise
between the longitudinal and lateral stability requirements for this
particular configuration.

Incremental results.- The incremental results for the BC-B and
BWC-BC configurations (fig. 8) were obtained as the incremental lift
and pitching-moment contributions produced by the canard and the wing.
The incremental results were obtained at corresponding angles of attack
and include the mutual interference effects between the lifting surface
and the body. As shown in figure 8, the canard contribution to lift
with the wing on is less than that for wing off; thus, there is an
adverse effect on the lift provided by that part of the wing in the
wake of the canard. The presence of the canard surface ($\delta_c = 0$) at
$M = 1.41$ results in little increase in total lift for either wing con-
figuration tested. (See fig. 8(a).) At $M = 2.01$, however, a substan-
tial portion of the lift due to the presence of the canard is realized.
At both Mach numbers the delta-wing configuration has a greater loss of
lift on the wing due to the presence of the canard surface than does
the trapezoidal-wing configuration. This effect, however, is not as
pronounced at a Mach number of 1.41 as at a Mach number of 2.01. The
greater loss of lift for the delta-wing configuration probably occurs

because more of its lift is in the inboard area which is most affected by the canard wake. It should be emphasized that both wing configurations tested have equal or greater lifts with the canard on than the wing-body configuration. (See figs. 4 and 5.)

The incremental wing data (fig. 8(a)) indicate that the pitching-moment nonlinearities shown at $M = 2.01$ (figs. 5 and 7) for the BWC configurations result primarily from body effects since the contribution of the wing in the presence of the body is reasonably linear.

At both Mach numbers the trapezoidal wing, which has less loss of lift due to the interference effects of the canard (figs. 8 and 9), has an increase in the moment increment provided by the canard because the interference lift (down load) does not act as far forward as that for the delta wing and the interference-moment increments act in the same direction as those provided by the canard. These effects on the moment increment provided by the canard may be only partially explained by the concentration of the induced loads on the inboard section of the wing. As reported in reference 5, there may be a chordwise variation in lift with the main interference effects concentrated near the wing leading edge. On this basis it might be expected that the delta wing, which has the leading edge of the wing closer to the canard surface and ahead of the center of moments, would have the greatest loss of lift on the wing and a decrease in the moment increment provided by the canard. Thus it would be reasonable to expect that an increase in the distance of the canard vortex from the wing surface would reduce the induced down load on the wing but not materially effect the chordwise lift distribution. An investigation of the effects of relative wing height behind a canard at $M = 2.01$ (ref. 6) indicated that a low-wing configuration does retain more of the canard lift than a high-wing configuration and that the increment of lift retained increases with angle of attack.

Estimated results.- The variation of lift and pitching moment with angle of attack for the various component configurations were estimated by the methods outlined in reference 7 and are compared with the experimental results in figures 9(a) and 9(b). In general, the results for the trapezoidal wing were in better agreement with the experimental results than those for the delta wing. Although the lift estimates were in good agreement for both wings, the theory underestimated C_{m_α} at

$M = 1.41$ for the delta wing but overestimated it at $M = 2.01$. Since no allowance for the chordwise variation in lift was made in the methods of reference 7, where the down load is assumed to act on the wing at the center of pressure, the good agreement with experiment shown in figure 9 for the trapezoidal-wing configuration (BWC) may result from a fortuitous location of the wing leading edge with respect to the canard vortex field.

Lift-drag ratio effects.- There was only a small decrease in $(L/D)_{max}$ from $M = 1.41$ to $M = 2.01$ for either wing configuration. The complete delta-wing configuration had an $(L/D)_{max}$ of 5.95 at $M = 2.01$ compared with the wing-body value of 6.8. For these tests the delta-wing configuration had slightly higher values of $(L/D)_{max}$ than those for the trapezoidal wing. The lift-drag ratios for the various component parts of the model are shown in figure 12.

Ventral fin effects.- The presence of the ventral fins (figs. 4 to 7) have little or no effect on lift but are slightly destabilizing in pitch and cause a small increase in drag for both wing configurations tested. The presence of the ventral fins caused a small decrease in $(L/D)_{max}$ for both wing configurations (fig. 13). The longitudinal control results obtained with the ventral fins removed are presented in figures 10 and 11.

Combined angles of attack and sideslip.- Conventional tail-rearward configurations have sometimes shown significant variations of lift and pitching moment with sideslip which have contributed to serious cross-coupling difficulties in flight. However, for the tail-forward configuration tested, there appears to be no serious effect of sideslip on these paraemters for control deflections of 0° to 15°.

Sideslip Characteristics

The basic sideslip data for several angles of attack are presented in figures 16 to 25. For clarity, the basic model buildup data are plotted for the wing-on and wing-off conditions for both Mach numbers.

Canard effects.- The lateral characteristics summarized in figures 26 and 27 indicate that at Mach number 1.41 (fig. 26(a)) the presence of the canard increased the directional-stability level for the delta-wing configuration but decreases the directional-stability level for the trapezoidal-wing configuration. There is little change in the C_{Y_β} results for either wing configuration. For both wings the presence of the canards provides a negative C_{l_β} increment or an increase in the positive effective dihedral.

At $M = 2.01$ (fig. 26(b)), the presence of the canards decreases the directional-stability level for both wing configurations, the delta-wing configuration having the largest decrease. The presence of the canards at $M = 2.01$ provides a positive increment in C_{Y_β} for both wing configurations; however, no improvement in C_{n_β} is shown. A

decrease in side force at the vertical tail due to the presence of the canards is consistent with the lower directional-stability level indicated for both wing configurations. As at $M = 1.41$ the presence of the canards provide a negative C_{l_β} increment.

The effects of a 15° canard deflection on the sideslip characteristics at $M = 2.01$ are shown for both wing configurations in figures 24 and 25. In general, deflecting the canard 15° does not materially affect the directional-stability level or the vertical-tail contribution for either wing configuration. There is little or no effect on C_{Y_β} due to canard deflection for either wing configuration; this result is consistent with the C_{n_β} results. However, deflecting the canard 15° provides an additional negative increment in C_{l_β} approximately equal to the negative increment provided by the presence of the vertical tail. The increase negative values of C_{l_β} occur for both wing configurations and apparently result from the effect of the canard wake on the leeward wing panel since about the same negative C_{l_β} increment is obtained whether the vertical tail is on or off. This effect of canard deflection on C_{l_β} might complicate the lateral-control problem in the case of a rolling pull-up maneuver.

Effect of component parts for $M = 2.01$.- The presence of either wing plan form (vertical tail on) causes a sizable reduction in the directional-stability level and in the vertical-tail contribution to directional stability (fig. 27). The C_{Y_β} results indicate only small changes in side force at the vertical tail; thus, the decrease in the directional-stability level due to the presence of either wing results primarily from a center-of-pressure movement at the vertical tail.

For the trapezoidal-wing configuration the presence of the wing on the vertical-tail-off configuration results in a substantial increase in the directional-stability level above an angle of attack of 8°. The stabilizing increment is not realized, however, when the vertical tail is installed. The presence of the delta wing on the vertical-tail-off configuration shows a decrease in the directional-stability level above an angle of attack of 15°. For both wing configurations the negative increment in the side-force parameter C_{Y_β} (stabilizing) added by the vertical-tail and ventral-fin arrangement decreased with increasing angles of attack until about 18° where the presence of the vertical tail no longer provided any increment in C_{Y_β}. These side-force results are

consistent with the directional-stability results which show a corresponding decrease in directional stability with increasing angle of attack. The loss of the side-force increment provided by the vertical tail and the subsequent loss of directional stability probably results from adverse flow effects at the vertical tail.

Although the presence of the canard on the body alone has no effect on C_{l_β}, the presence of either wing provides large negative C_{l_β} values with increasing angles of attack. The presence of the vertical-tail—ventral-fin arrangement with the wing off provides a large initial increment in C_{l_β} that decreases with increasing angle of attack; thus, the increment provided by the vertical tail reaches zero near an angle of attack of 16°. The complete model (trapezoidal wing on) has a similar negative level of C_{l_β} ($\alpha = 0$) which becomes more negative as the angle of attack is increased. The effect of the wing is not as great for the delta-wing configuration.

In general, the complete-model canard configurations have the same characteristic decrease in directional stability with angle of attack as most conventional high-fineness-ratio supersonic configurations. The presence of the canard surface may be beneficial or detrimental depending upon Mach number and the geometry of the configuration.

CONCLUSIONS

An investigation has been made in the Langley 4- by 4-foot supersonic pressure tunnel at Mach numbers of 1.41 and 2.01 to determine the longitudinal and lateral stability and control characteristics of the various component parts of a generalized canard airplane equipped with either a delta-plan-form or a trapezoidal-plan-form wing. The results of the investigation indicate the following conclusions:

1. The interference effects of the canard wake on either wing at a Mach number of 1.41 results in the loss of most of the lift increment produced by the canard. At a Mach number of 2.01, however, a substantial portion of the canard lift is retained.

2. Because the interference effects of the canard wake appear to be concentrated near the leading edge of the wing, the proper location of the wing leading edge with respect to the center of moments may result in a substantial increase in the pitching-moment increment provided by the canard even though the total lift of the canard is small.

3. The canard configurations have the same characteristic decrease in directional stability with angle of attack as most conventional high-fineness-ratio supersonic configurations. Although the presence of the canard surface caused a small increase in the directional stability at a Mach number of 1.41 for the delta-wing configuration, the presence of the canards resulted in small decreases in the directional-stability level at a Mach number of 2.01 for both wing configurations.

4. A canard deflection of 15° provided an increase in the positive effective dihedral approximately as large as that provided by the presence of the vertical tail. This effect of canard deflection might complicate the lateral-control problem in the case of a rolling pull-up maneuver.

Langley Research Center,
      National Aeronautics and Space Administration,
            Langley Field, Va., July 10, 1958.

REFERENCES

1. Driver, Cornelius: Longitudinal and Lateral Stability and Control Characteristics of Two Canard Airplane Configurations at Mach Numbers of 1.41 and 2.01. NACA RM L56L19, 1957.

2. Sleeman, William C., Jr.: Investigation at High Subsonic Speeds of the Static Longitudinal and Lateral Stability Characteristics of Two Canard Airplane Configurations. NACA RM L57J08, 1957.

3. Spearman, M. Leroy, and Driver, Cornelius: Effects of Canard Surface Size on Stability and Control Characteristics of Two Canard Airplane Configurations at Mach Numbers of 1.41 and 2.01. NACA RM L57L17a, 1958.

4. Spearman, M. Leroy, and Driver, Cornelius: Longitudinal and Lateral Stability and Control Characteristics at Mach Number 2.01 of a 60° Delta-Wing Airplane Configuration Equipped With a Canard Control and With Wing Trailing-Edge Flap Controls. NACA RM L58A20, 1958.

5. Watts, P. E., and Beecham, L. J.: A Wind Tunnel Investigation of the Longitudinal and Lateral Aerodynamic Characteristics of a Canard Aircraft Model. - Part I. Tests at M = 1.40 and 2.02. Rep. No. Aero. 2575, British R.A.E., June 1956.

6. Spearman, M. Leroy, and Driver, Cornelius: Some Factors Affecting the Stability and Performance Characteristics of Canard Aircraft Configurations. NACA RM L58D16, 1958.

7. Pitts, William C., Nielsen, Jack N., and Kaattari, George E.: Lift and Center of Pressure of Wing-Body-Tail Combinations at Subsonic, Transonic, and Supersonic Speeds. NACA Rep. 1307, 1957.

TABLE I.- GEOMETRIC CHARACTERISTICS OF MODEL

Body:
Maximum diameter, in. 3.50
Length, in. 37.00
Base area, sq in. 9.582
Fineness ratio 10.57

Trapezoidal wing:
Span, in. 25.72
Chord at body-wing intersection, in. 13.25
Area, sq ft 1.53
Aspect ratio 3
Taper ratio 0.143
Thickness ratio 0.04
Mean geometric chord, in. 10.184
Sweep angle of leading edge, deg . . . . 38° 40'
Sweep angle of trailing edge, deg . . . . -11° -18'
Leading-edge half-angle, normal to leading edge, deg 5
Trailing-edge half-angle, normal to trailing edge, deg . . . 5

Delta wing:
Span, in. 22.56
Chord at body-wing intersection, in. 16.51
Mean geometric chord, in. 13.027
Area, sq ft 1.53
Aspect ratio 2.31
Taper ratio . . . .
Thickness ratio 0.036
Sweep angle of leading edge, deg 60
Leading-edge half-angle, normal to leading edge, deg 5
Trailing-edge half-angle, normal to trailing edge, deg . . . 5

Canard:
Area, exposed (each canard), sq in. 6.742
Span, exposed, in. 2.25
Mean geometric chord, in. 3.33

Vertical tail:
Area (exposed), sq ft 0.279
Span (exposed), in. 4.25
Aspect ratio 0.439
Sweep of leading edge, deg 70
Sweep of trailing edge, deg . . . . 15° 13'
Section . . . . 3/16 inch slab
Leading-edge half-angle, normal to leading edge, deg 5

Ventral fins:
Area, each fin, sq ft 0.13
Span (exposed), in. 2.25
Aspect ratio 0.271
Sweep of leading edge, deg 60
Sweep of trailing edge, deg . . . . -77° 30'
Leading-edge half-angle, normal to leading edge, deg 5
Trailing-edge half-angle, normal to trailing edge, deg . . . 5

TABLE II.- FUSELAGE ORDINATES

Body station	Radius	
0	0	
.297	.076	
.627	.156	
.956	.233	
1.285	.307	
1.615	.378	
1.945	.445	
2.275	.509	
2.605	.573	
2.936	.627	
3.267	.682	
3.598	.732	
3.929	.780	
4.260	.824	
4.592	.865	
4.923	.903	
5.255	.940	
5.587	.968	
5.920	.996	
6.252	1.020	
6.583	1.042	Conical
18.648	1.75	section
37.000	1.75	
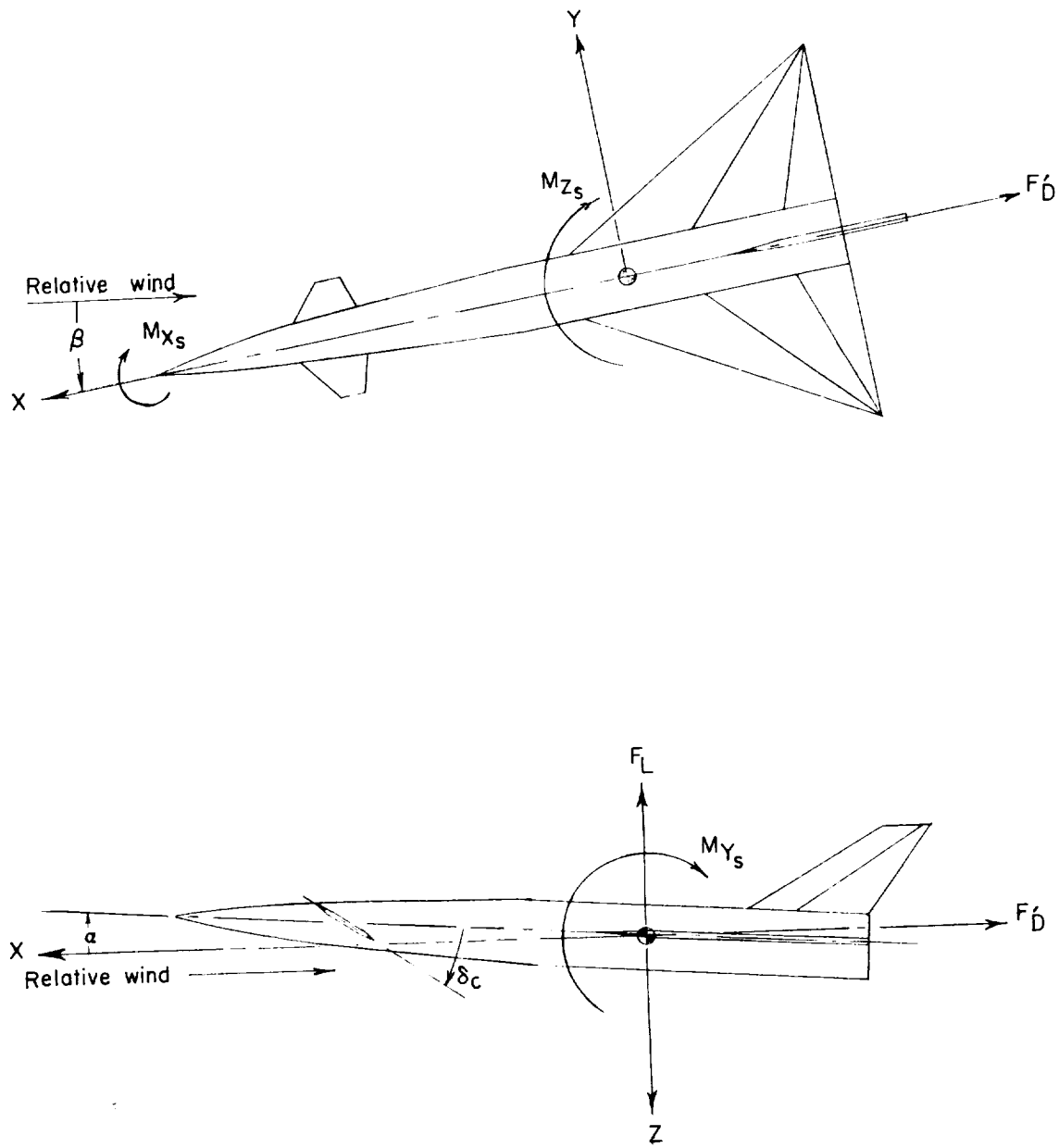
(a) Stability axes.

Figure 1.- Axes systems. Arrows indicate positive directions.
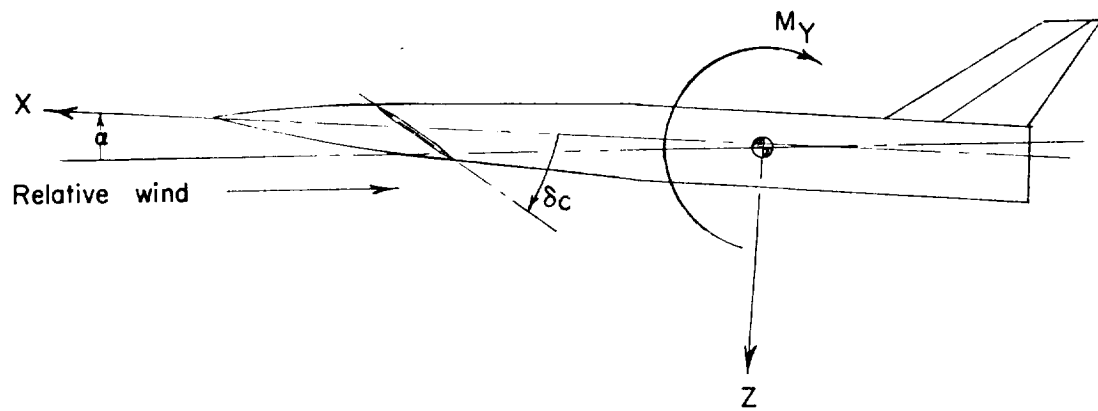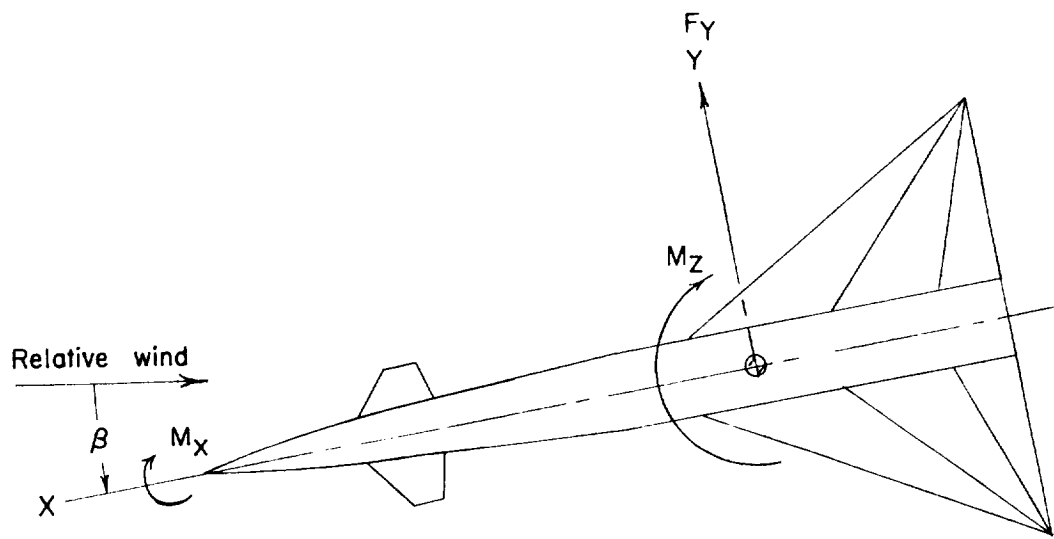
(b) Body axes.

Figure 1.- Concluded.
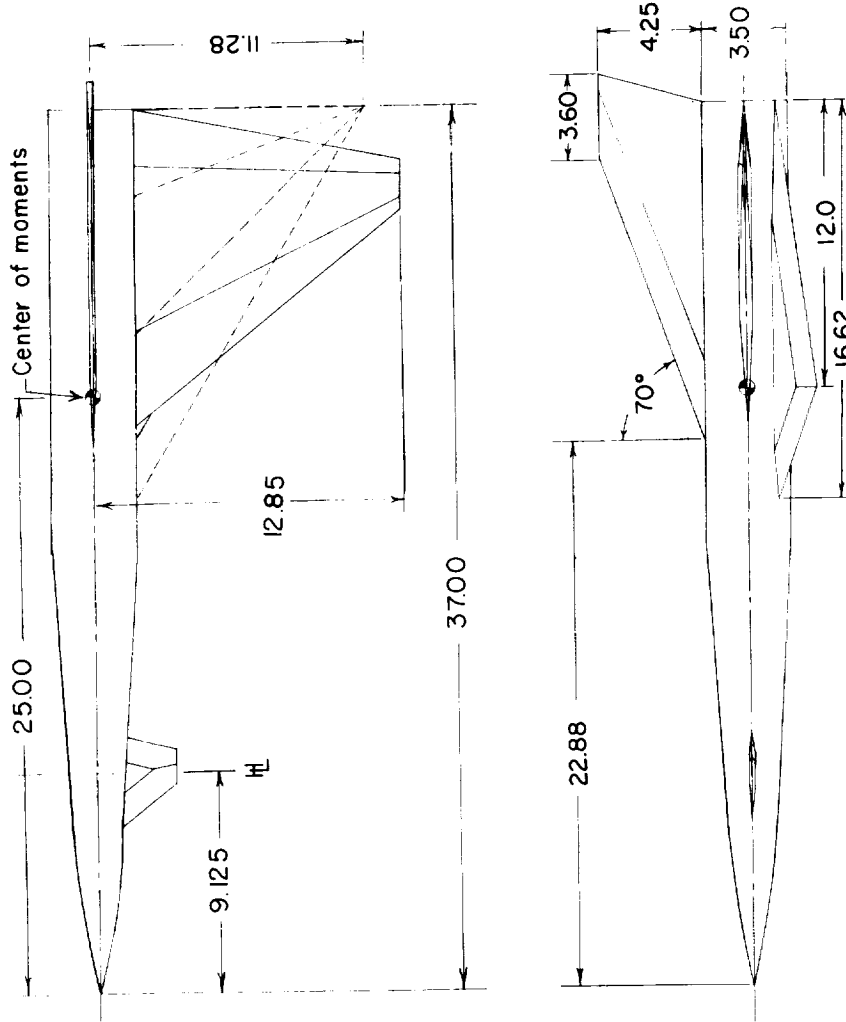
(a) Three-view drawing of model arrangement.

Figure 2.- Details of generalized canard airplane model.

Trapezoidal wing $(\Lambda_{.80c}=0°)$

60° delta wing
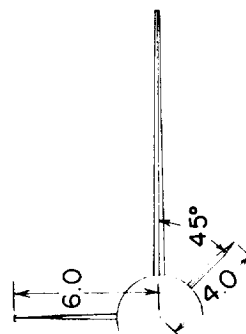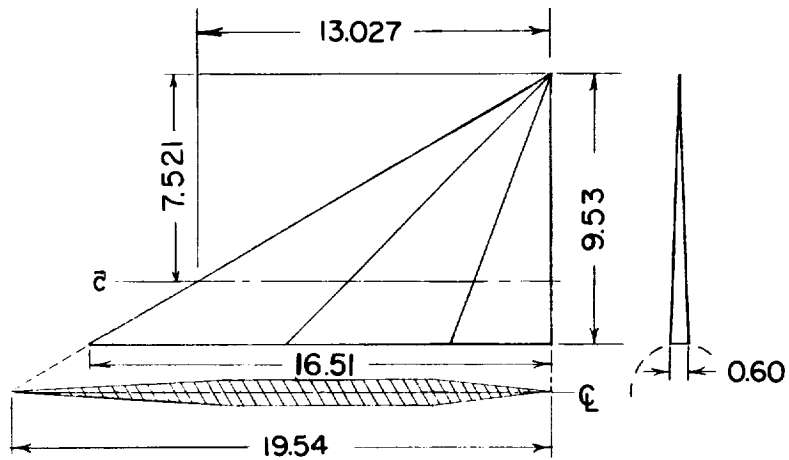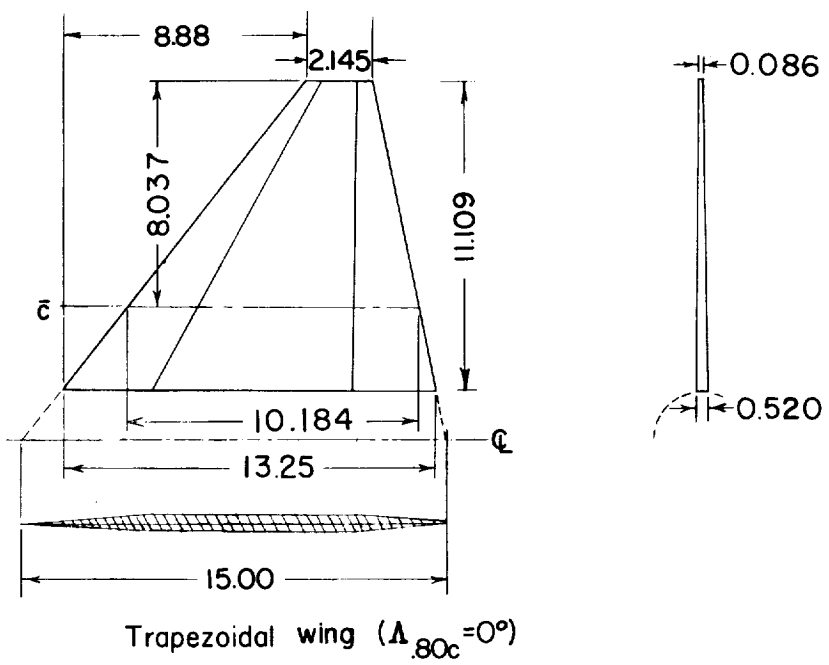
(b) Details of wings.

Figure 2.- Continued.
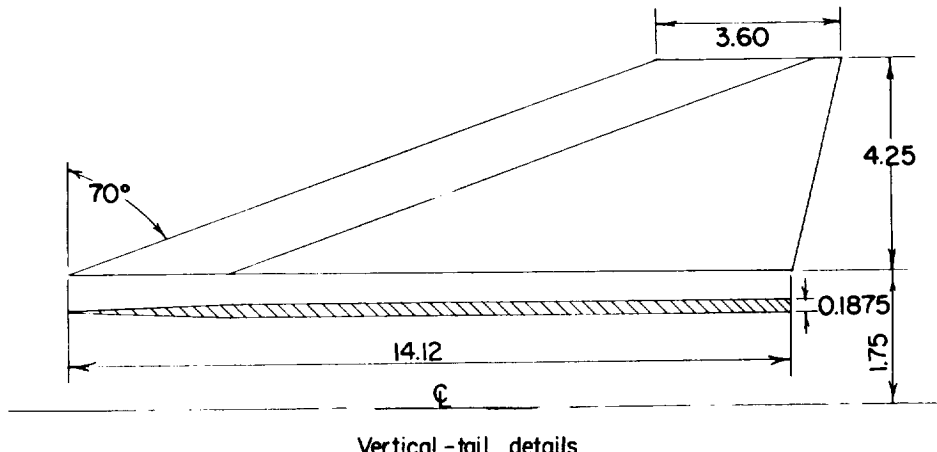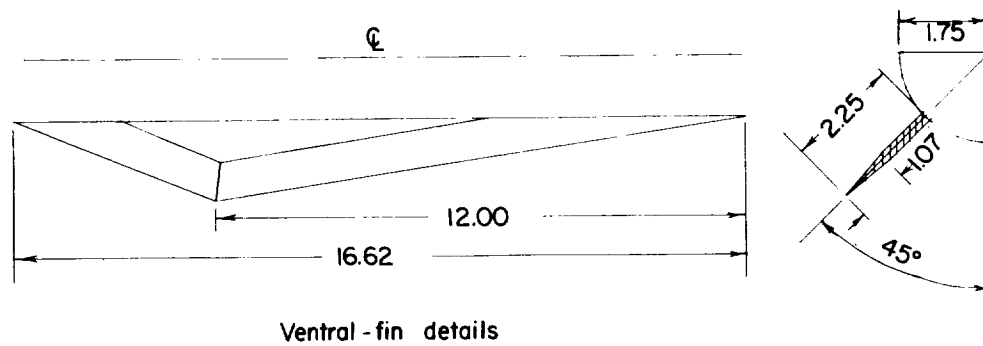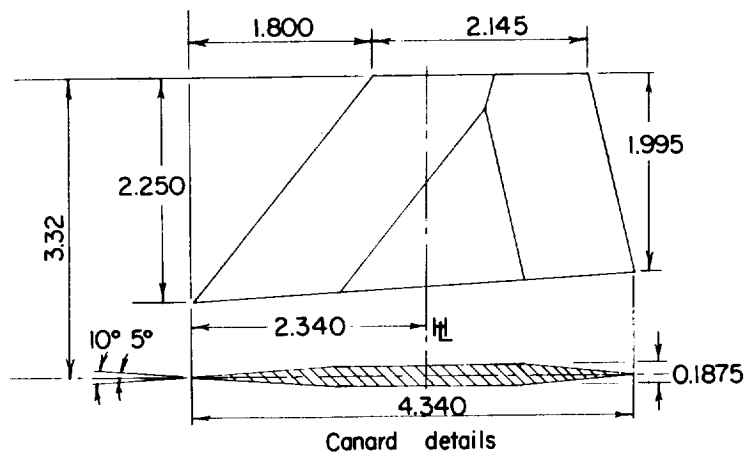
(c) Details of the canard surface, ventral fin, and vertical fin.

Figure 2.- Concluded.
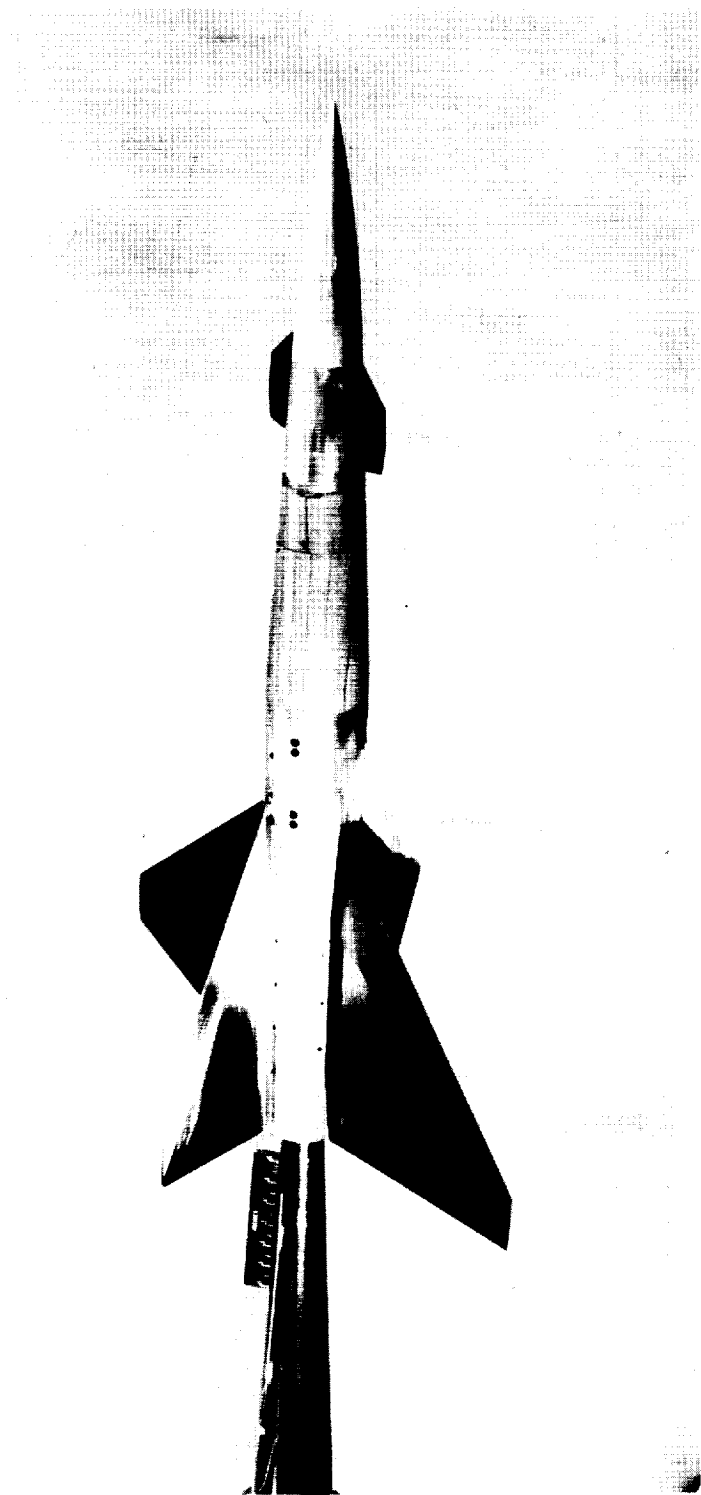
Figure 3.- Photographs of models.

L-94457

Figure 3.- Concluded.
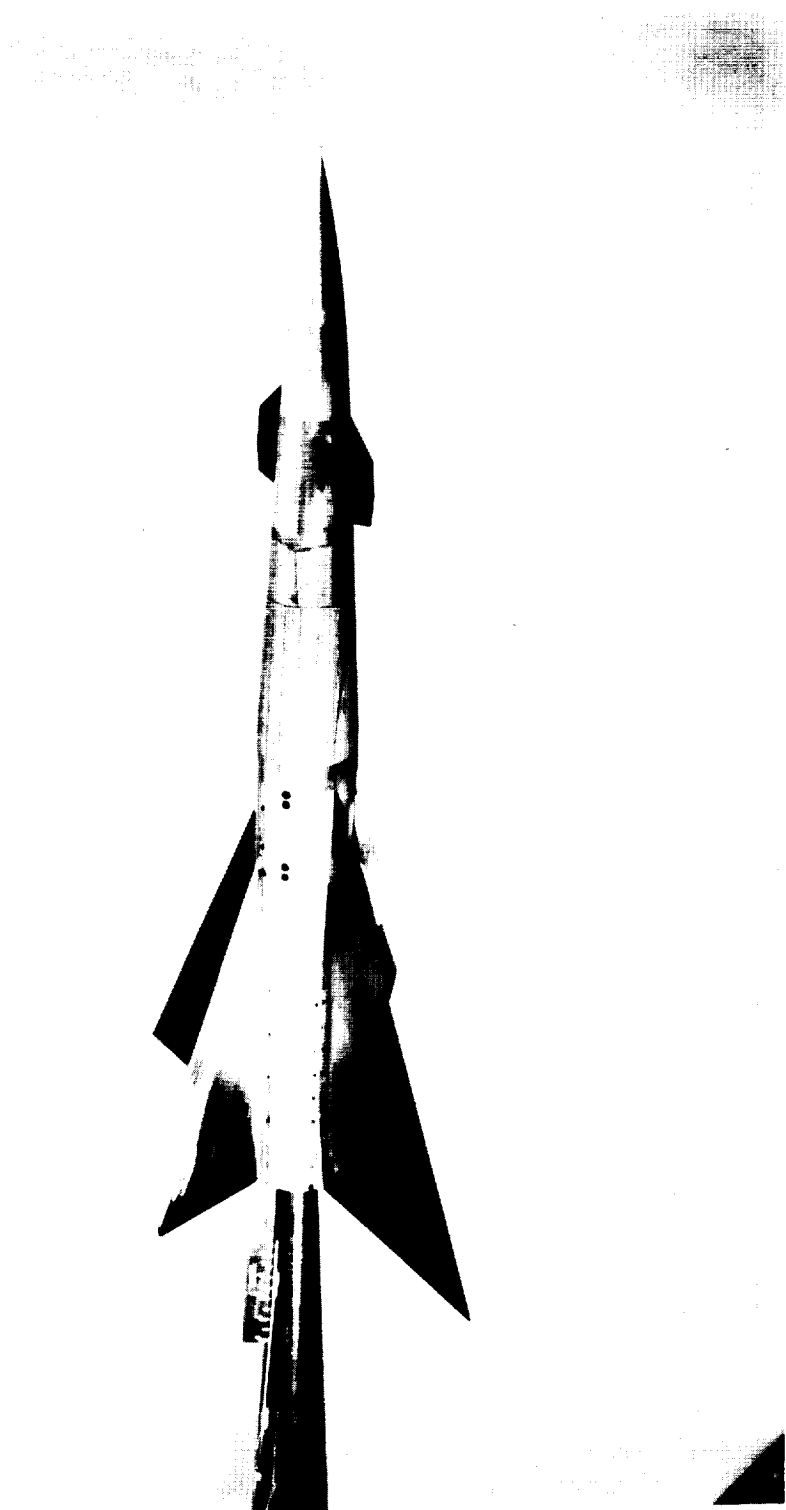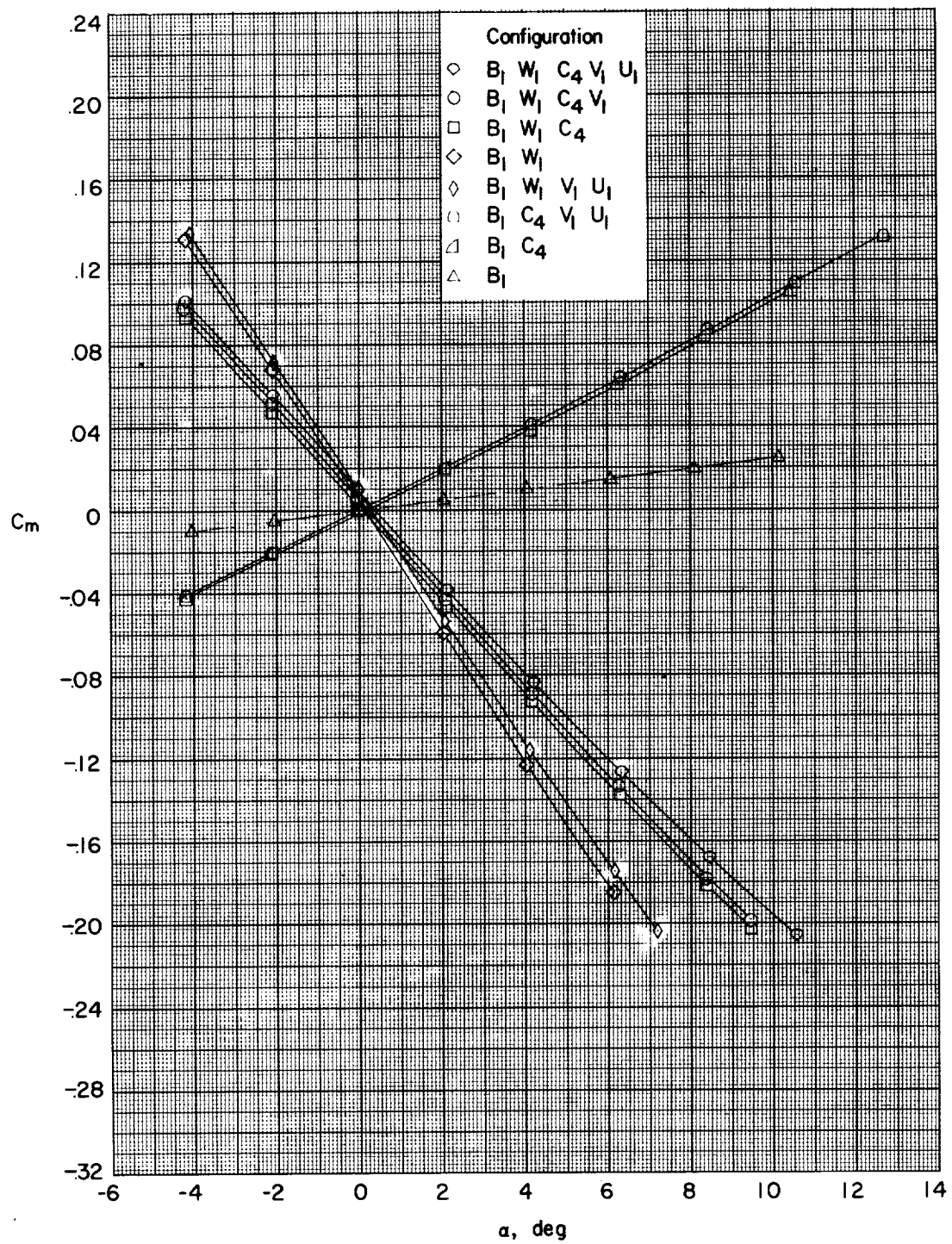
Figure 4.- The aerodynamic characteristics of various components of the trapezoidal-wing configurations. M = 1.41.
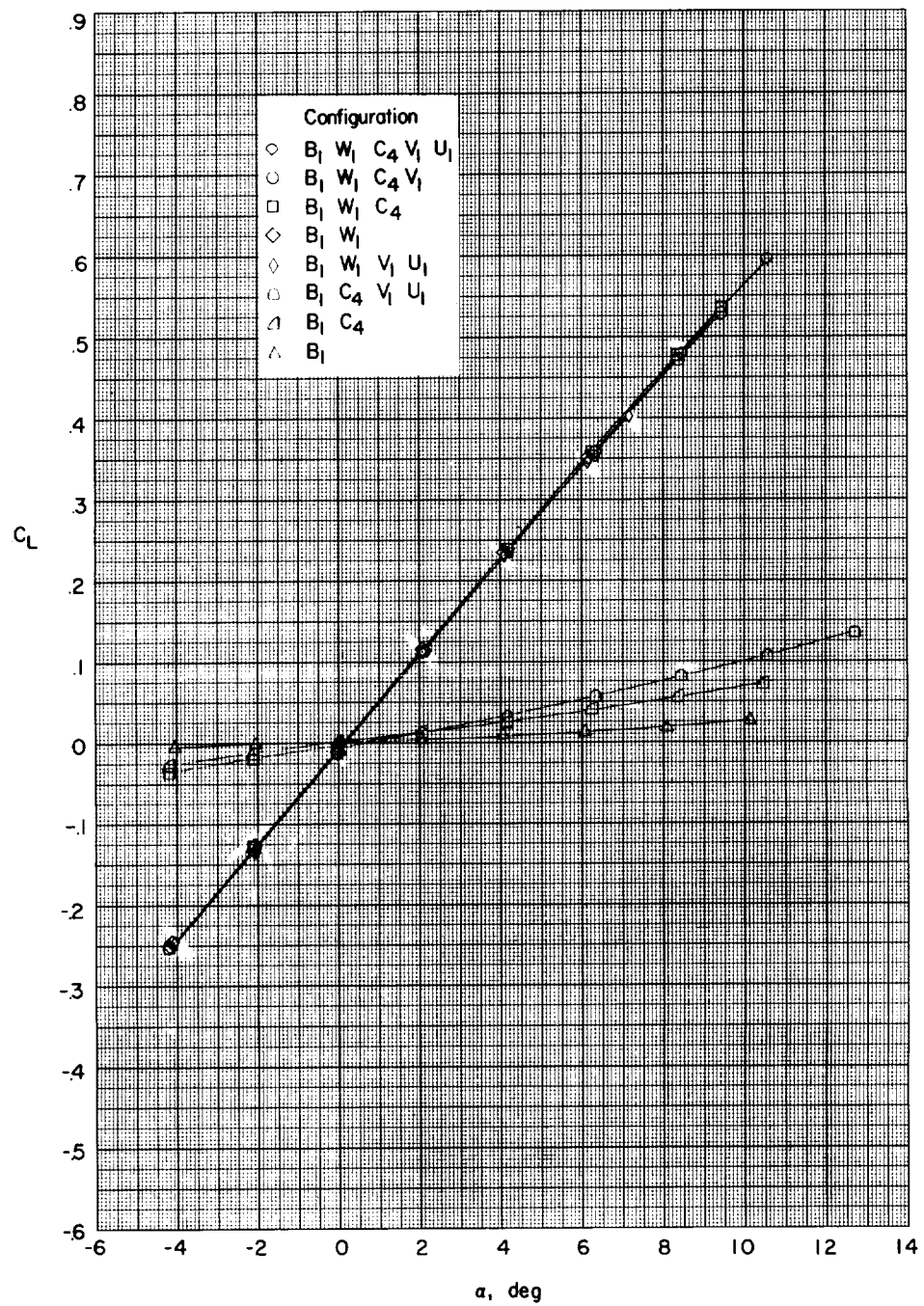
Figure 4.- Continued.

24
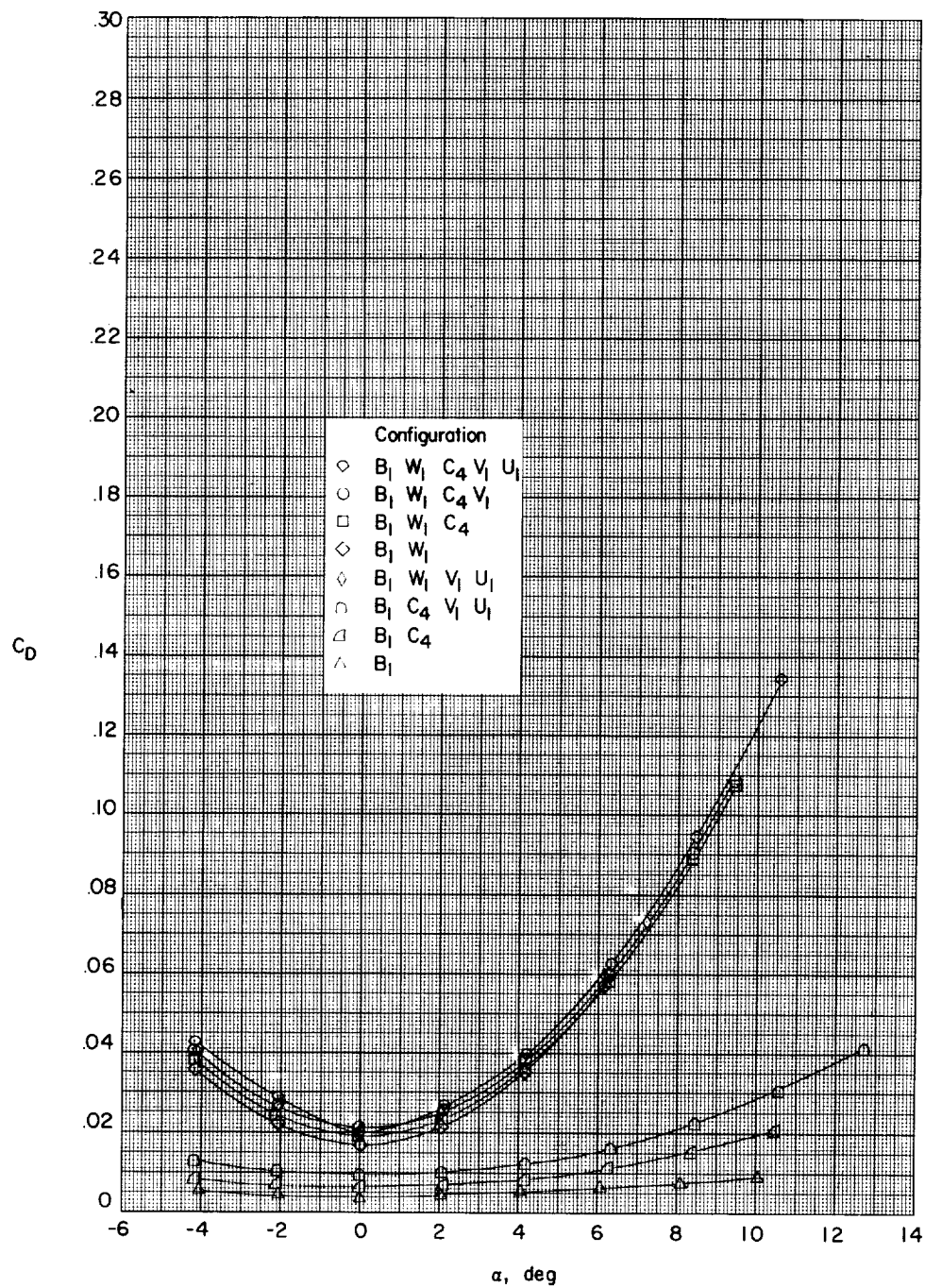
Figure 4.- Concluded.
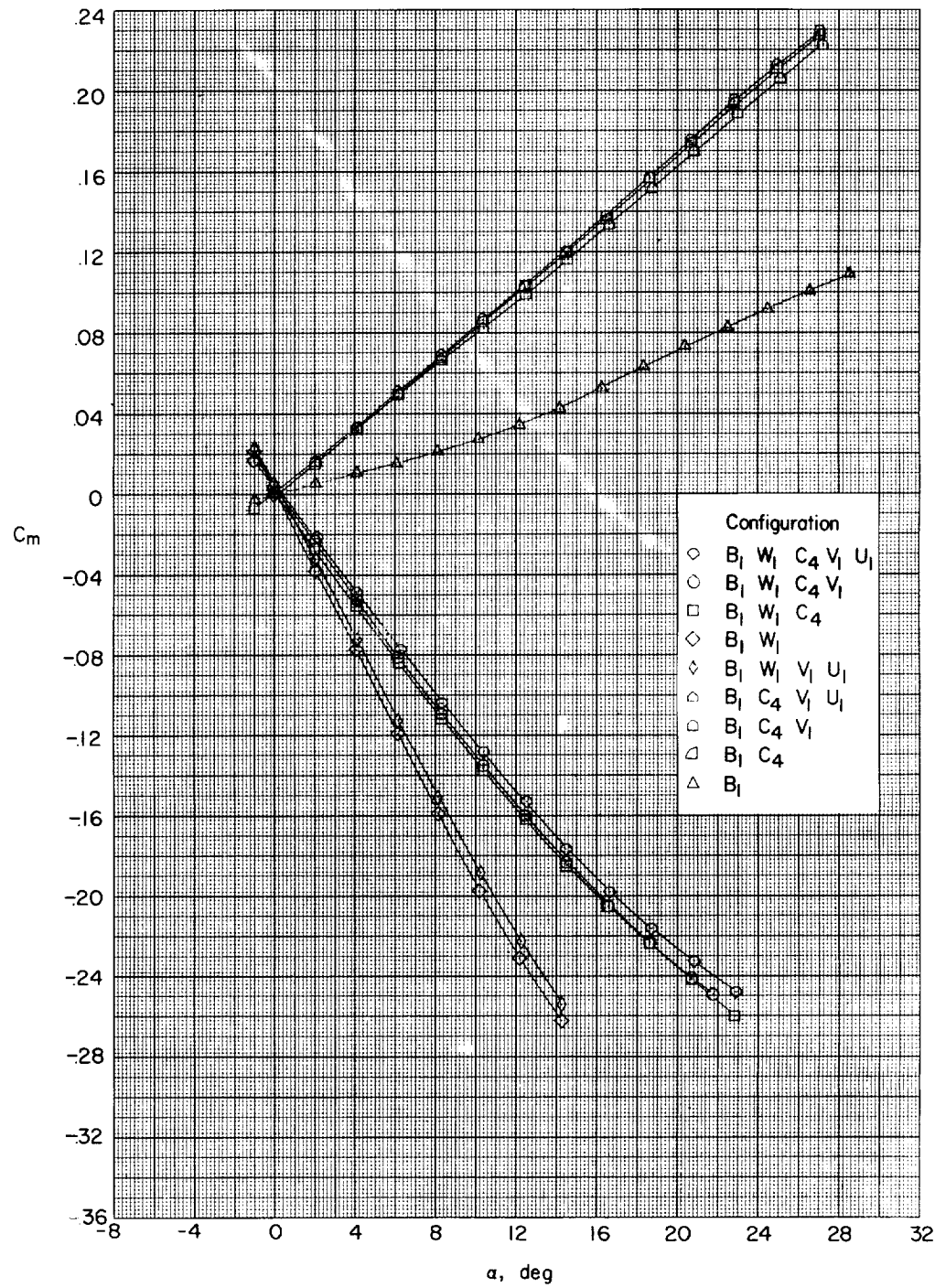
Figure 5.- The aerodynamic characteristics of various components of the trapezoidal-wing configuration. M = 2.01.
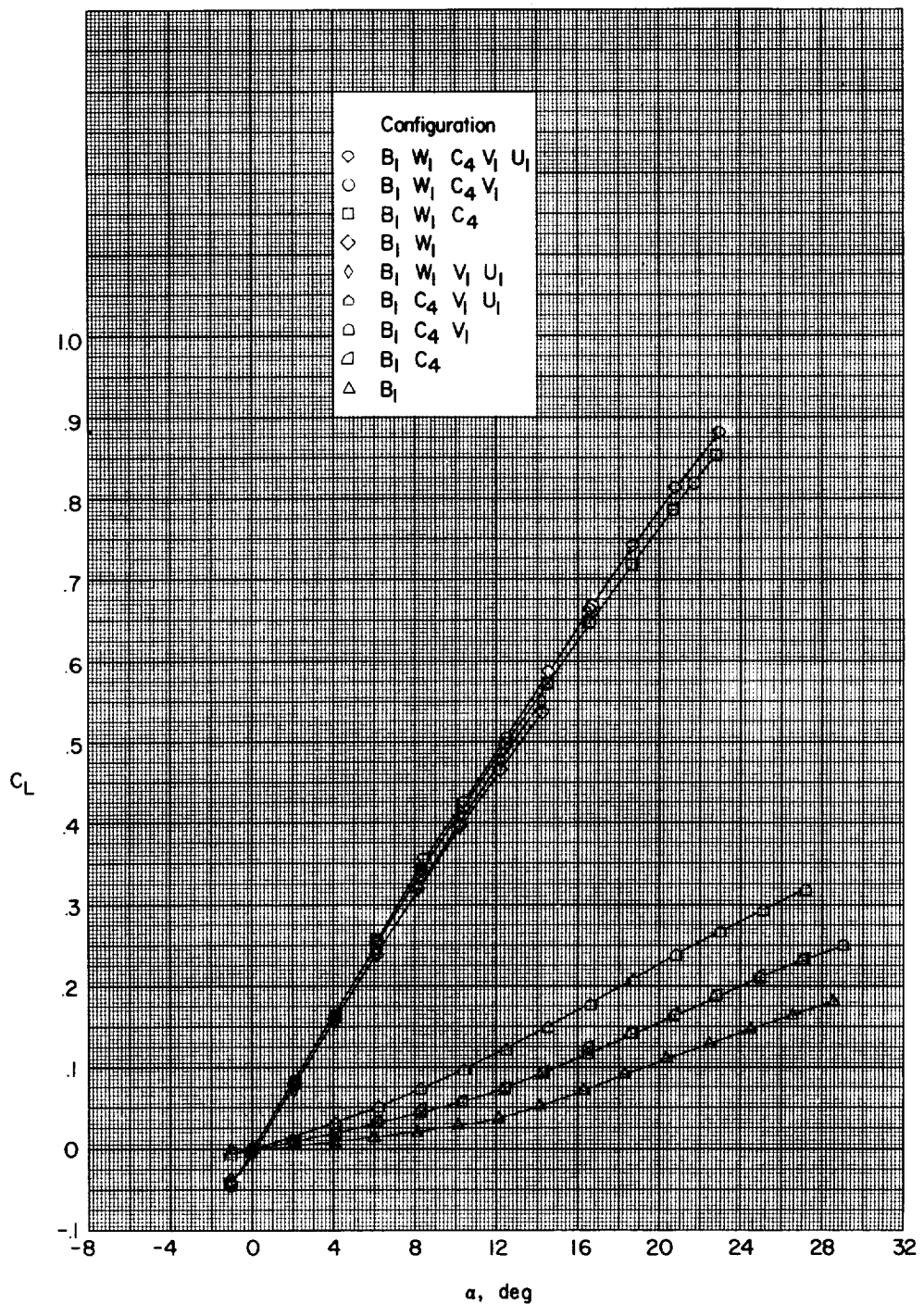
Figure 5.- Continued.
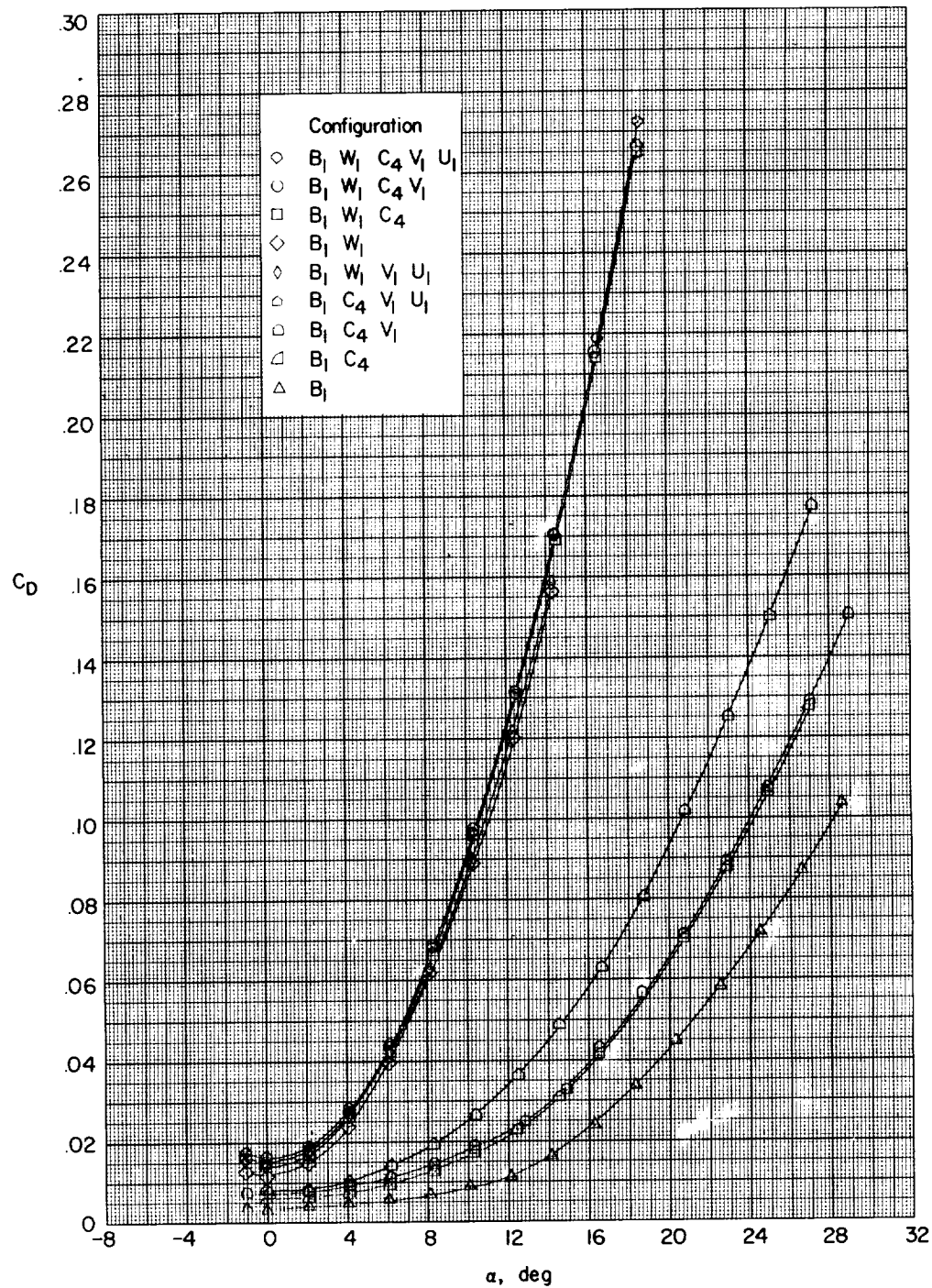
Figure 5.- Concluded.
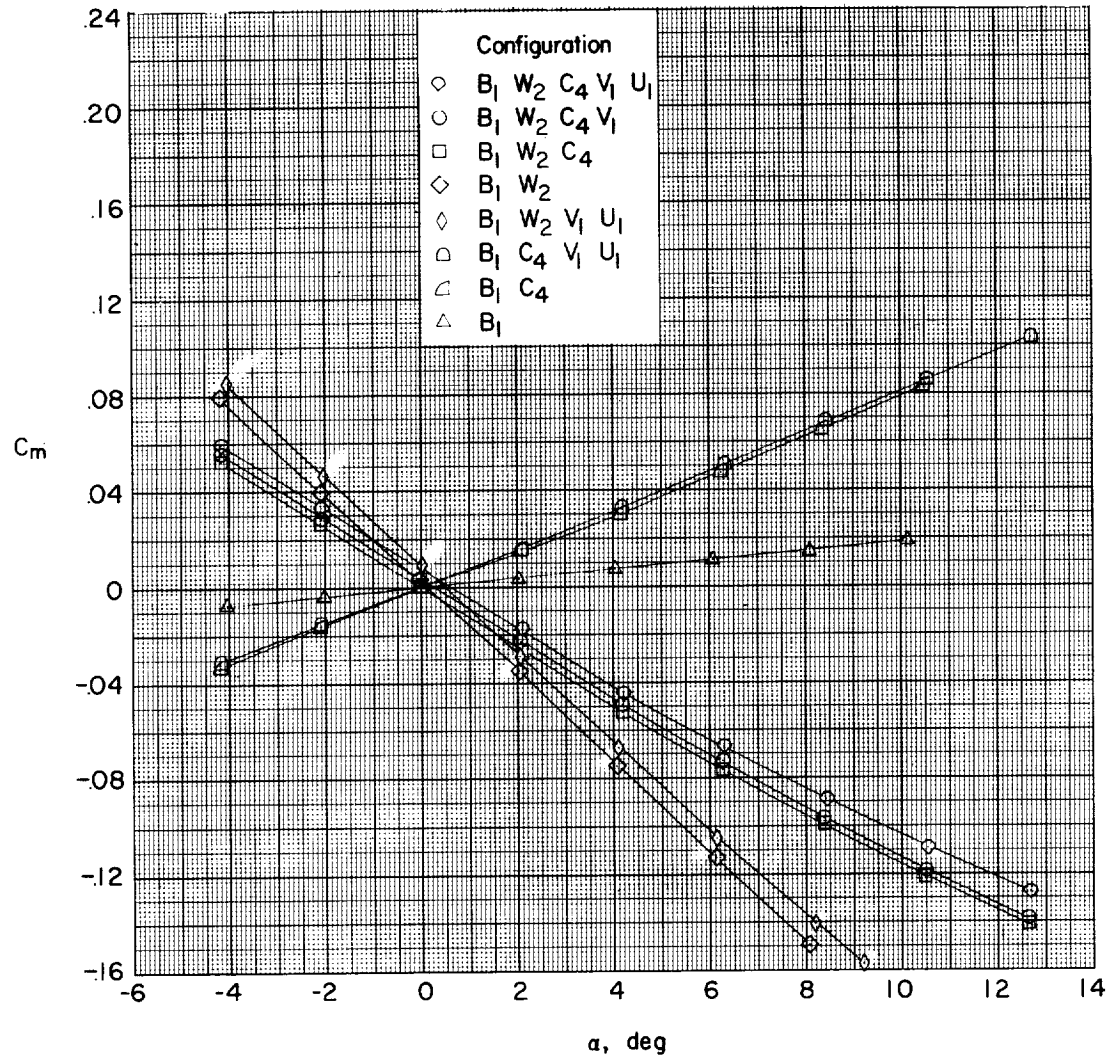
Figure 6.- The aerodynamic characteristics of various components of the delta-wing configuration. M = 1.41.
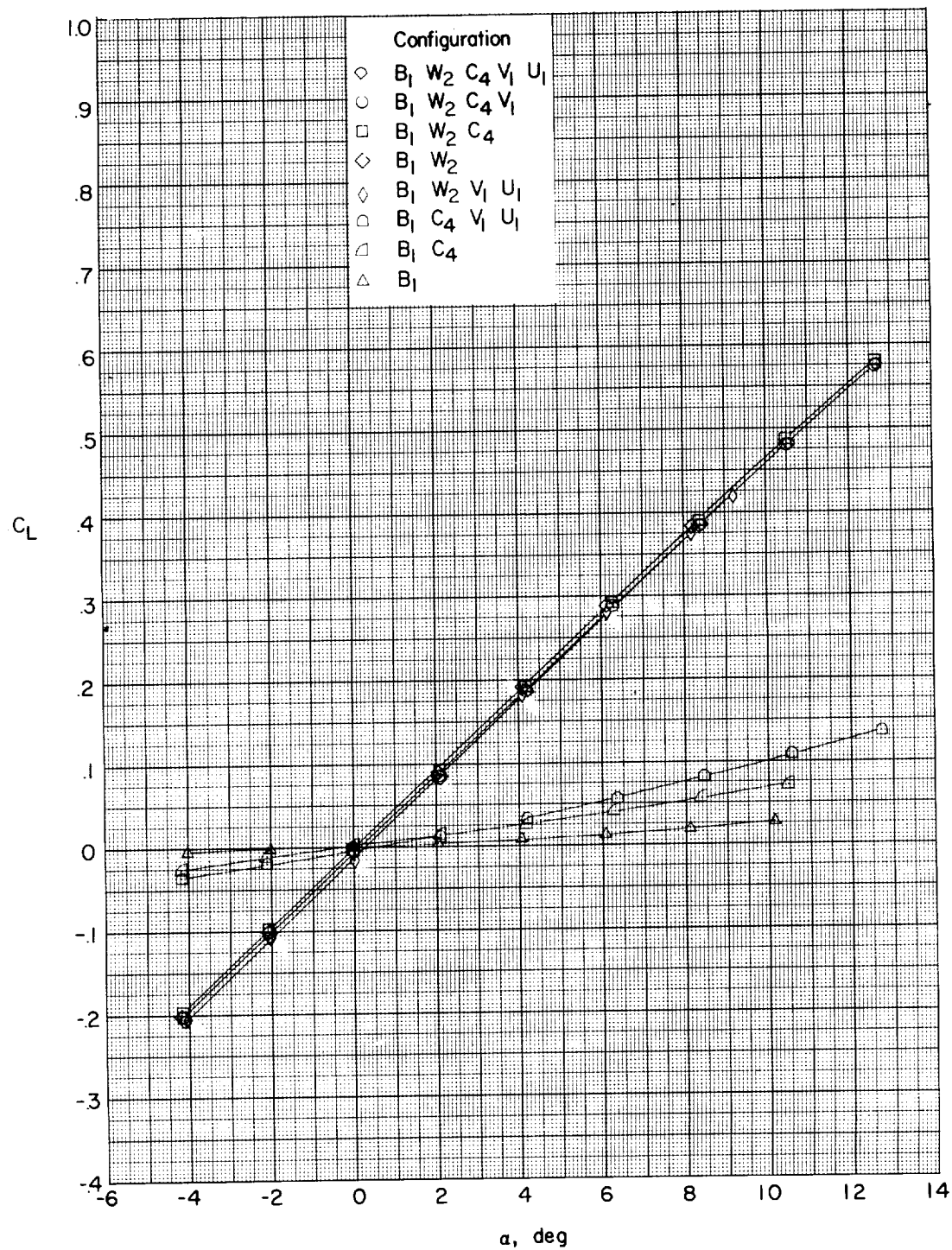
Figure 6.- Continued.
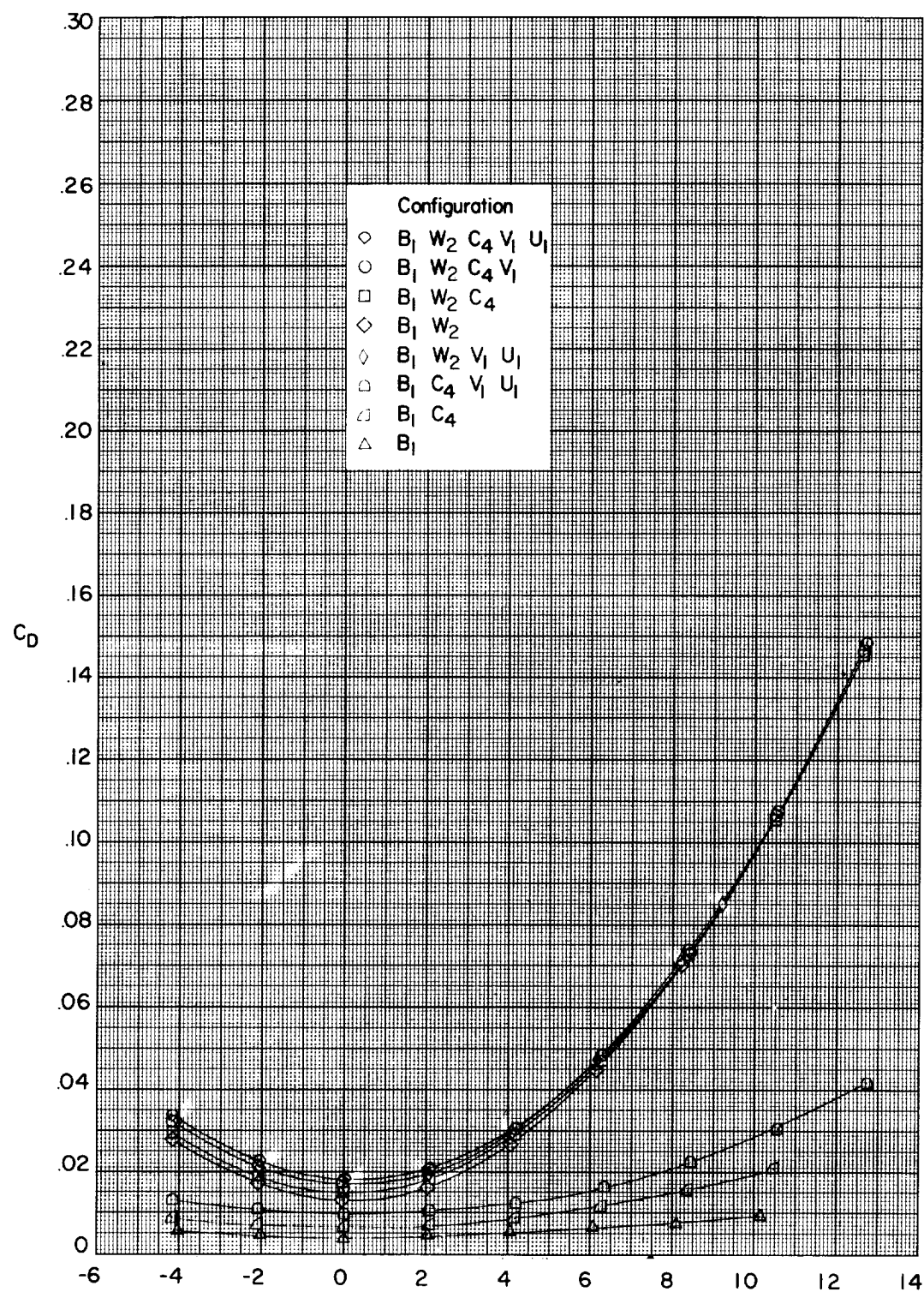
Figure 6.- Concluded.
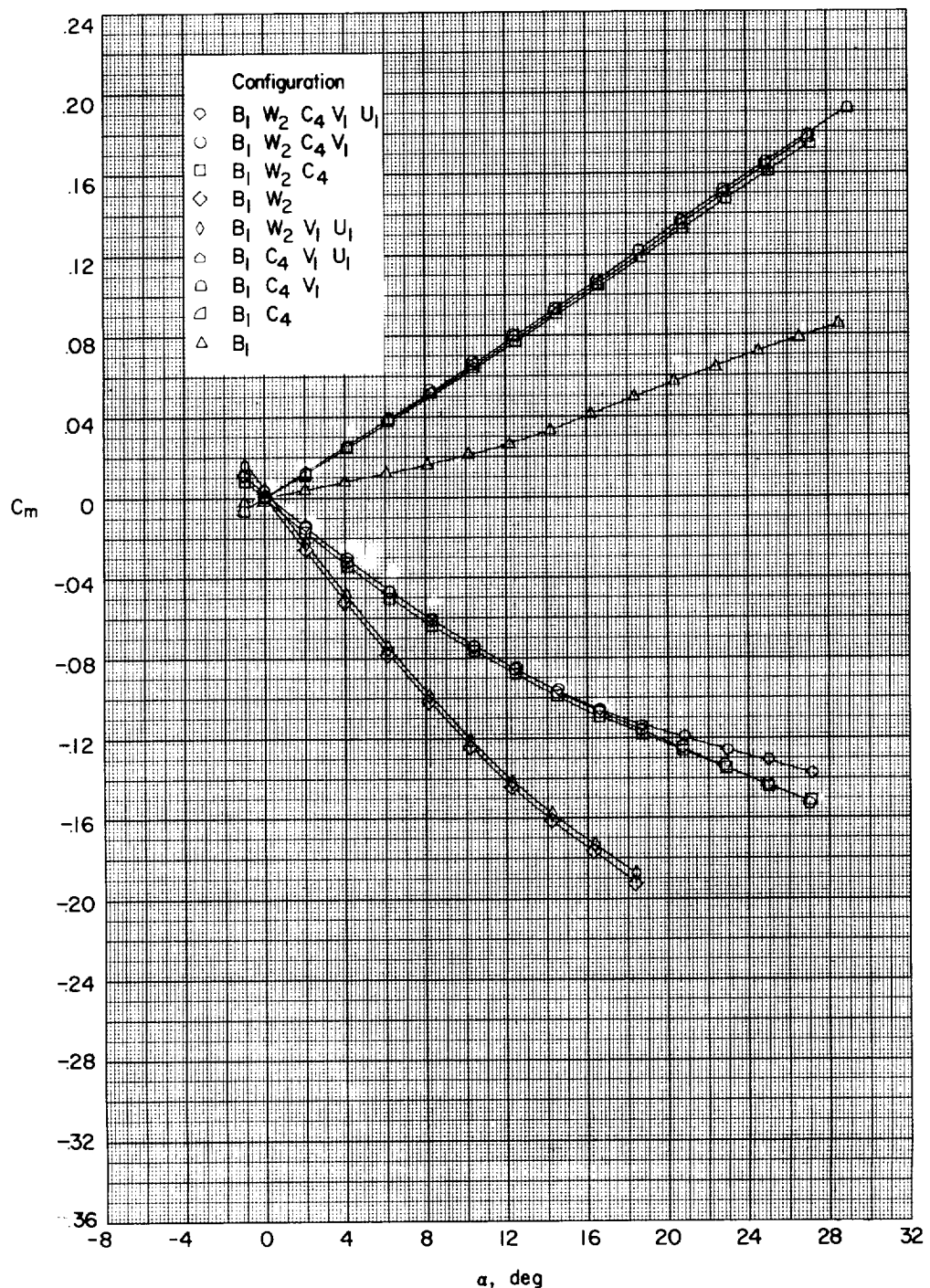
Figure 7.- The aerodynamic characteristics of various components of the delta-wing configuration. M = 2.01.
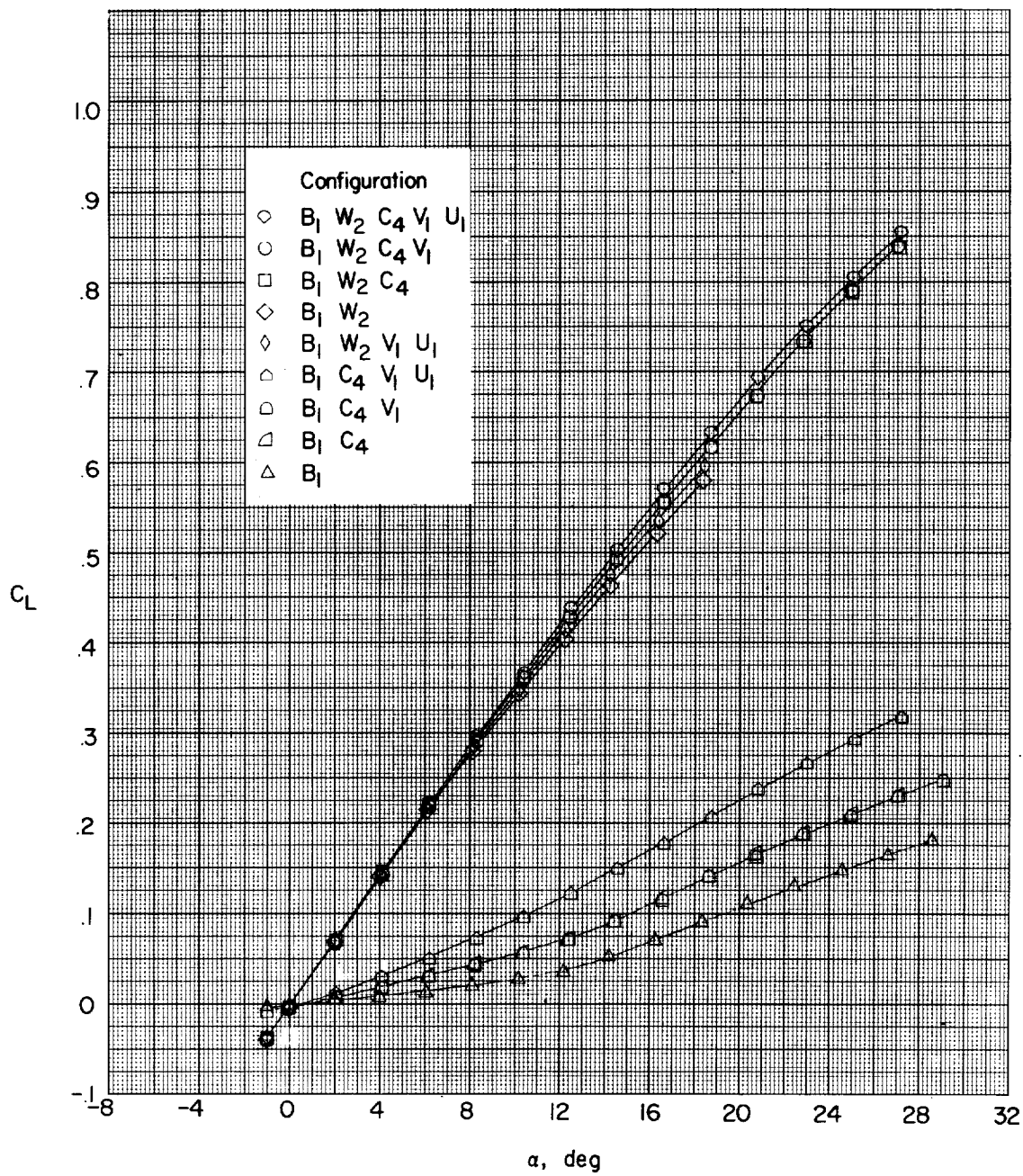
Figure 7.- Continued.
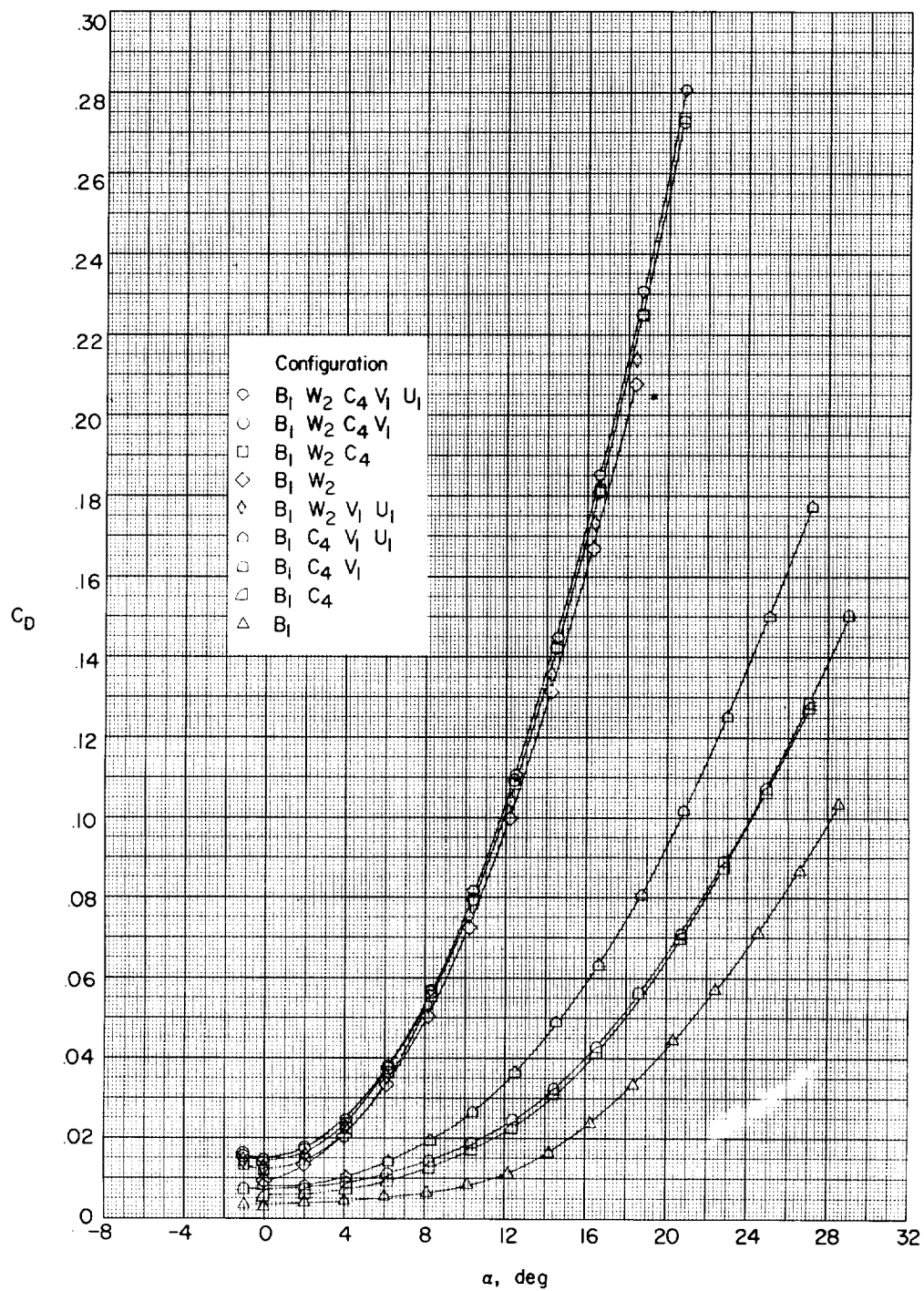
Figure 7.- Concluded.
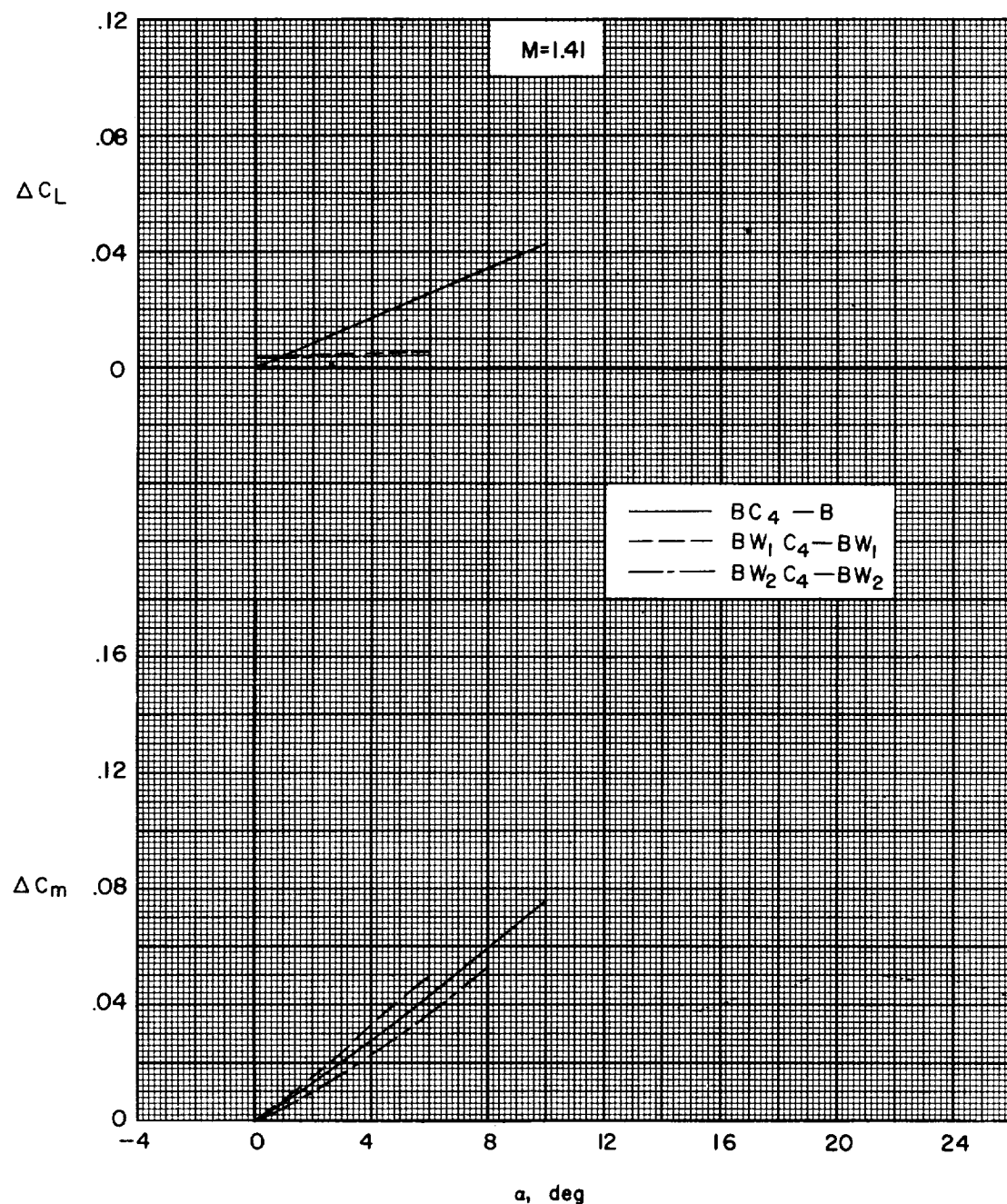
(a) Canard increments.

Figure 8.- Incremental canard and wing results.
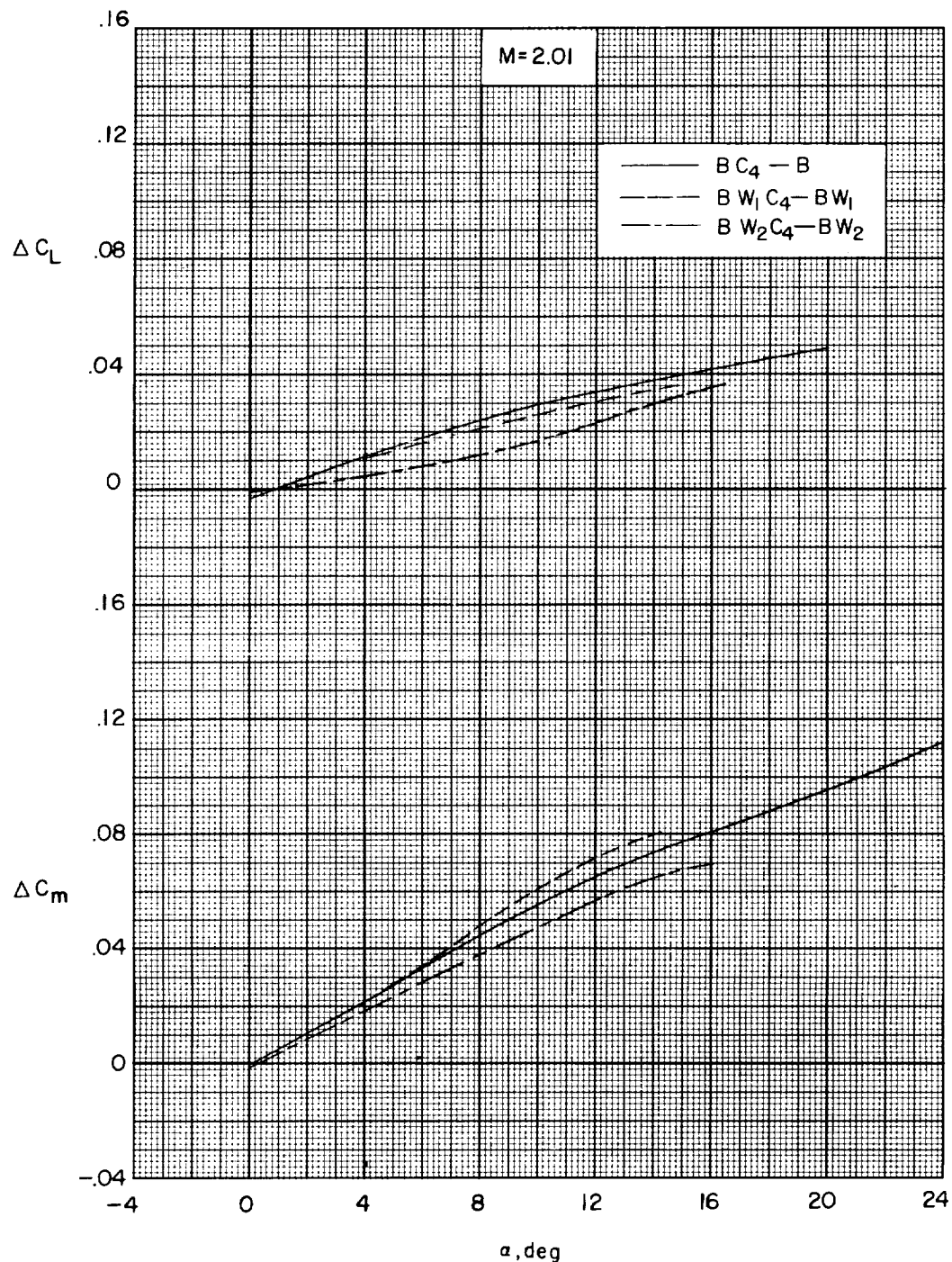
(a) Concluded.

Figure 8.- Continued.
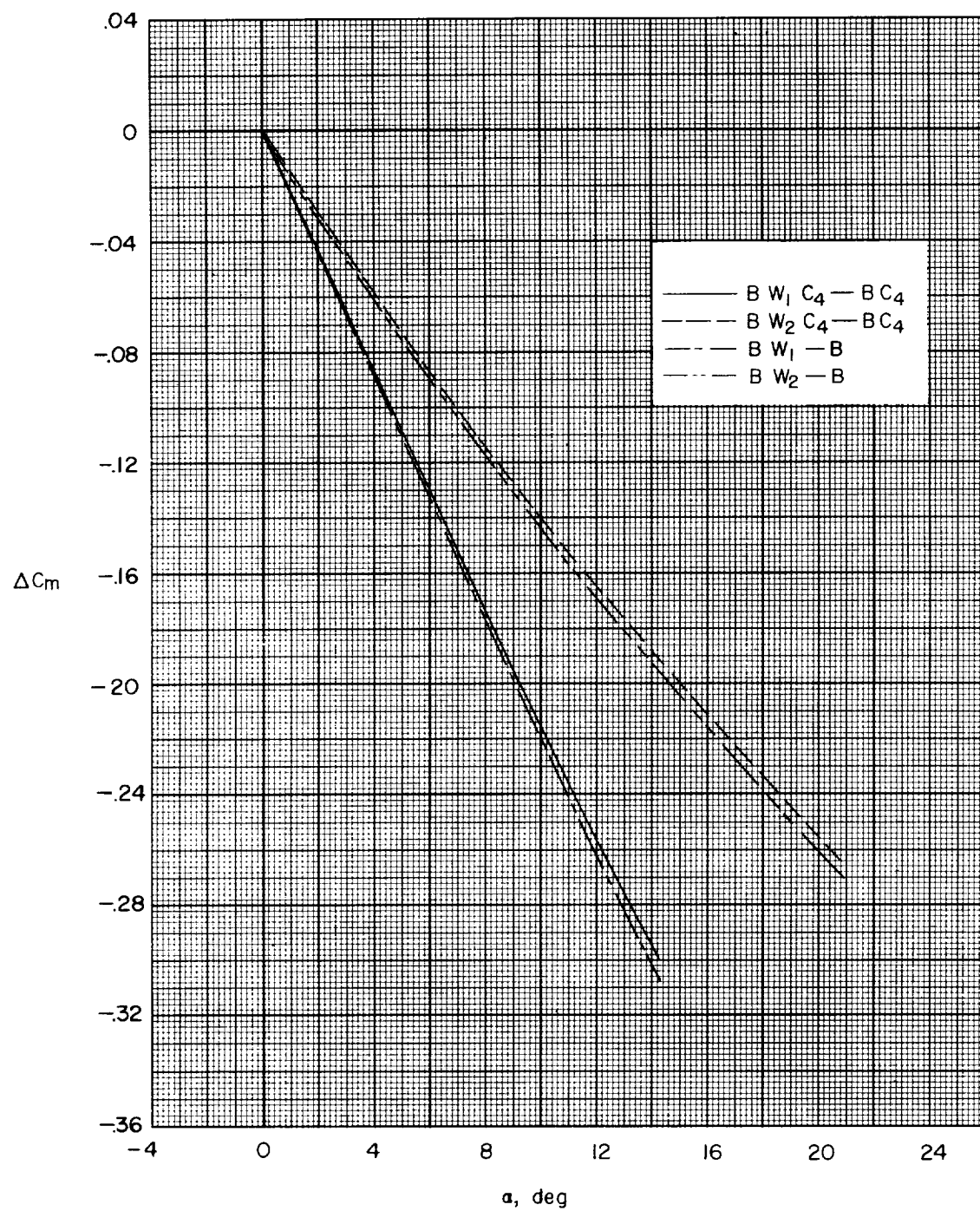
(b) Wing increment. M = 1.41.

Figure 8.- Continued.
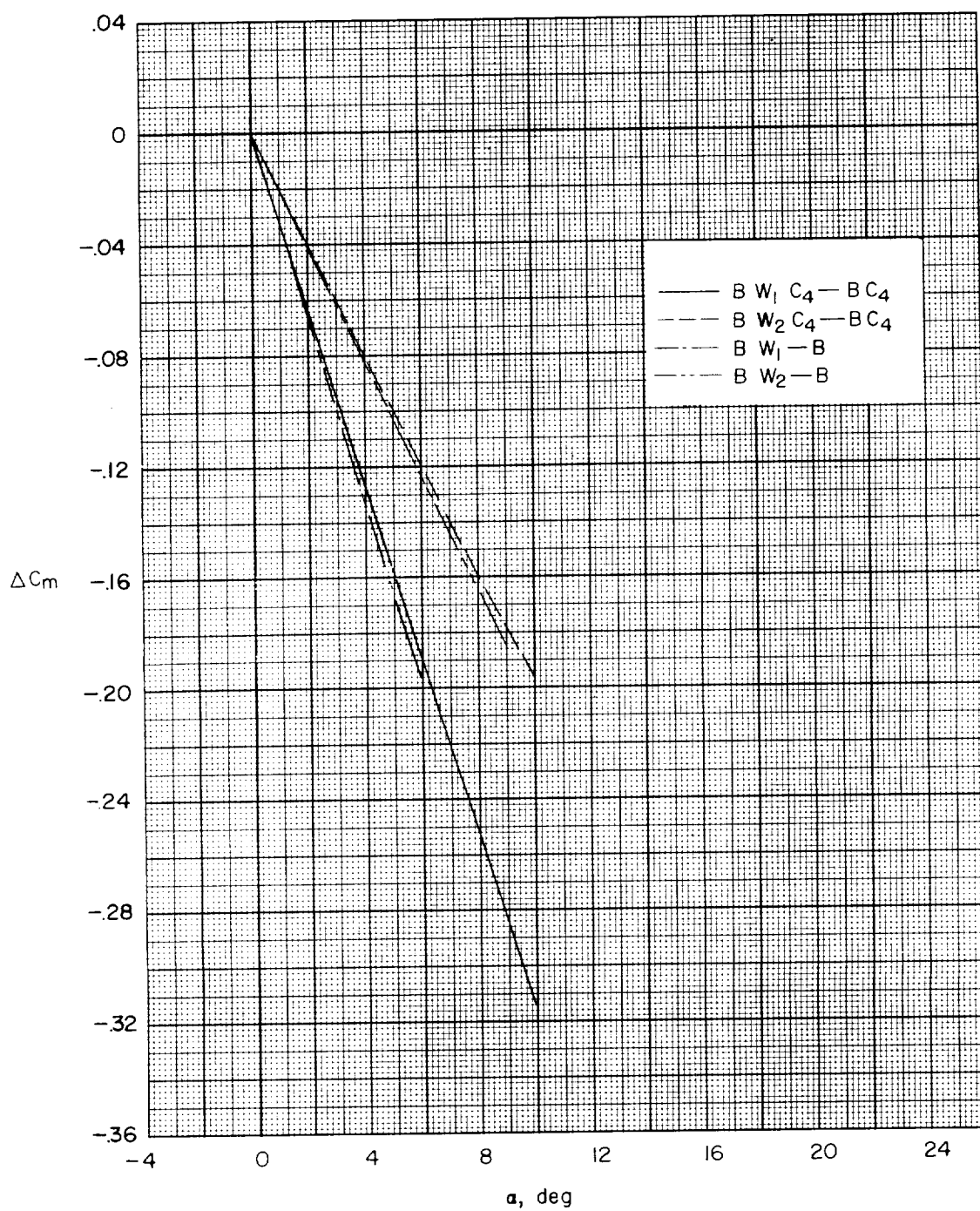
(b) Continued. M = 2.01.

Figure 8.- Continued.
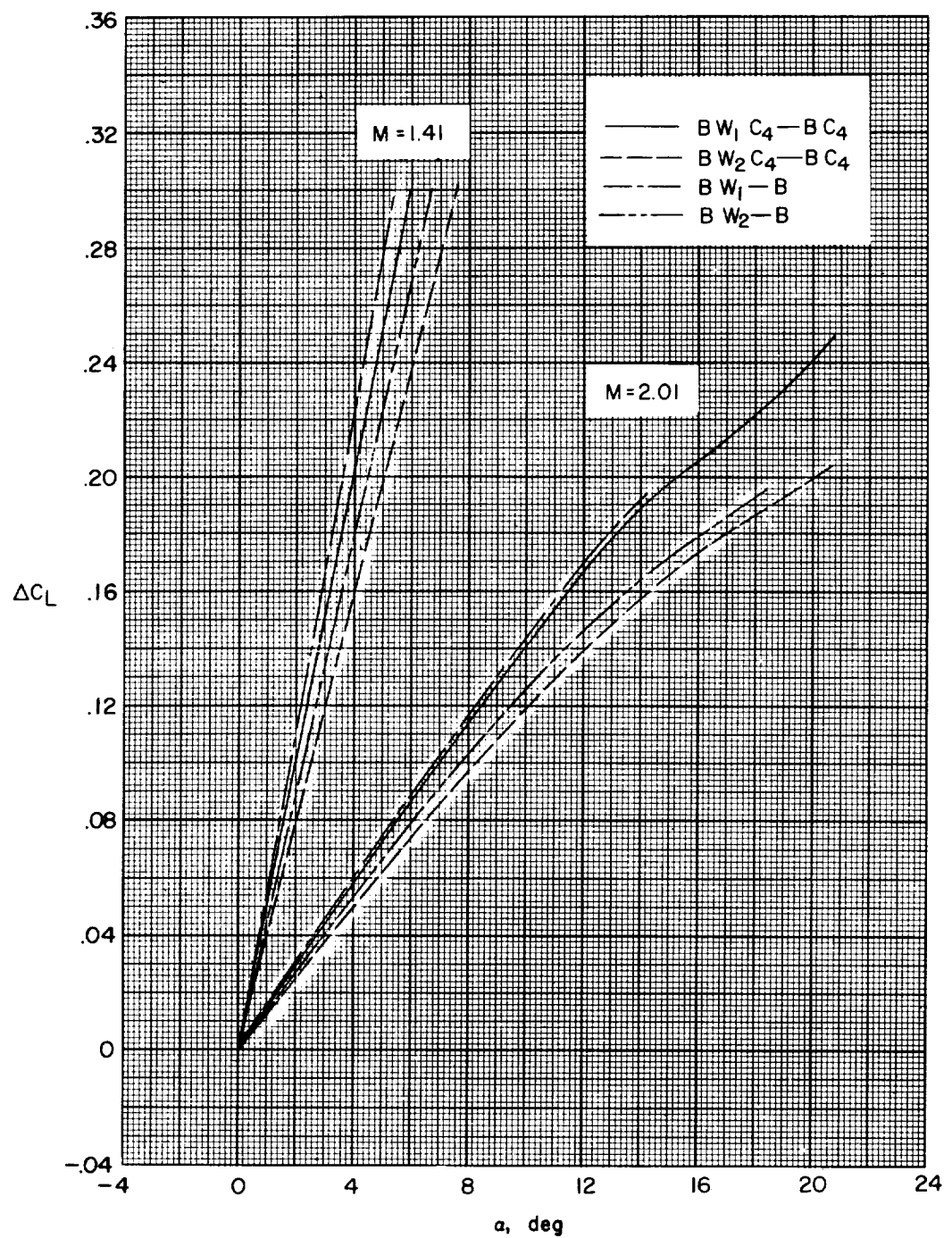
(b) Concluded.

Figure 8.- Concluded.
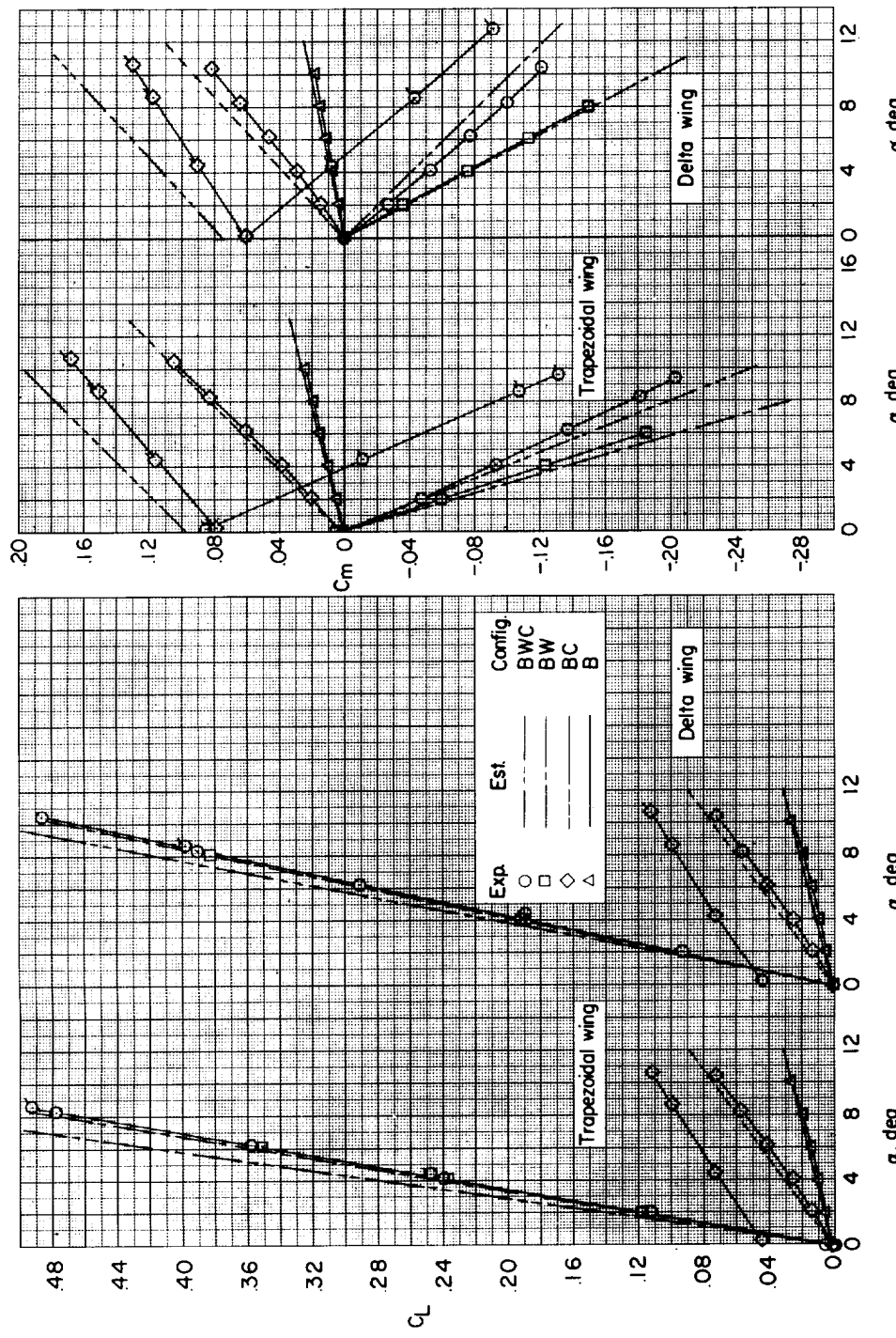
Figure 9.- The aerodynamic characteristics in pitch of various component parts of the model. (Flagged symbols denote 15° canard deflection, trailing edge down.)
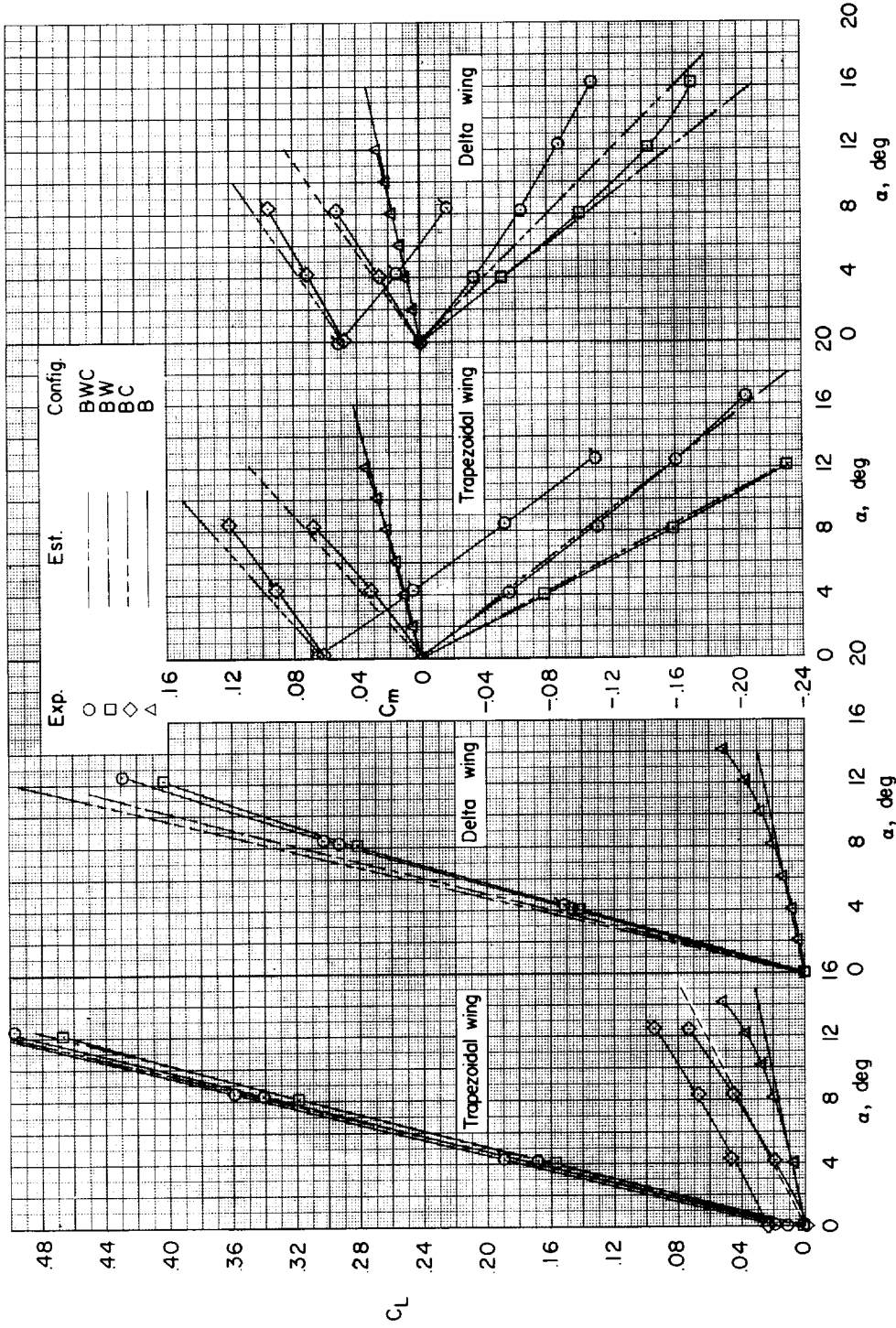
(a) M = 1.41.

(b) M = 2.01.

Figure 9.- Concluded.
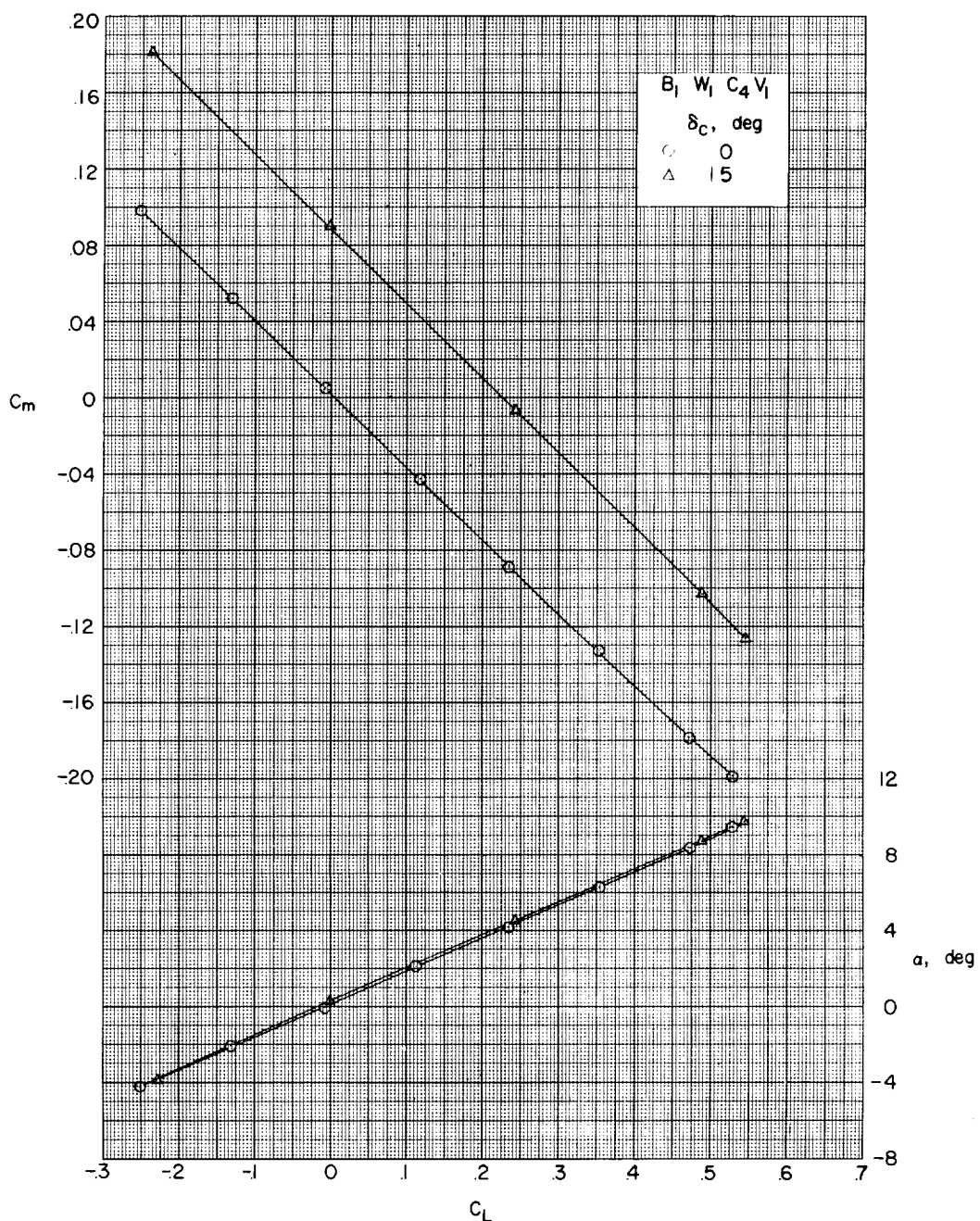
(a) M = 1.41.

Figure 10.- The aerodynamic characteristics of the trapezoidal-wing
configuration with the ventral fins removed.
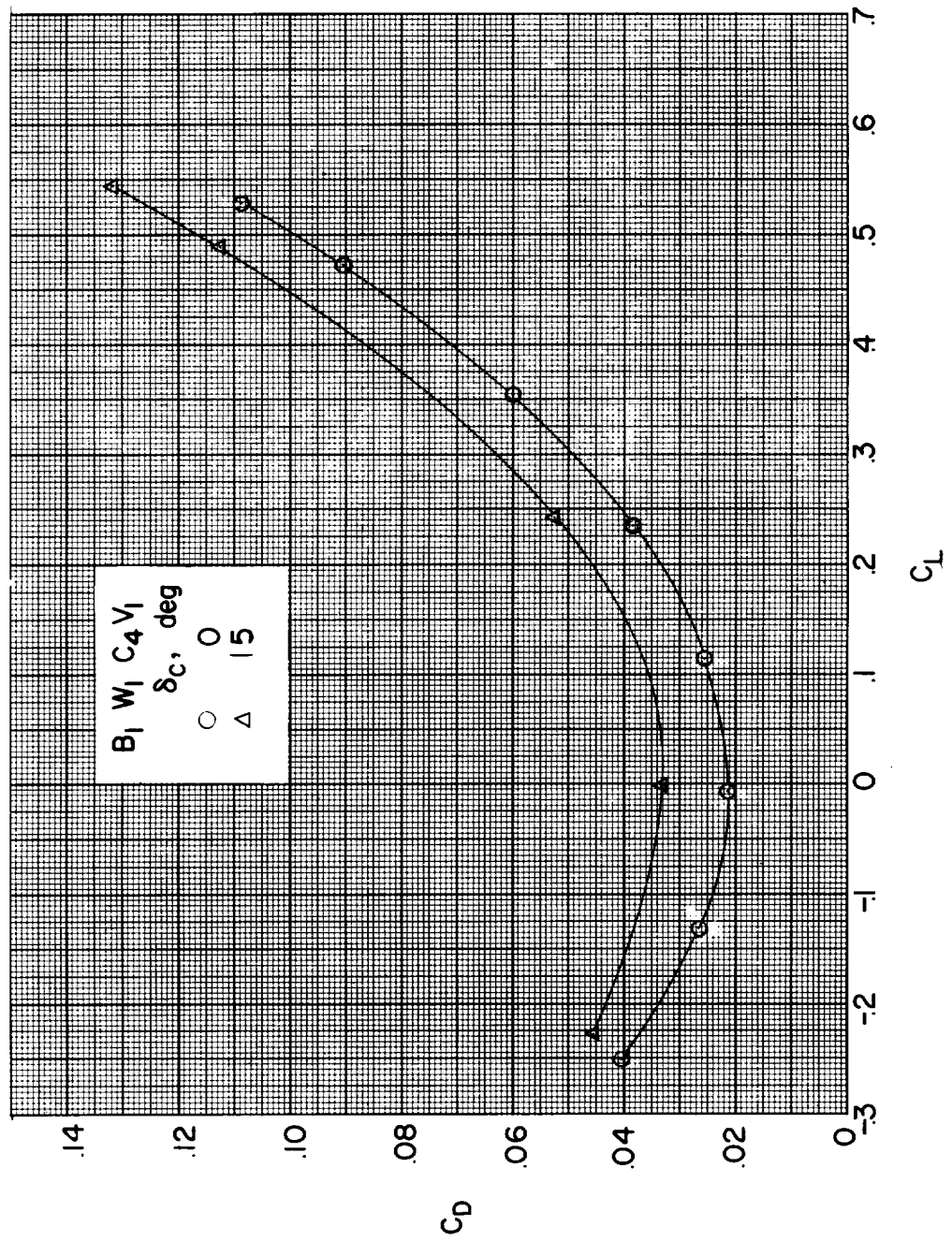
(a) Concluded.

Figure 10.- Continued.
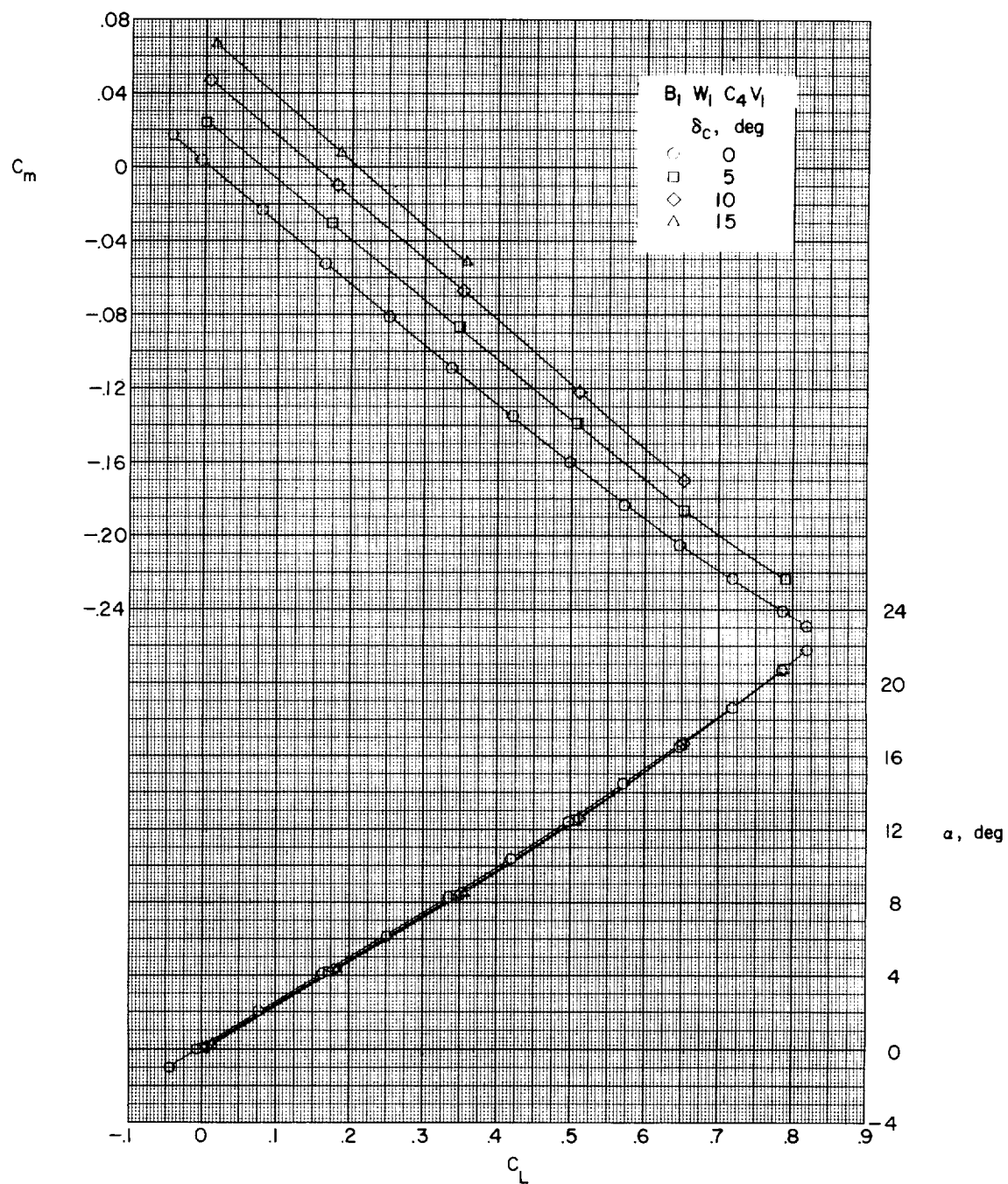
(b) M = 2.01.

Figure 10.- Continued.
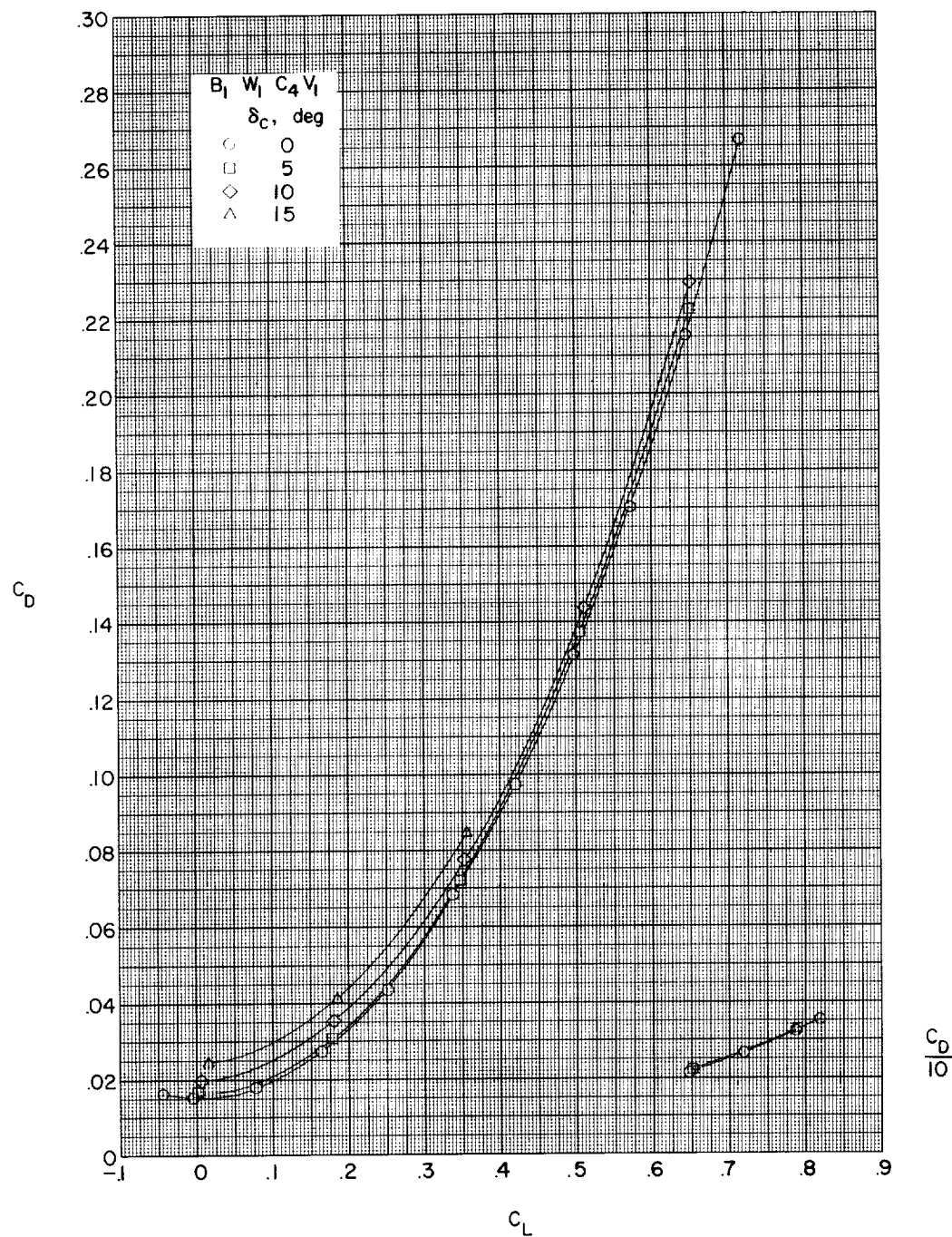
(b) Concluded.

Figure 10.- Concluded.
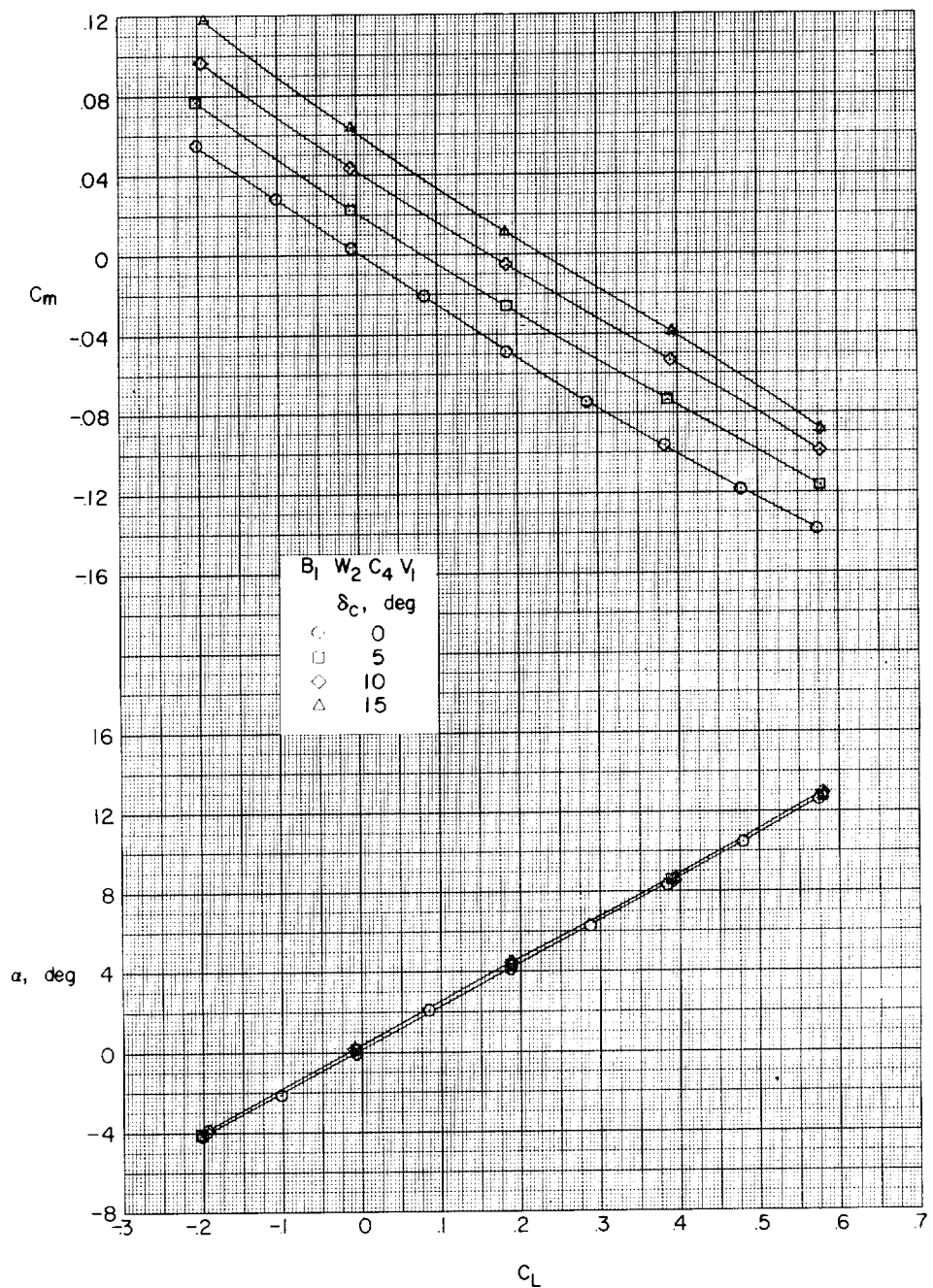
(a) M = 1.41.

Figure 11.- The aerodynamic characteristics of the delta-wing
configuration with the ventral fins removed.
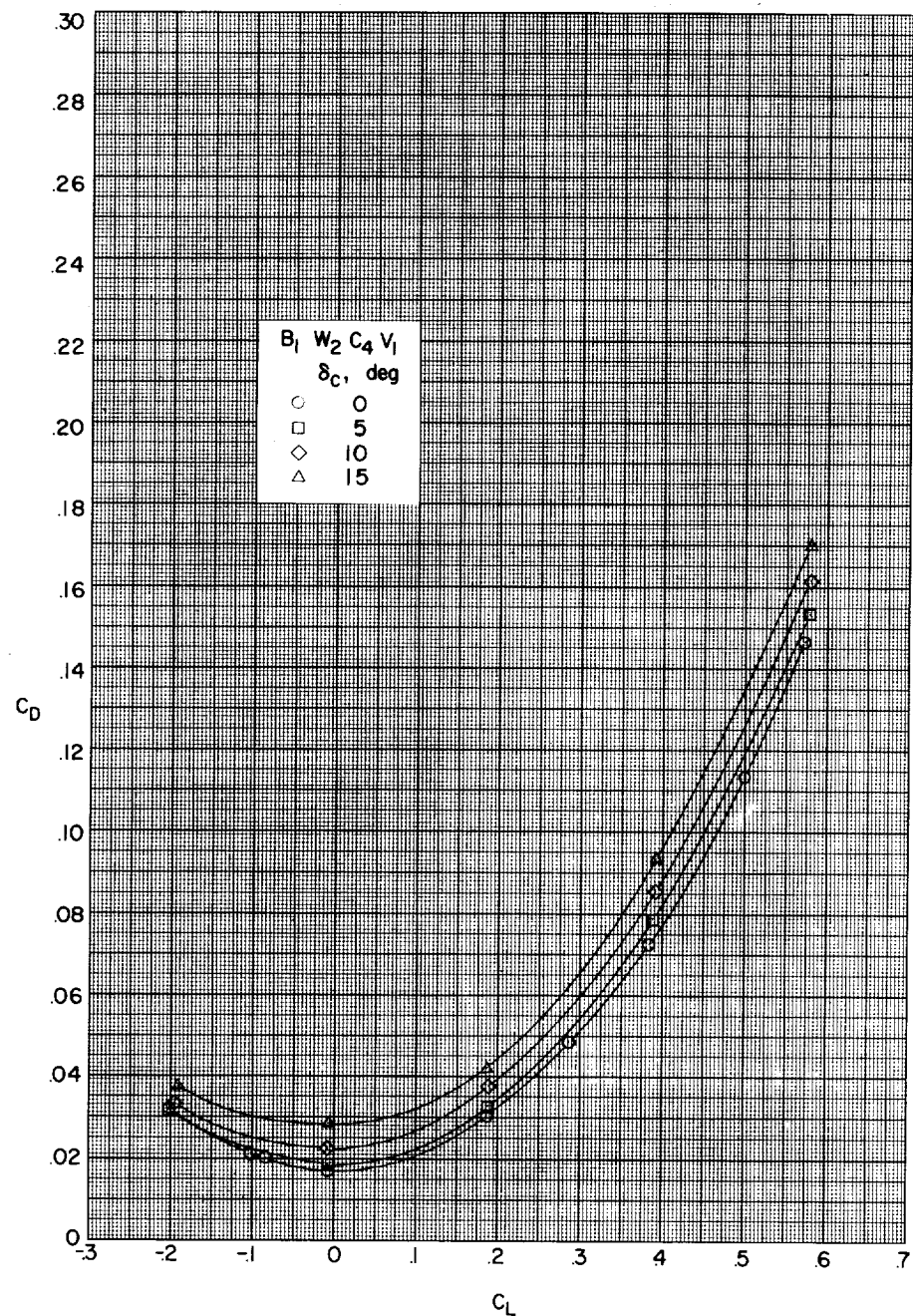
(a) Concluded.

Figure 11.- Continued.
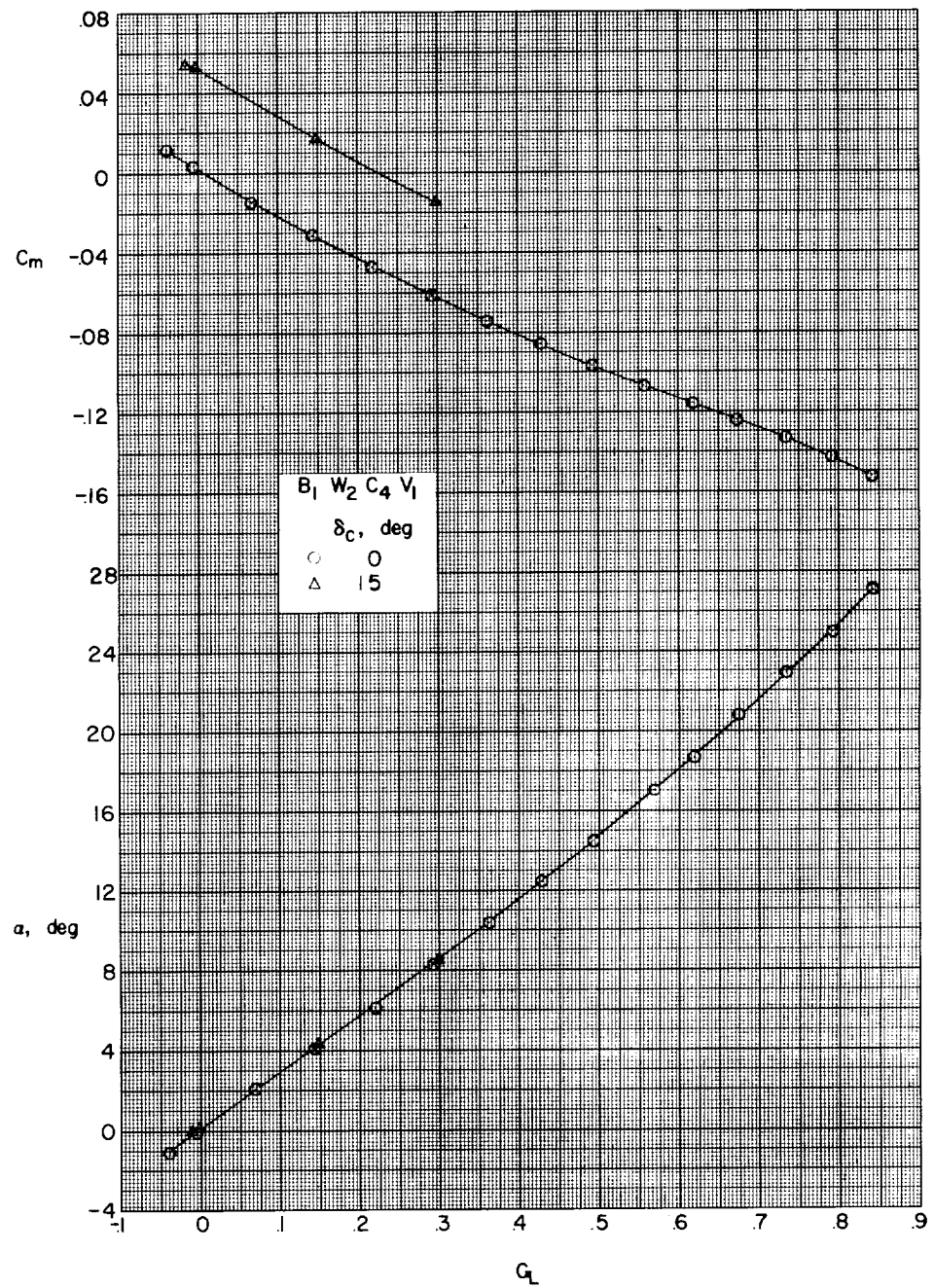
(b) M = 2.01.

Figure 11.- Continued.
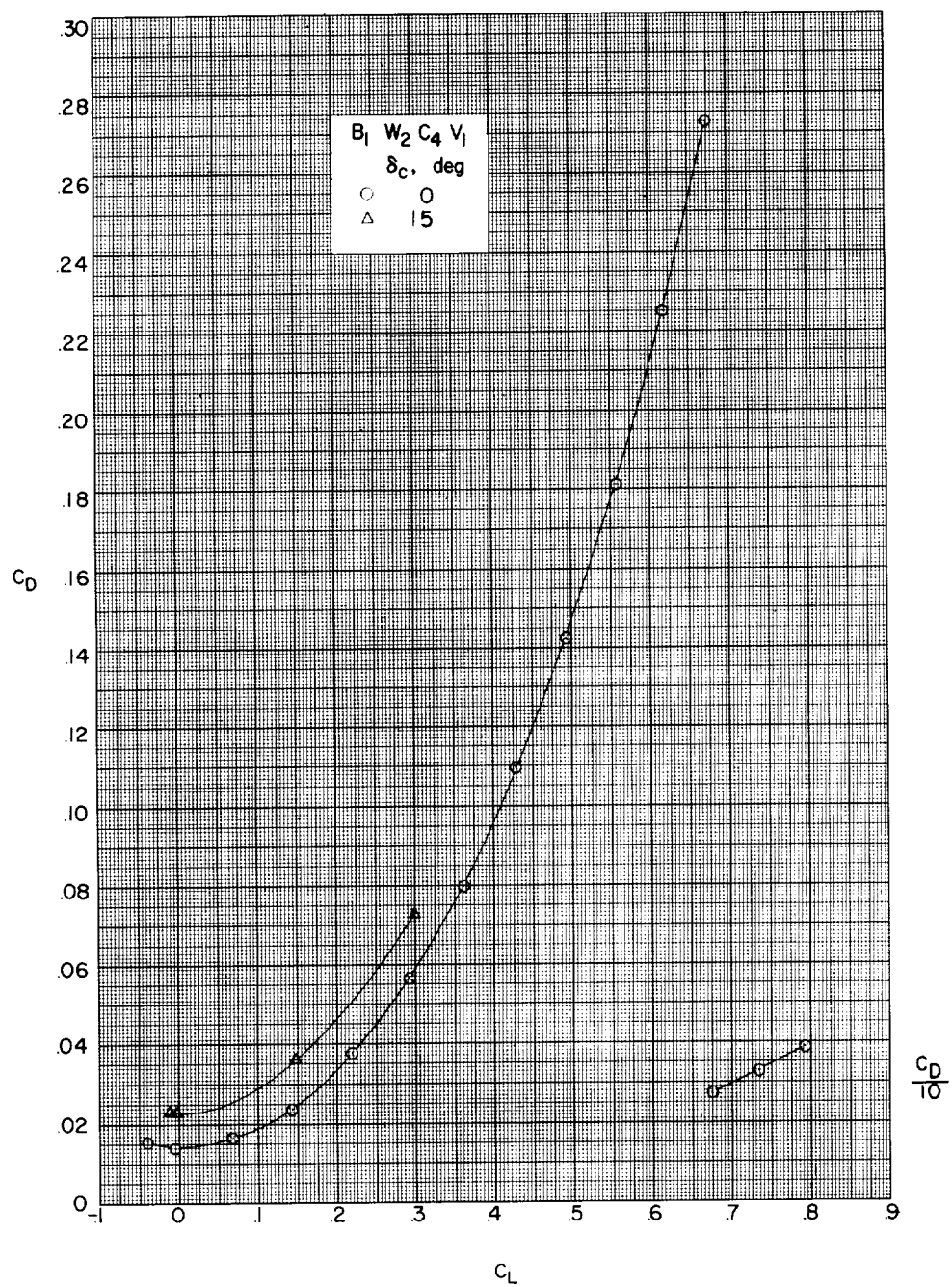
(b) Concluded.

Figure 11.- Concluded.
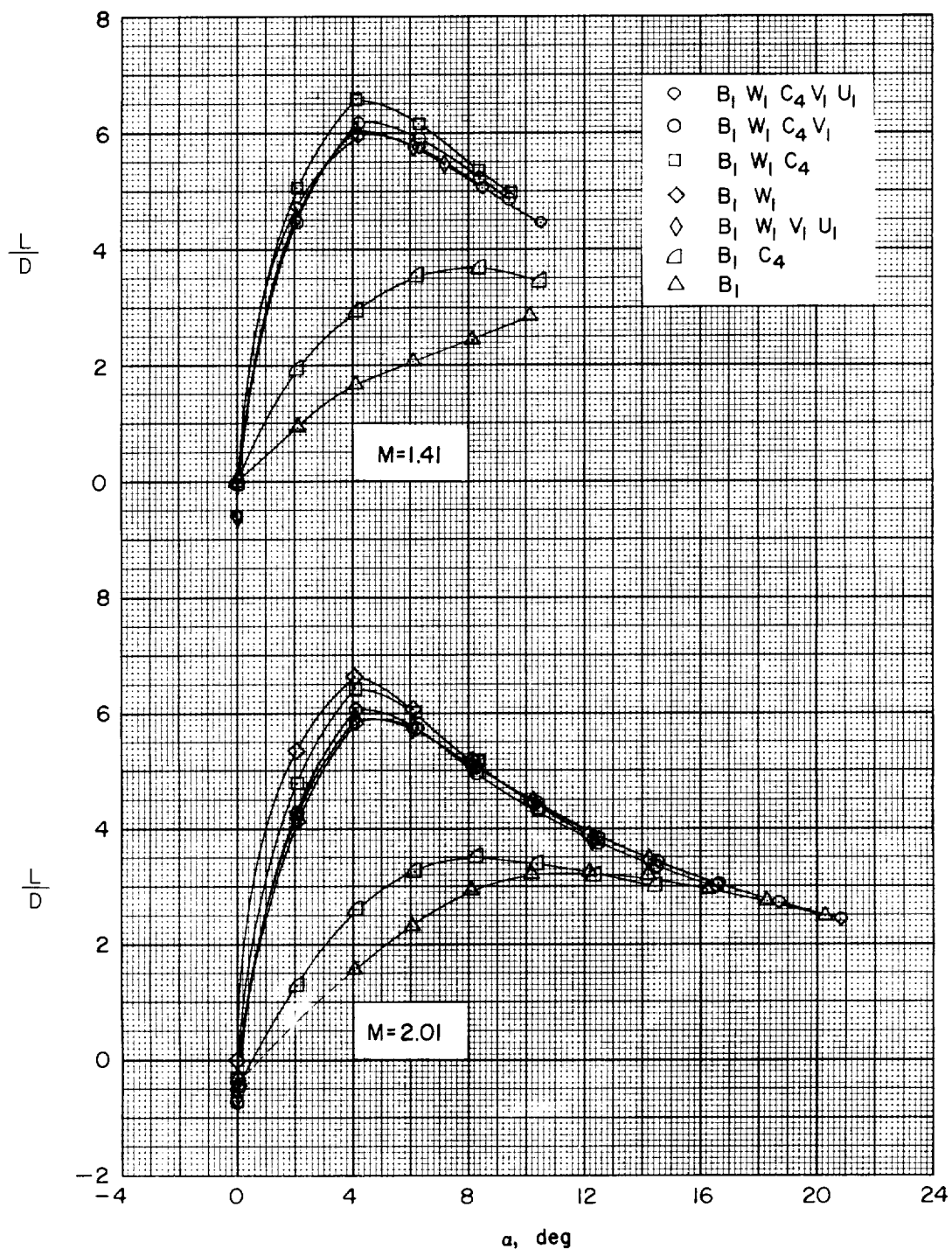
Figure 12.- Lift-drag ratios of the various component parts of the trapezoidal-wing model.
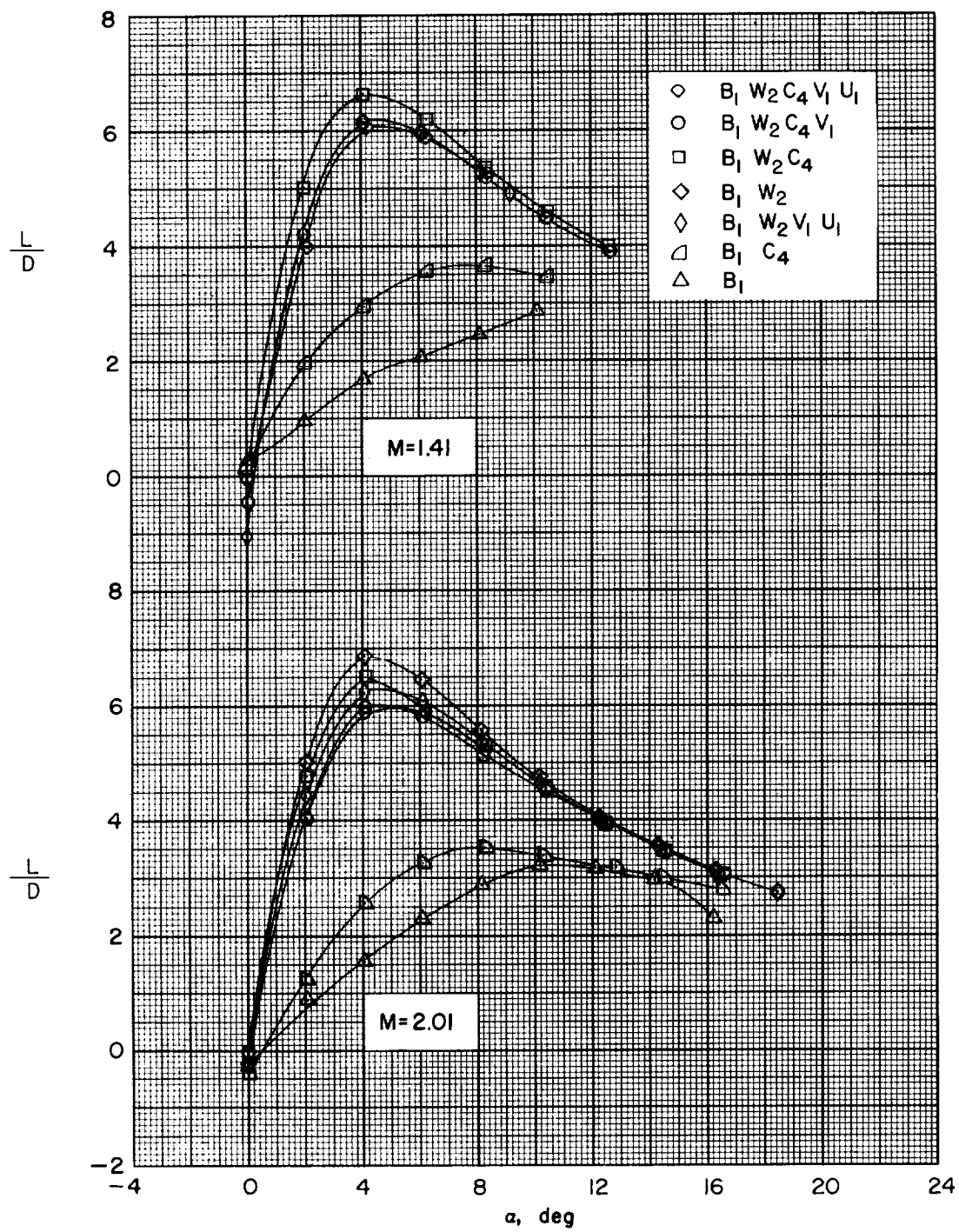
Figure 13.- Lift-drag ratios of the various component parts of the delta-wing model.
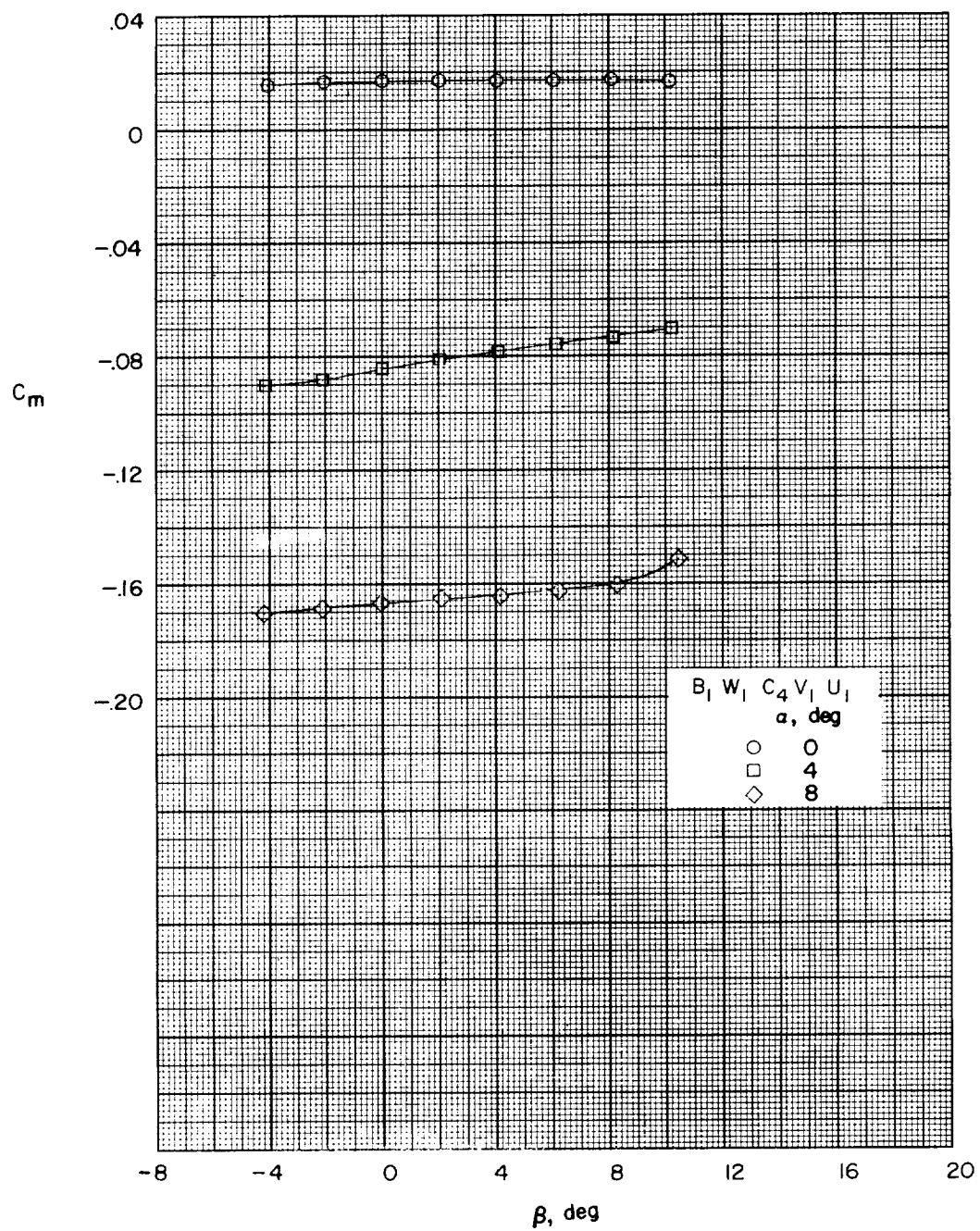
(a) M = 1.41.

Figure 14.- The variation of the longitudinal characteristics with sideslip of the trapezoidal-wing configuration.
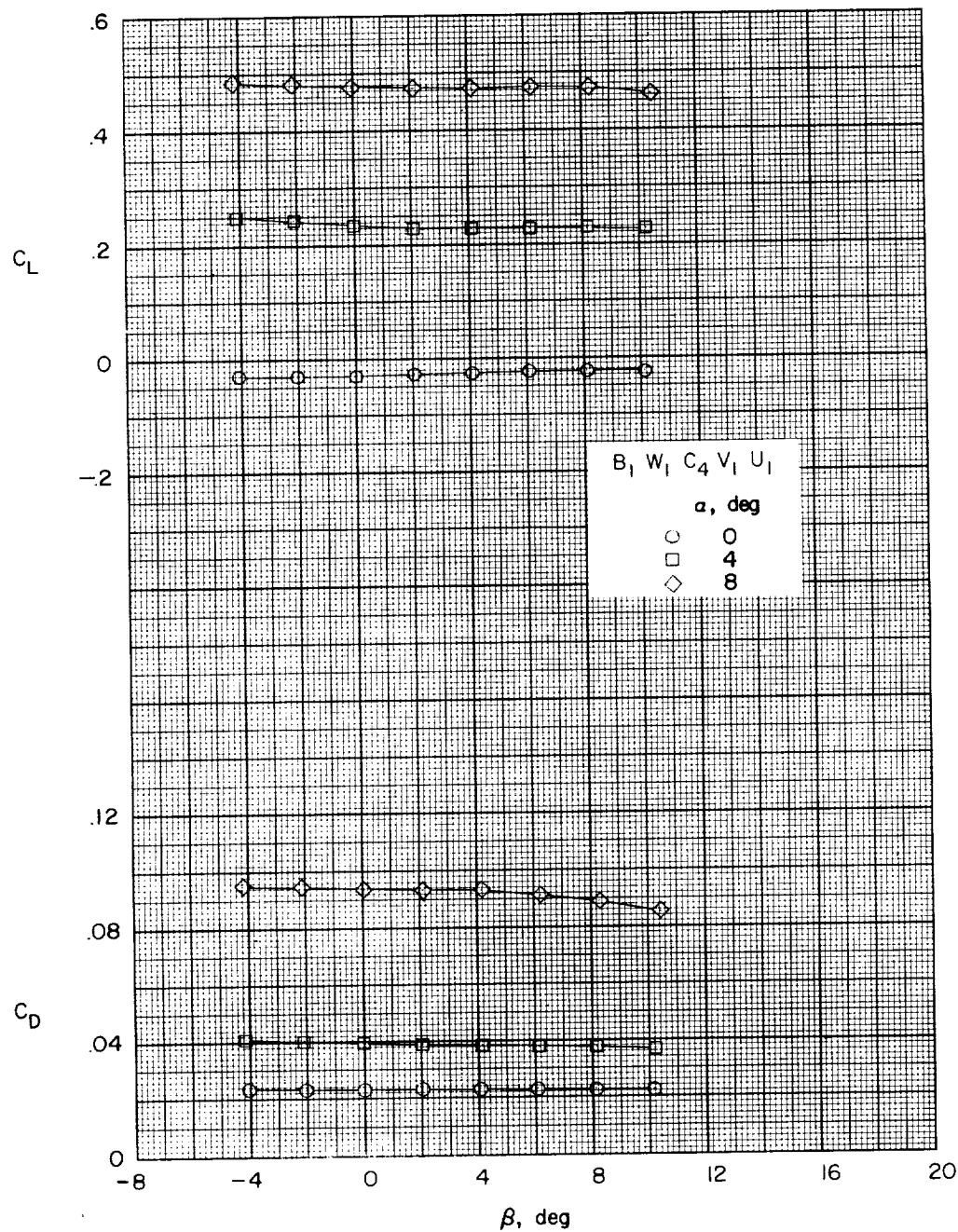
(a) Concluded.

Figure 14.- Continued.
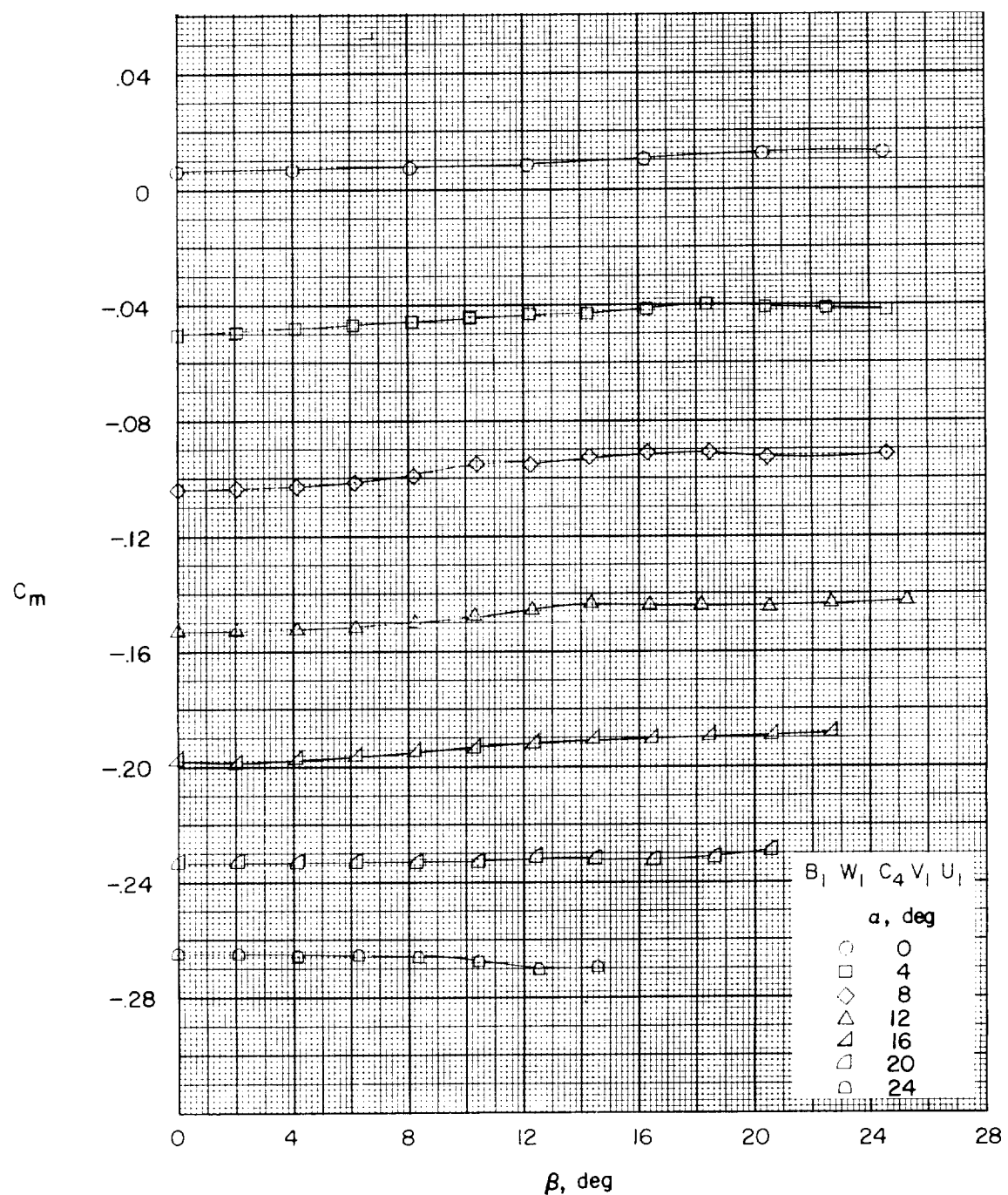
(b) M = 2.01.

Figure 14.- Continued.
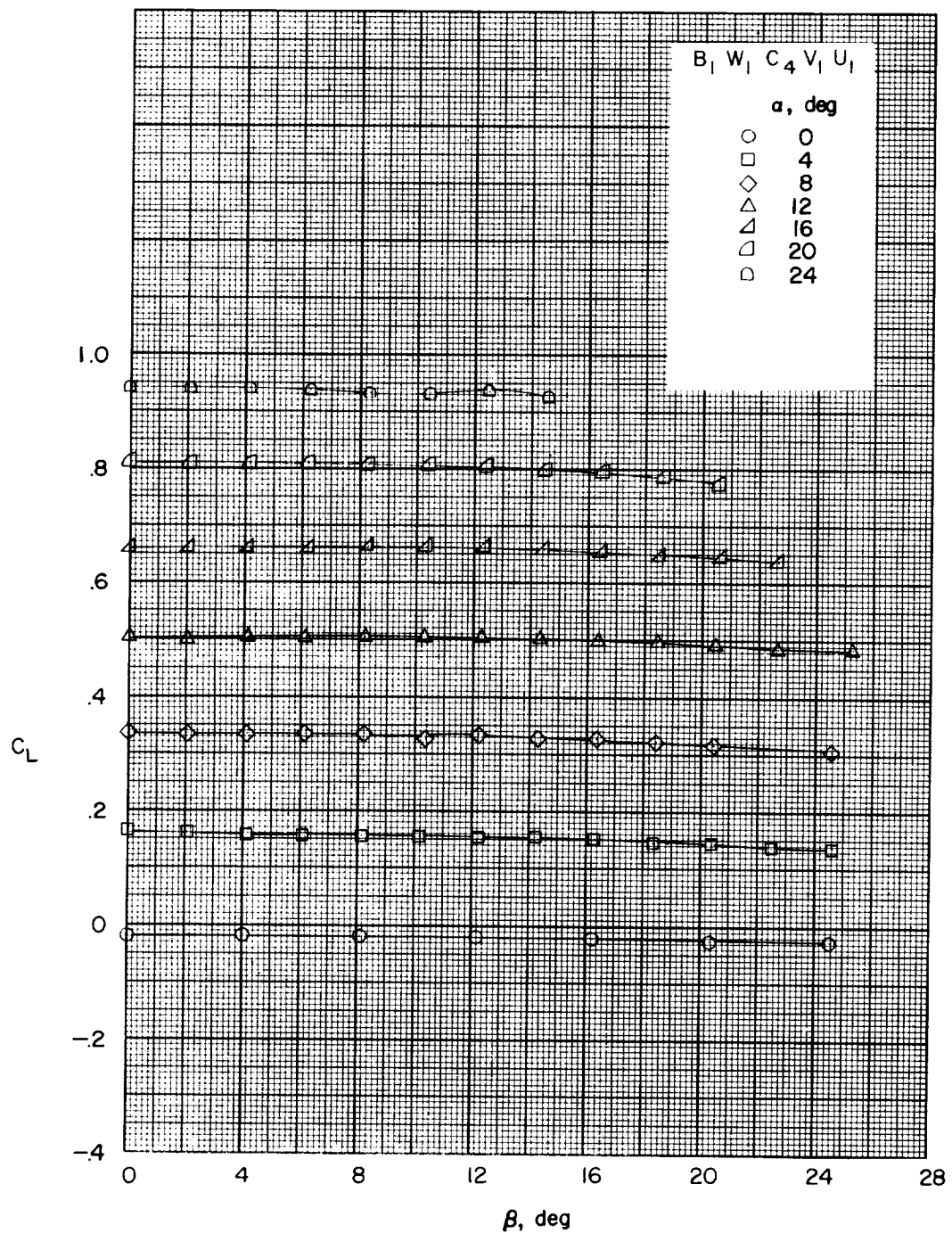
(b) Continued.

Figure 14.- Continued.
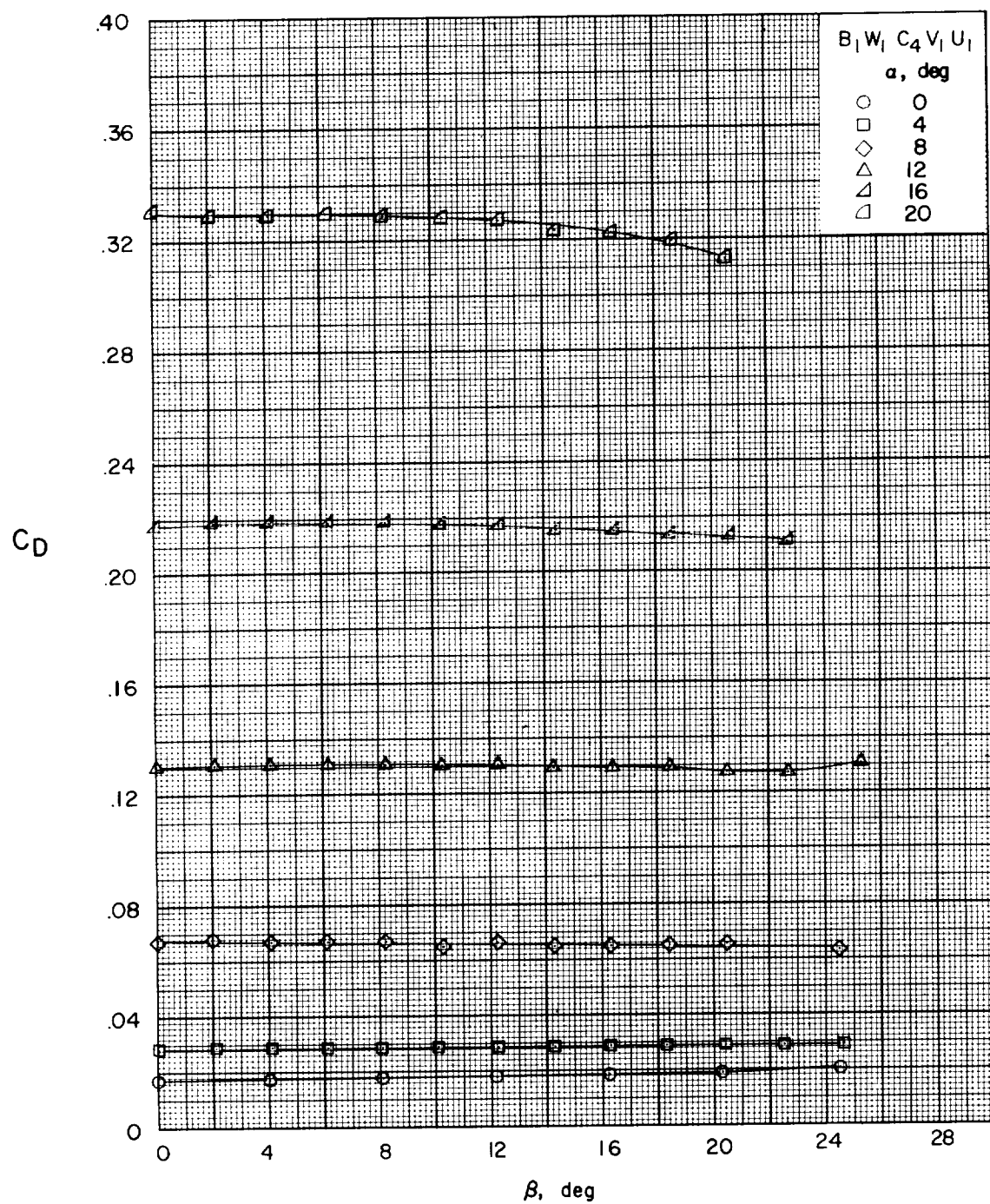
(b) Concluded.

Figure 14.- Concluded.
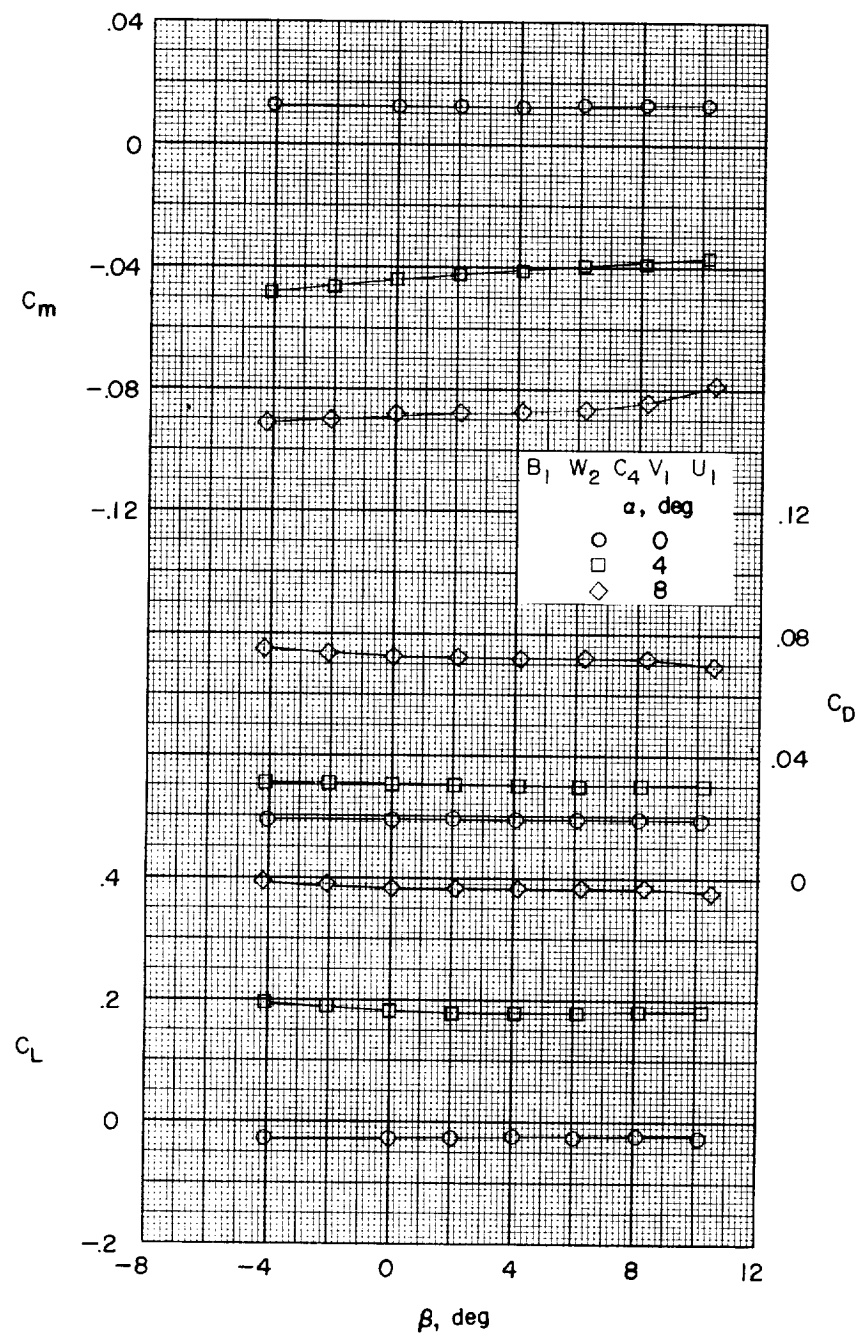
(a) M = 1.41.

Figure 15.- The variation of the longitudinal characteristics with sideslip of the delta-wing configuration.
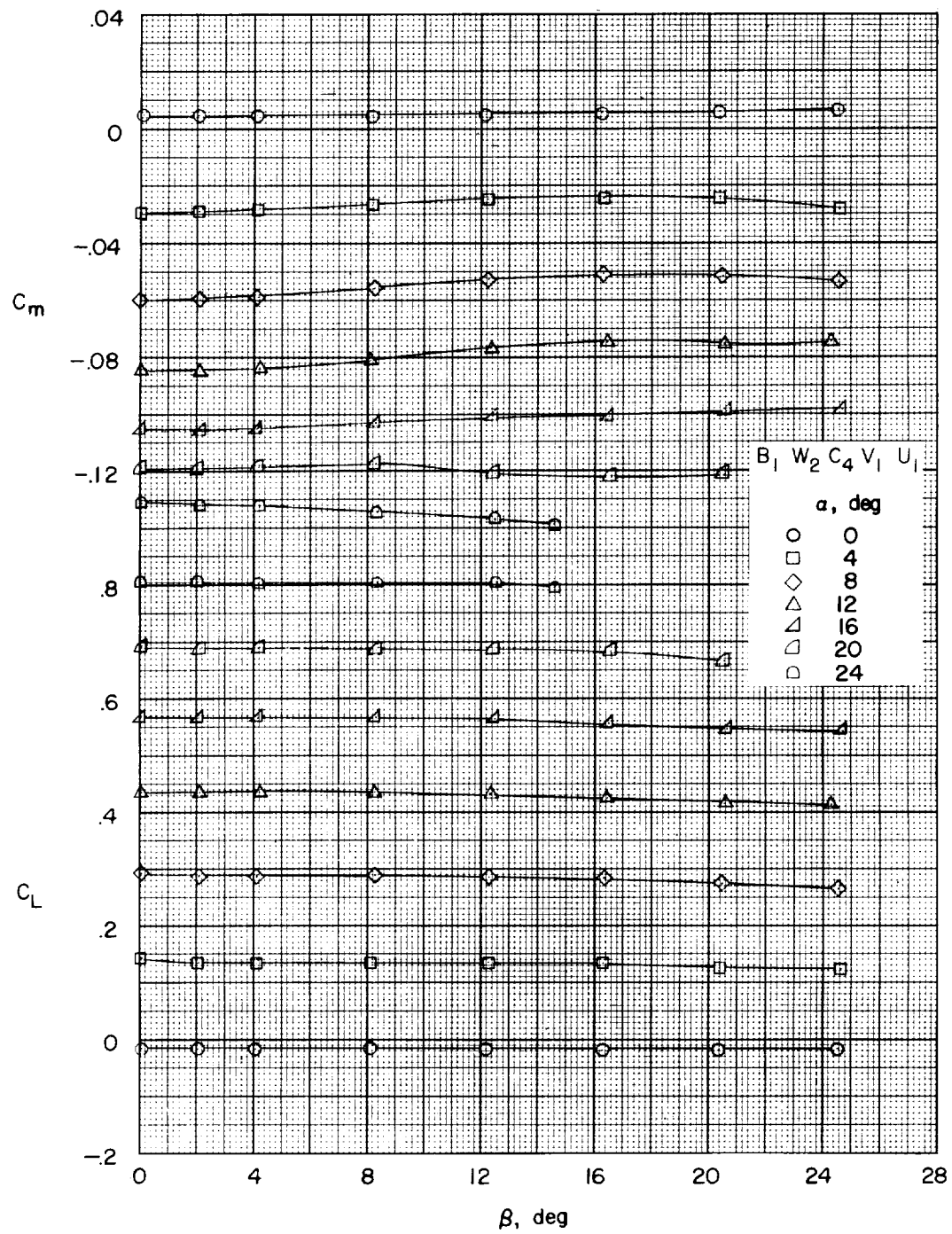
(b) M = 2.01.

Figure 15.- Continued.

58
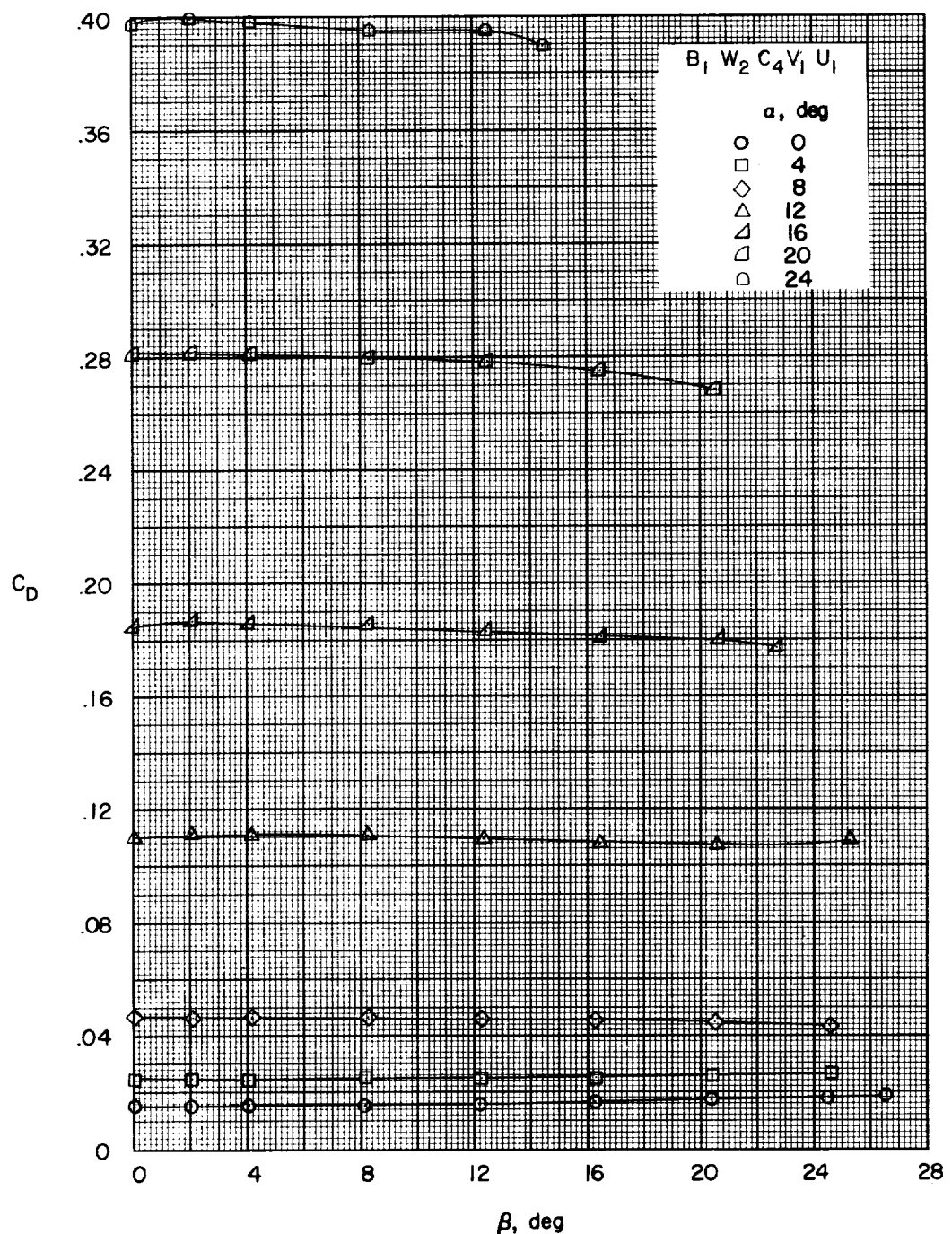
(b) Concluded.

Figure 15.- Concluded.
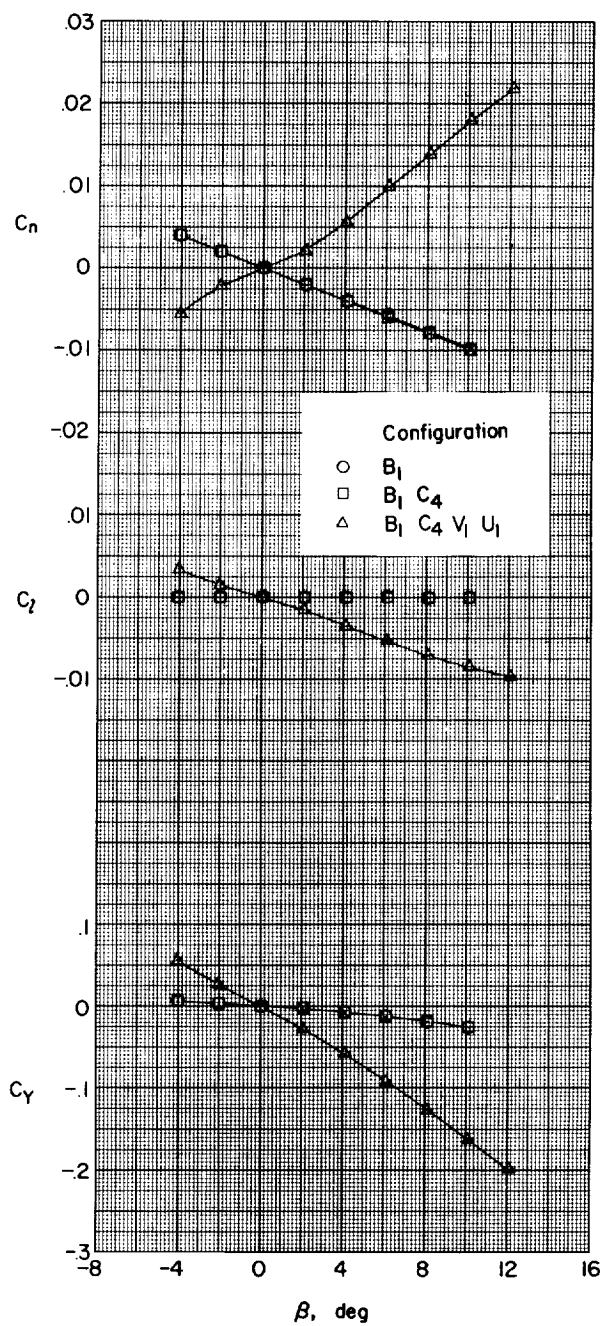
(a) α = 0°.

Figure 16.- The aerodynamic characteristics in sideslip of the trapezoidal-wing configuration. Wing off; M = 1.41.
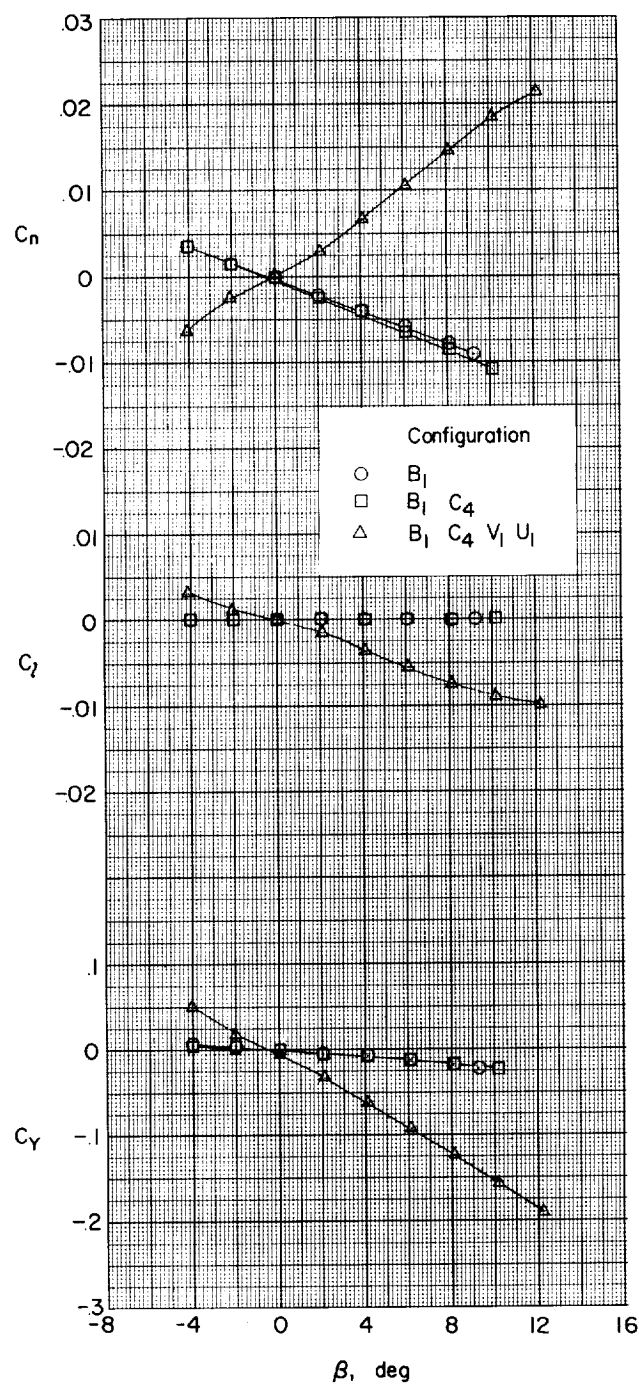
(b) $\alpha = 4.1^\circ$.

Figure 16.- Continued.
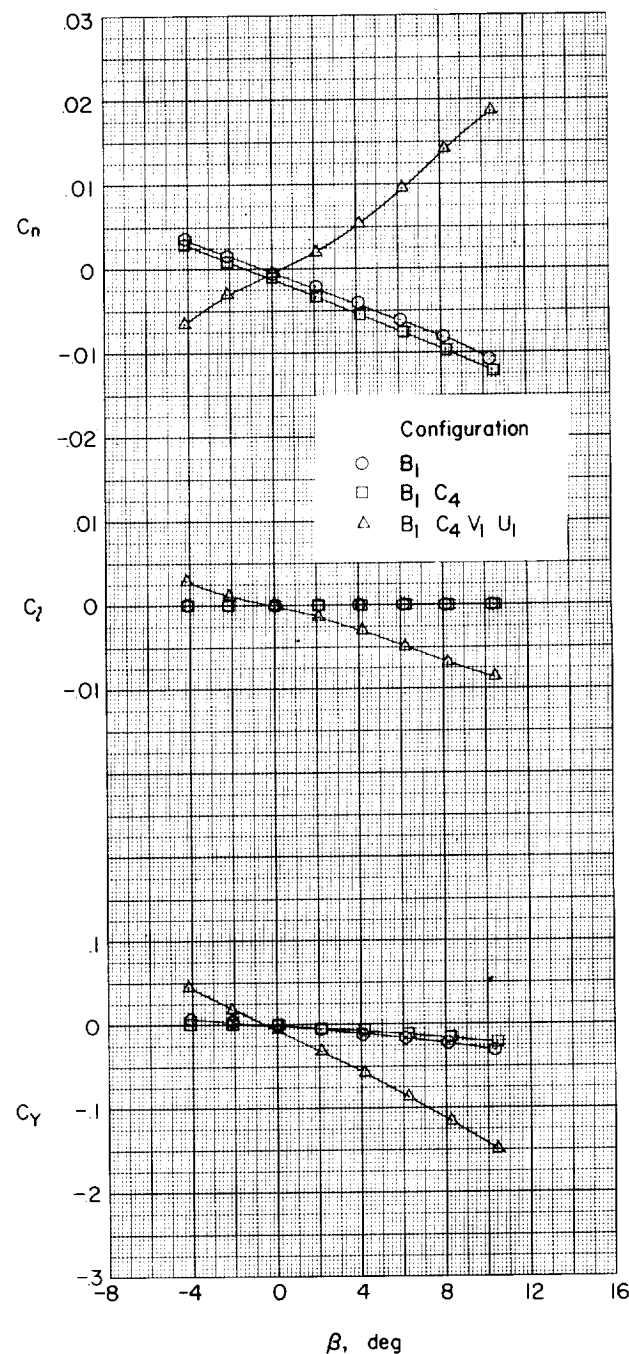
(c) $\alpha = 8.2^\circ$.

Figure 16.- Concluded.
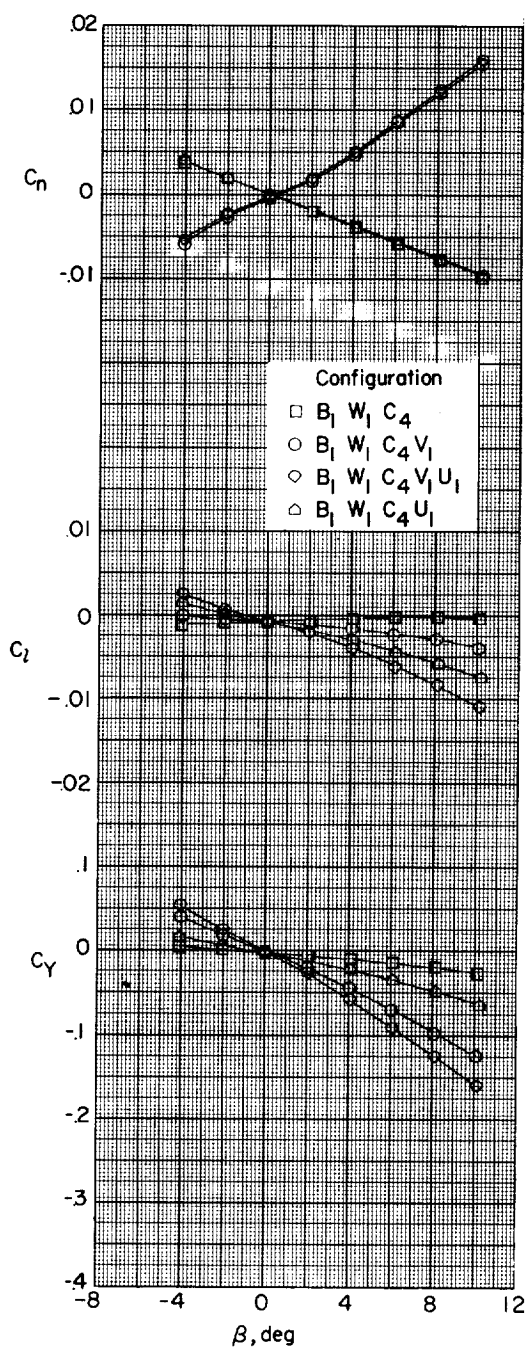
(a) $\alpha = 0^{\circ}$.

Figure 17.- The aerodynamic characteristics in sideslip of the trapezoidal-wing configuration. Wing on; M = 1.41.
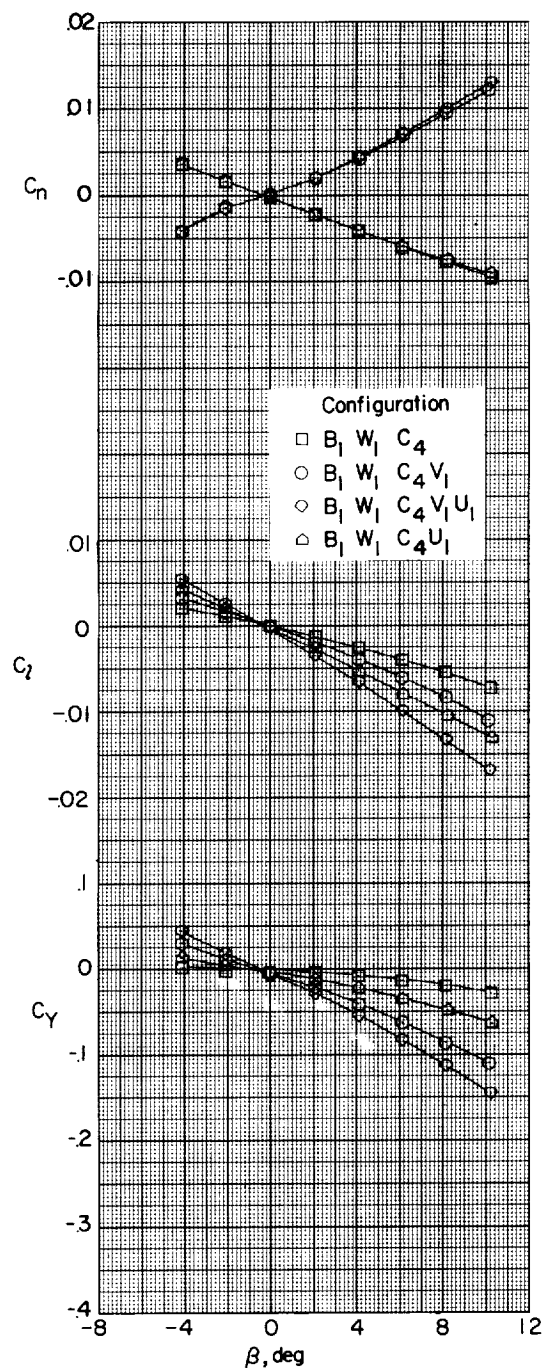
(b) $\alpha = 4.1°$.

Figure 17.- Continued.
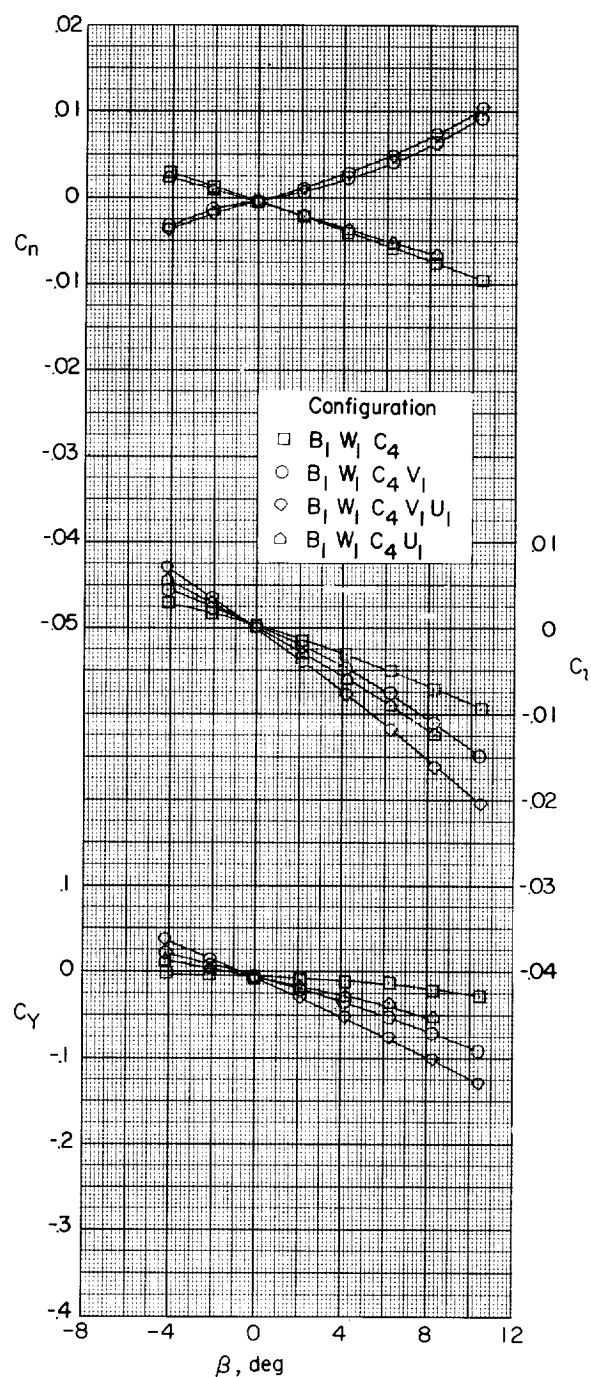
(c)   α = 8.2°.

Figure 17.- Concluded.
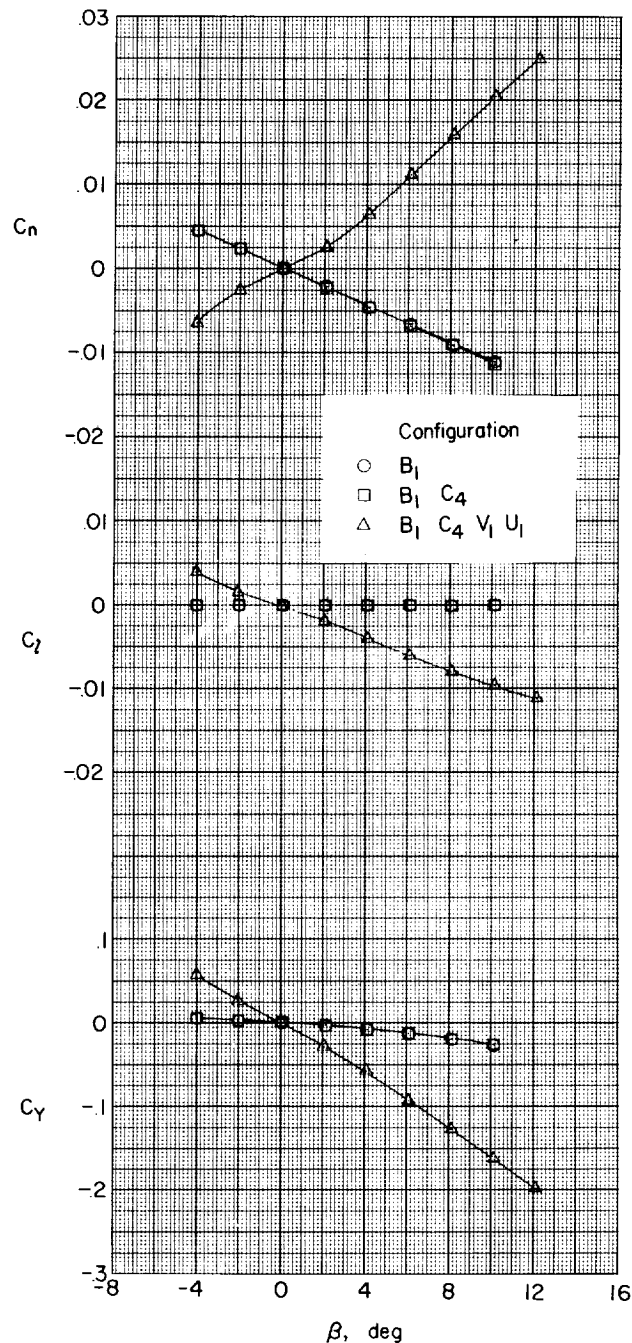
(a) α = 0°.

Figure 18.- The aerodynamic characteristics in sideslip of the delta-wing configuration. Wing off; M = 1.41.
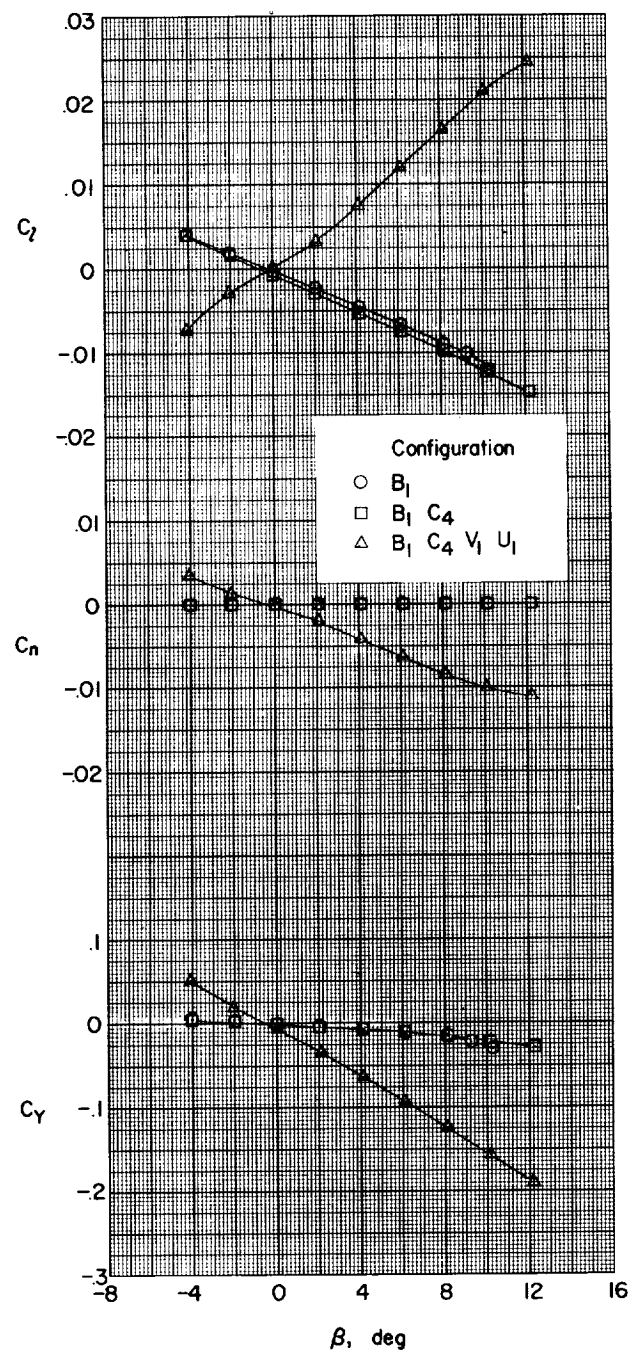
(b) $\alpha = 4.1^\circ$.

Figure 18.- Continued.
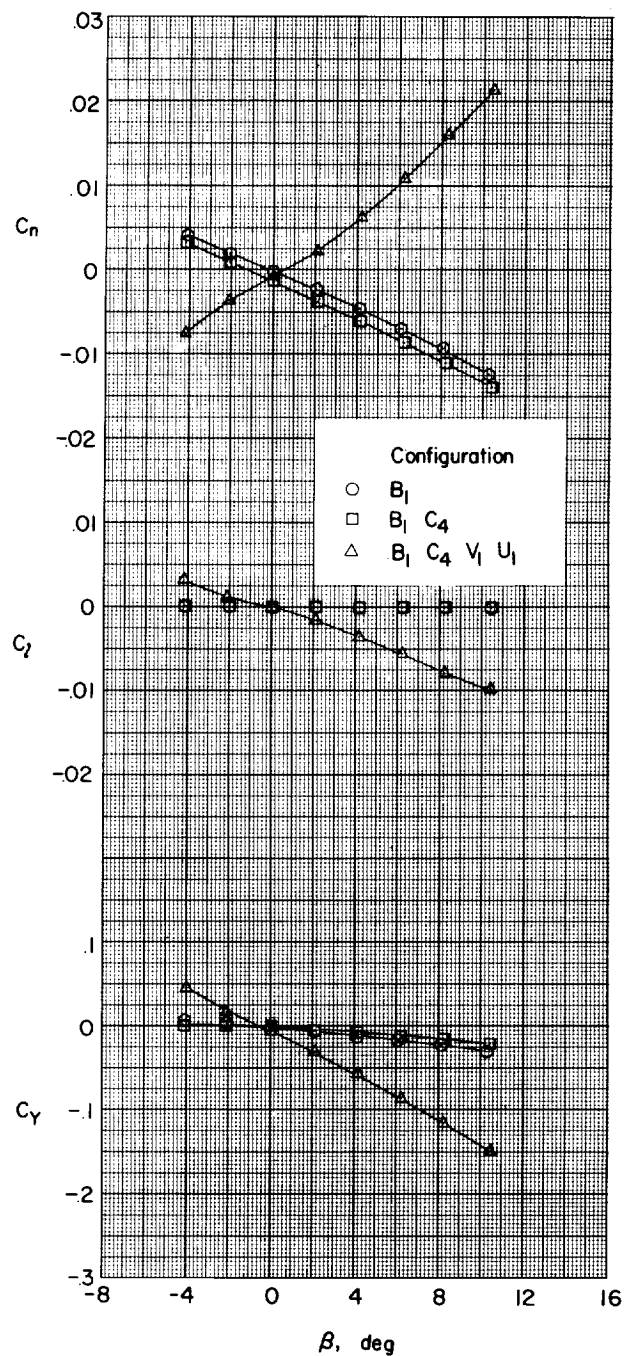
(c) $\alpha = 8.2°$.

Figure 18.- Concluded.

68
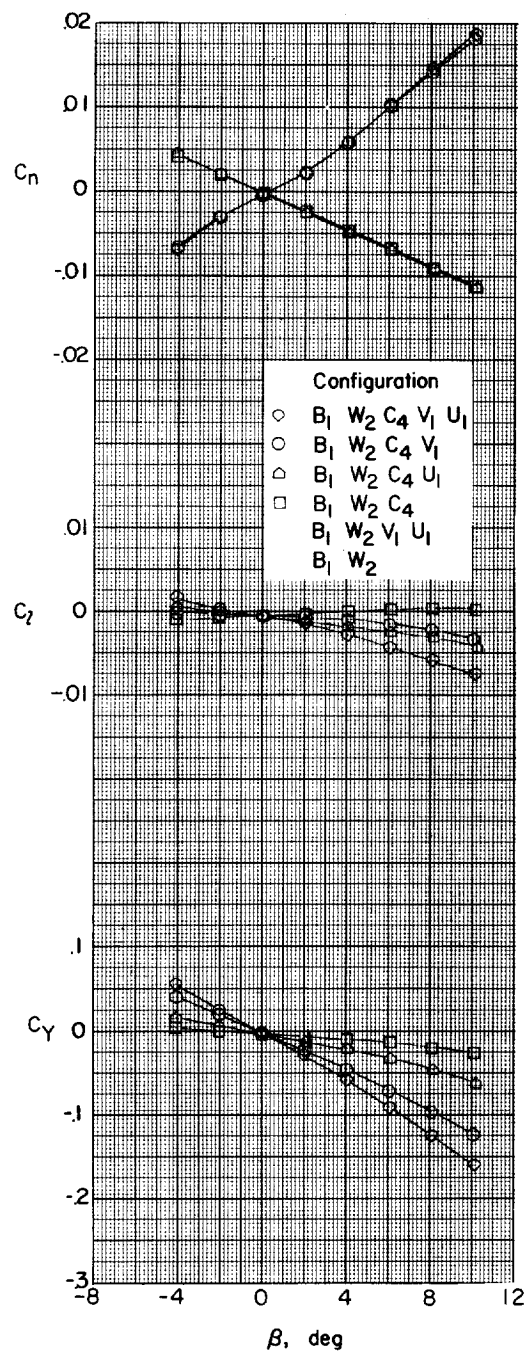
(a) $\alpha = 0^{\circ}$.

Figure 19.- The aerodynamic characteristics in sideslip of the delta-wing configuration. Wing on; M = 1.41.
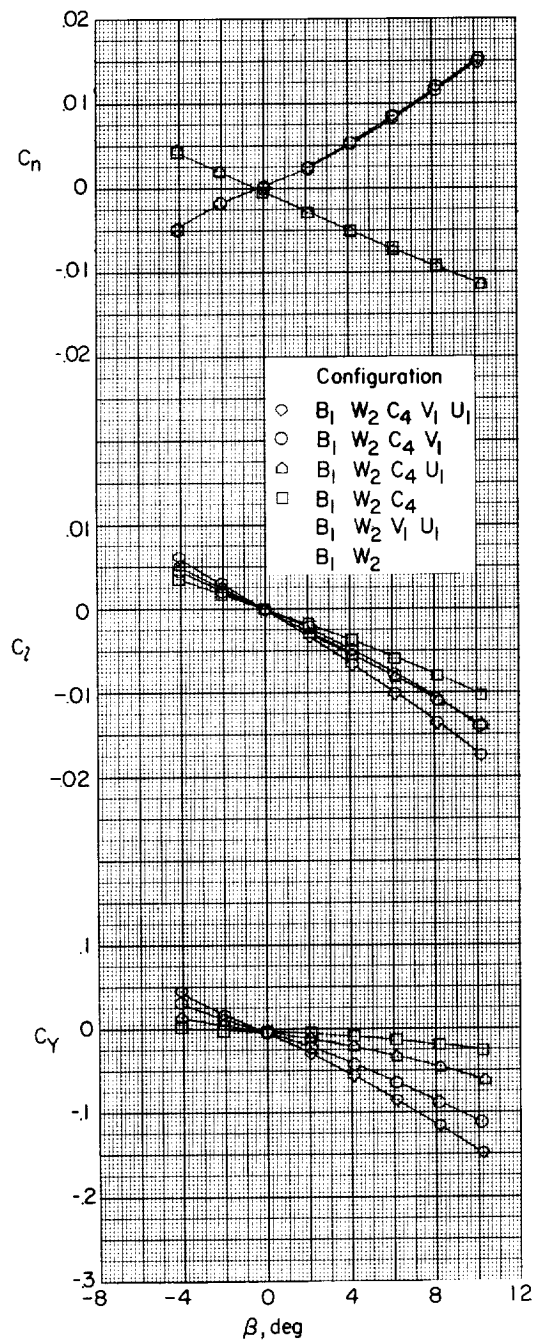
(b) $\alpha = 4.1^{\circ}$.

Figure 19.- Continued.

Cn

.02

.01

0

-.01

-.02

Configuration
◇ B₁ W₂ C₄ V₁ U₁
○ B₁ W₂ C₄ V₁
△ B₁ W₂ C₄ U₁
□ B₁ W₂ C₄
   B₁ W₂ V₁ U₁
   B₁ W₂

.01

0

Cₗ -.01

-.02

-.03

.1

0

Cʏ -.1

-.2

-.3

-8   -4   0   4   8   12

β, deg
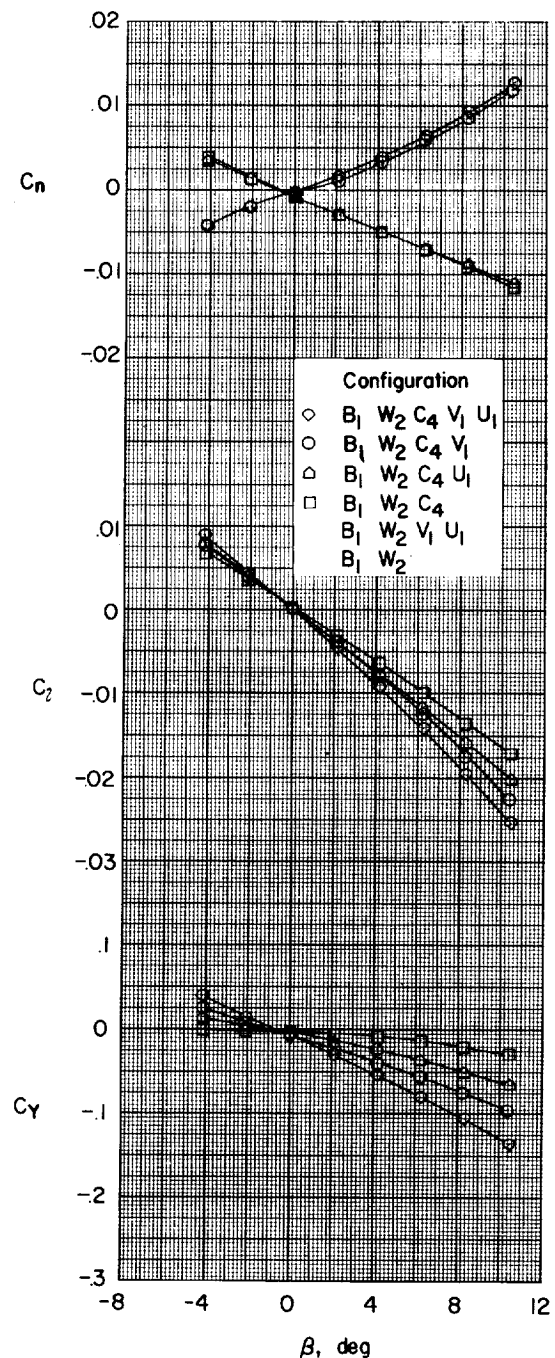
(c) $\alpha = 8.2°$.

Figure 19.- Concluded.
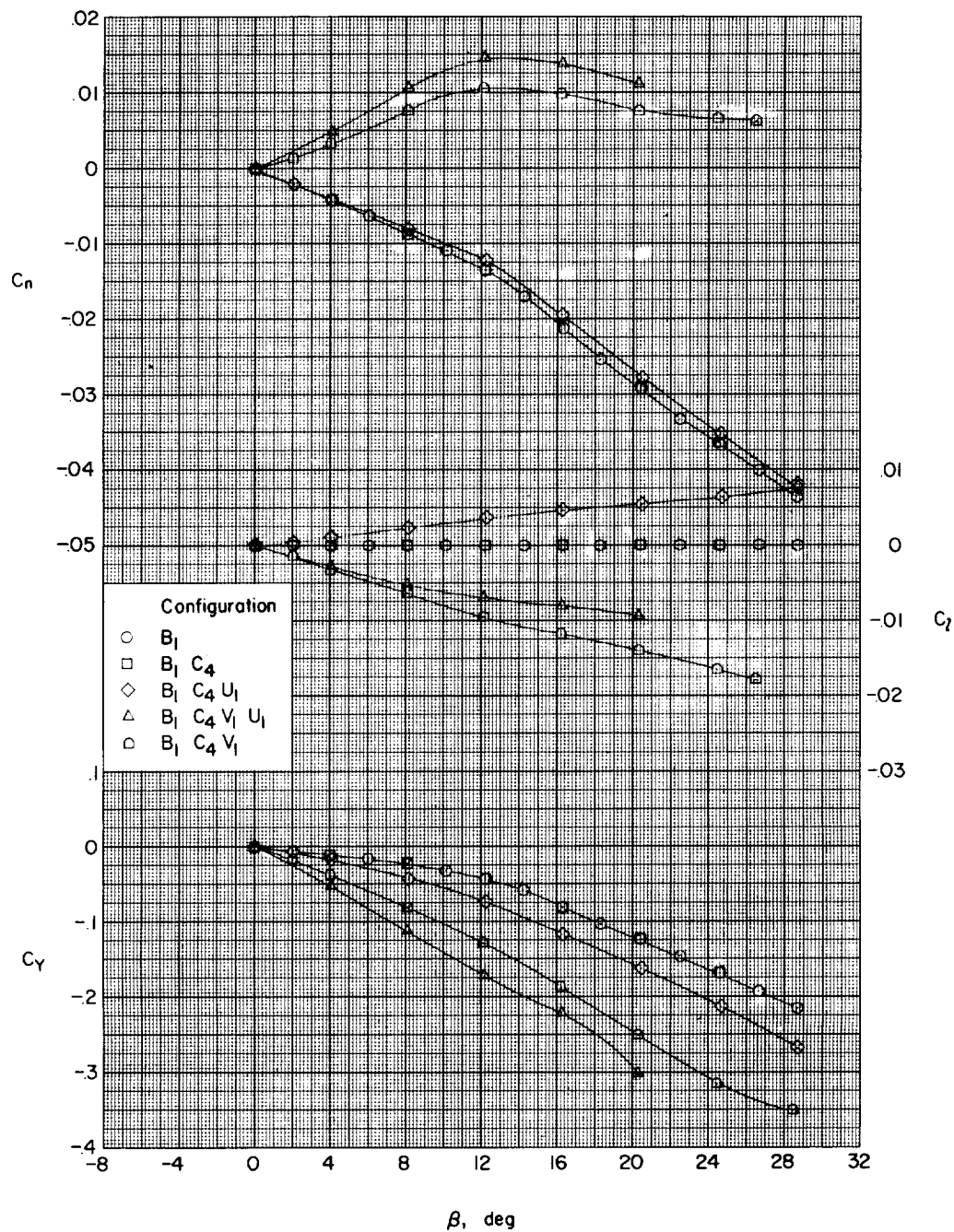
(a) α = 0°.

Figure 20.- The aerodynamic characteristics in sideslip of the
trapezoidal-wing configuration. Wing off; M = 2.01.
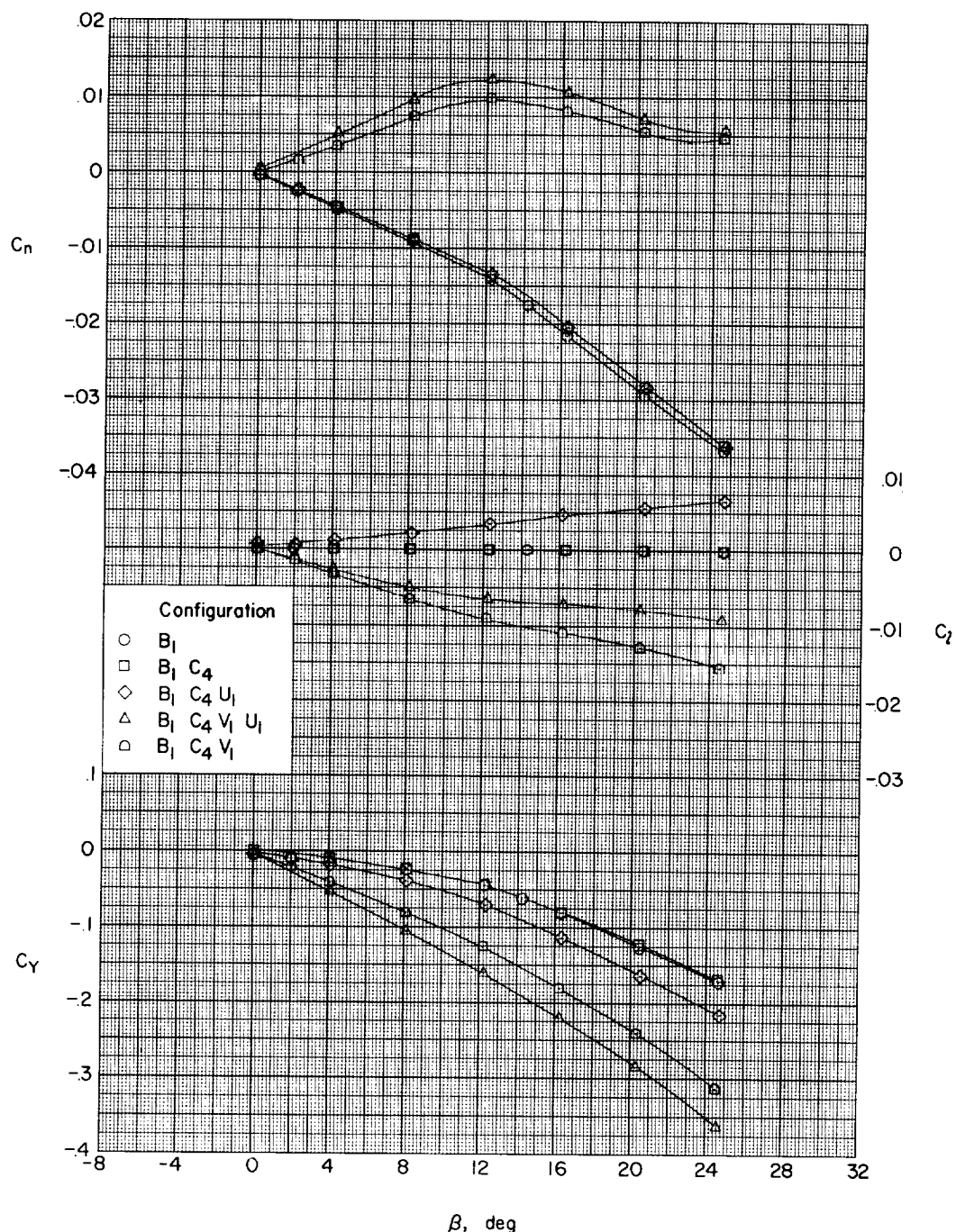
(b) $\alpha = 4.2^\circ$.

Figure 20.- Continued.
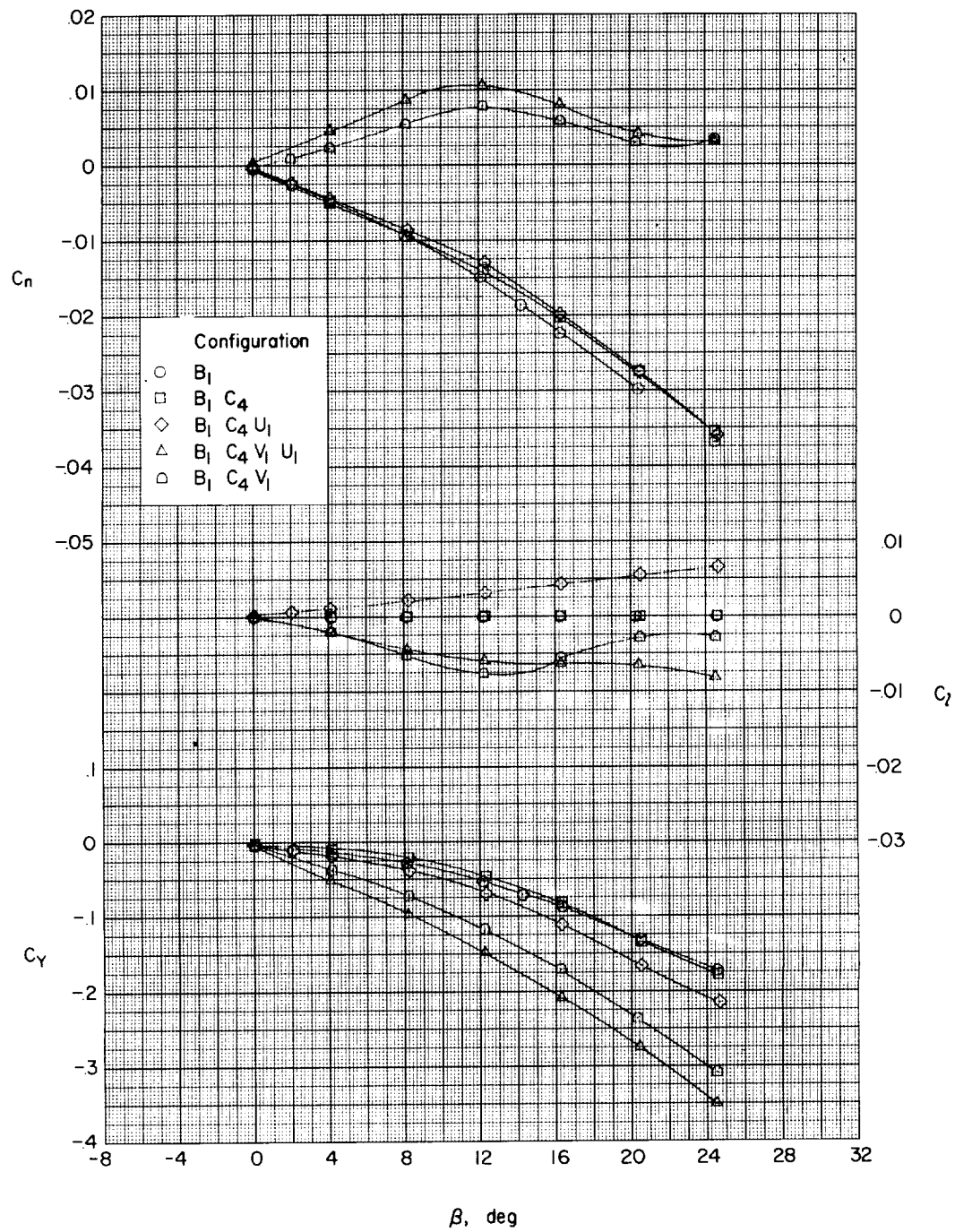
(c) $\alpha = 8.3^{\circ}$.

Figure 20.- Continued.
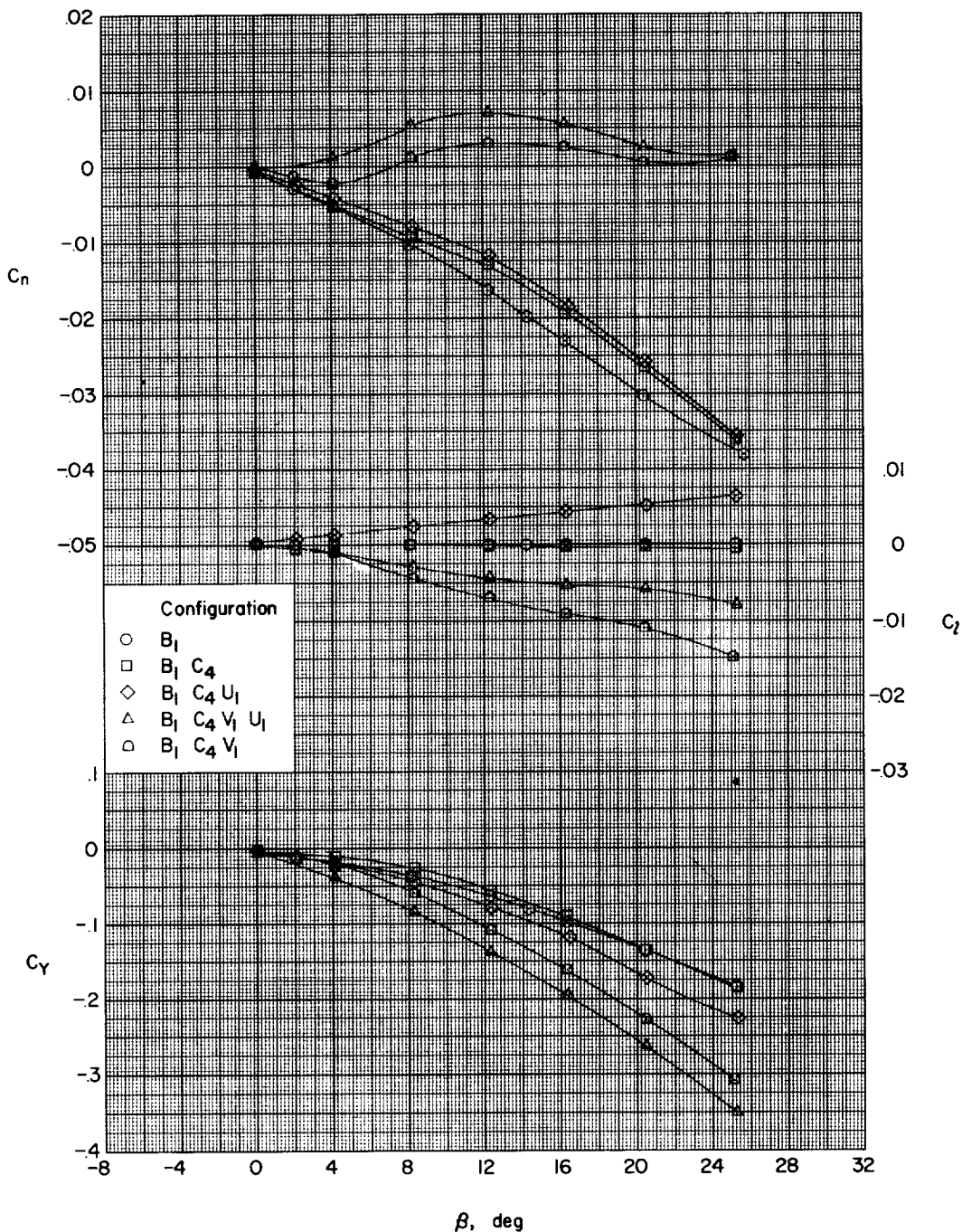
(d) $\alpha = 12.4°$.

Figure 20.- Continued.
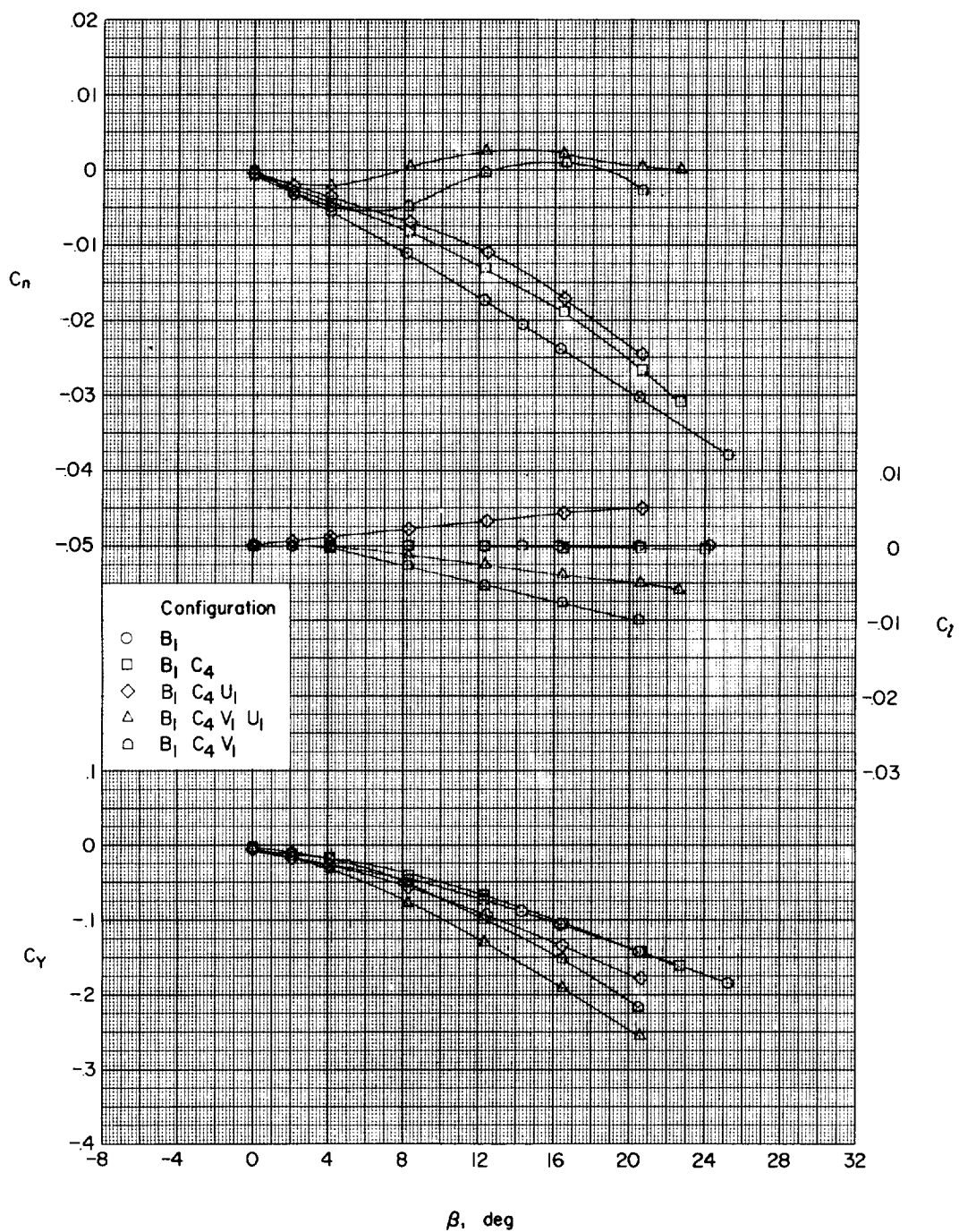
(e) $\alpha = 16.5°$.

Figure 20.- Continued.
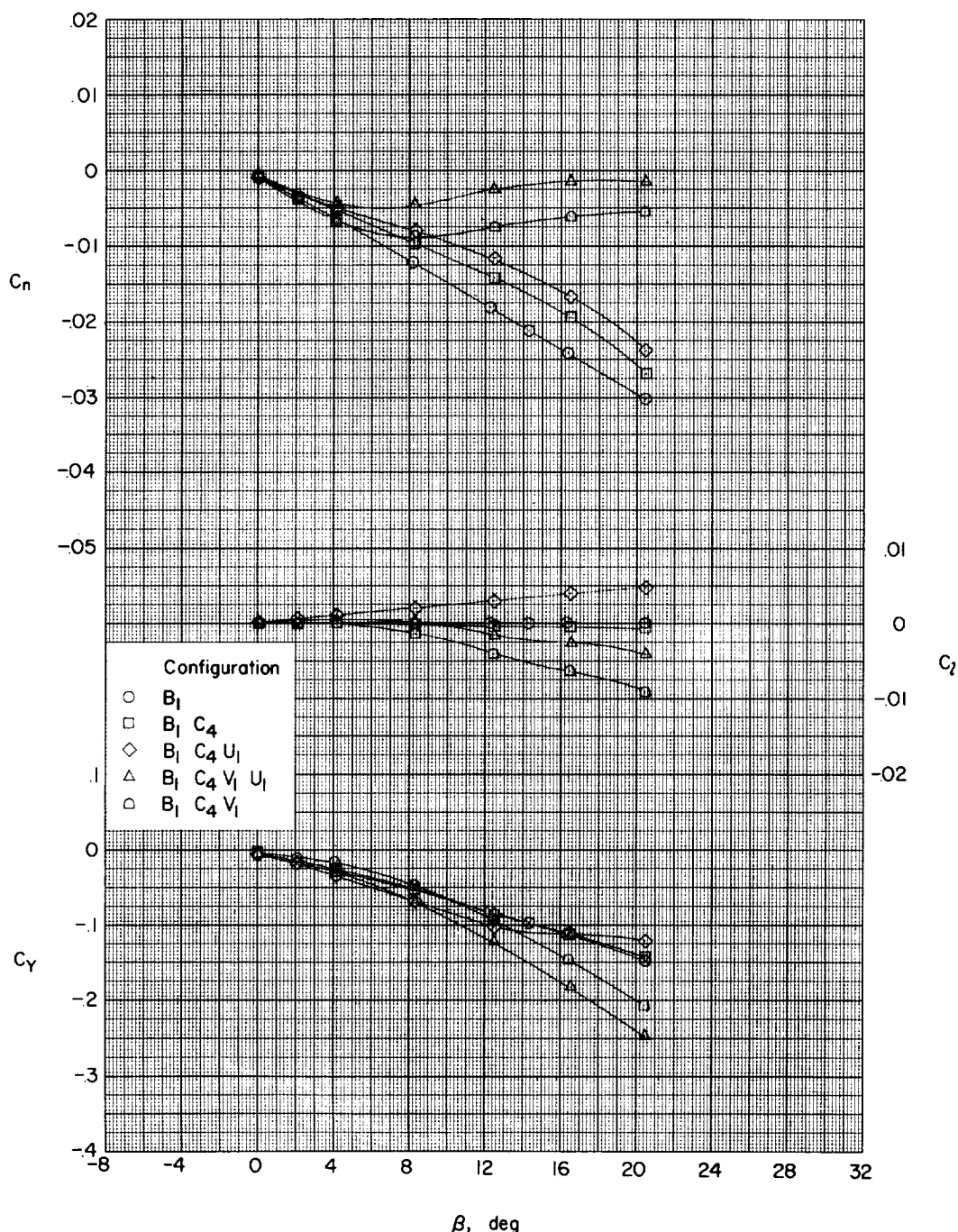
(f) $\alpha = 20.7^{\circ}$.

Figure 20.- Concluded.
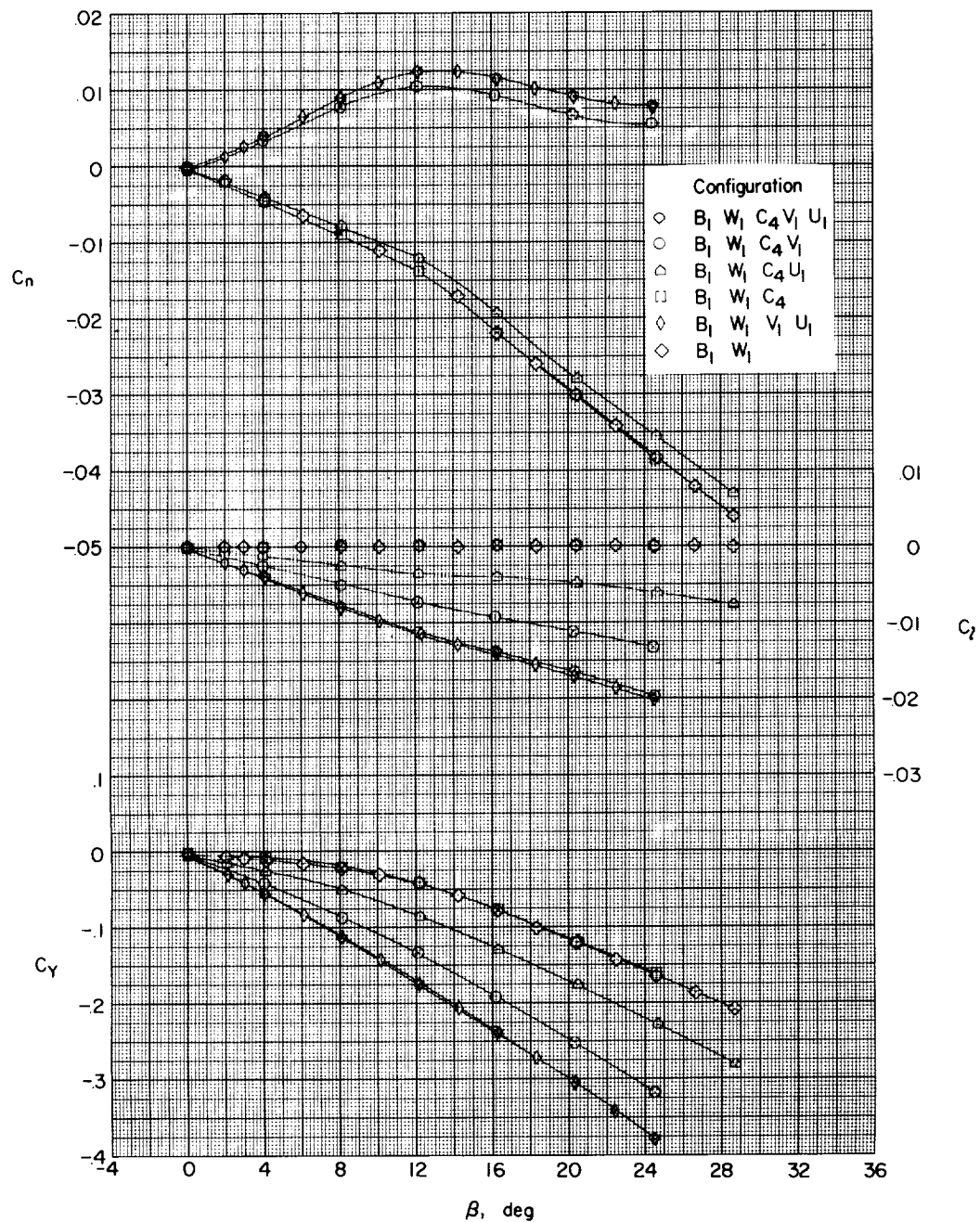
(a) α = 0°.

Figure 21.- The aerodynamic characteristics in sideslip of the trapezoidal-wing configuration. Wing on; M = 2.01.
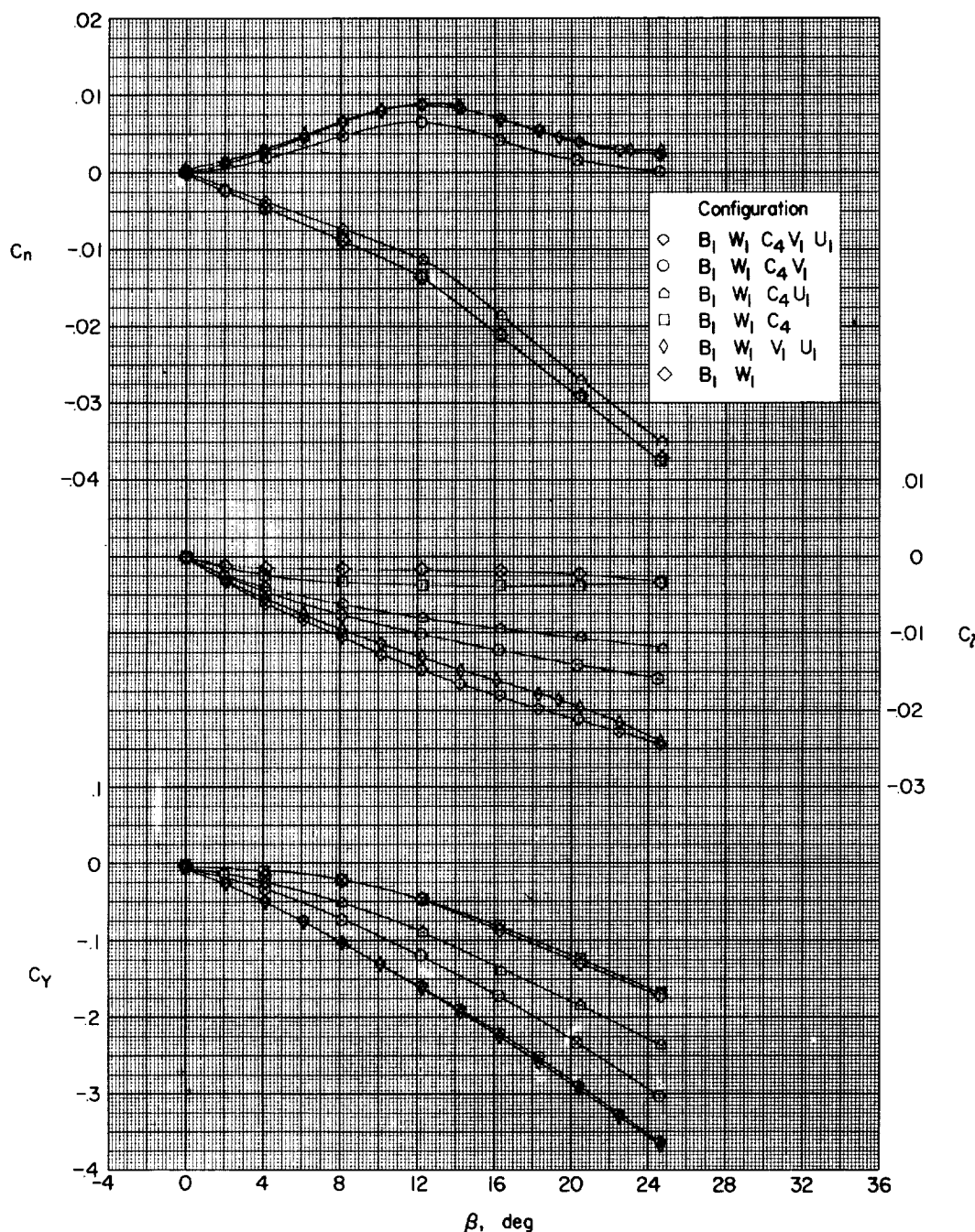
(b) α = 4.1°.

Figure 21.- Continued.
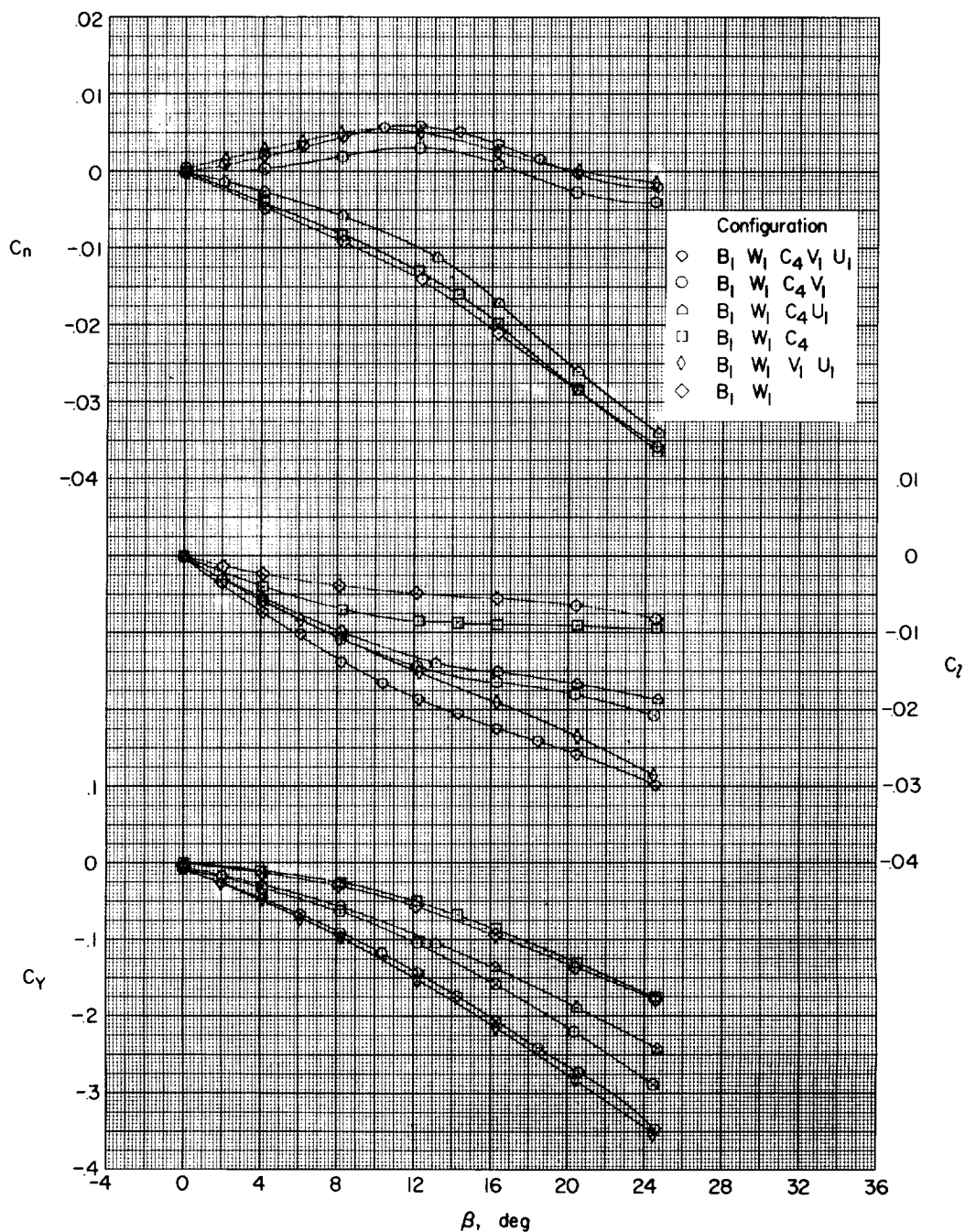
(c) α = 8.2°.

Figure 21.- Continued.
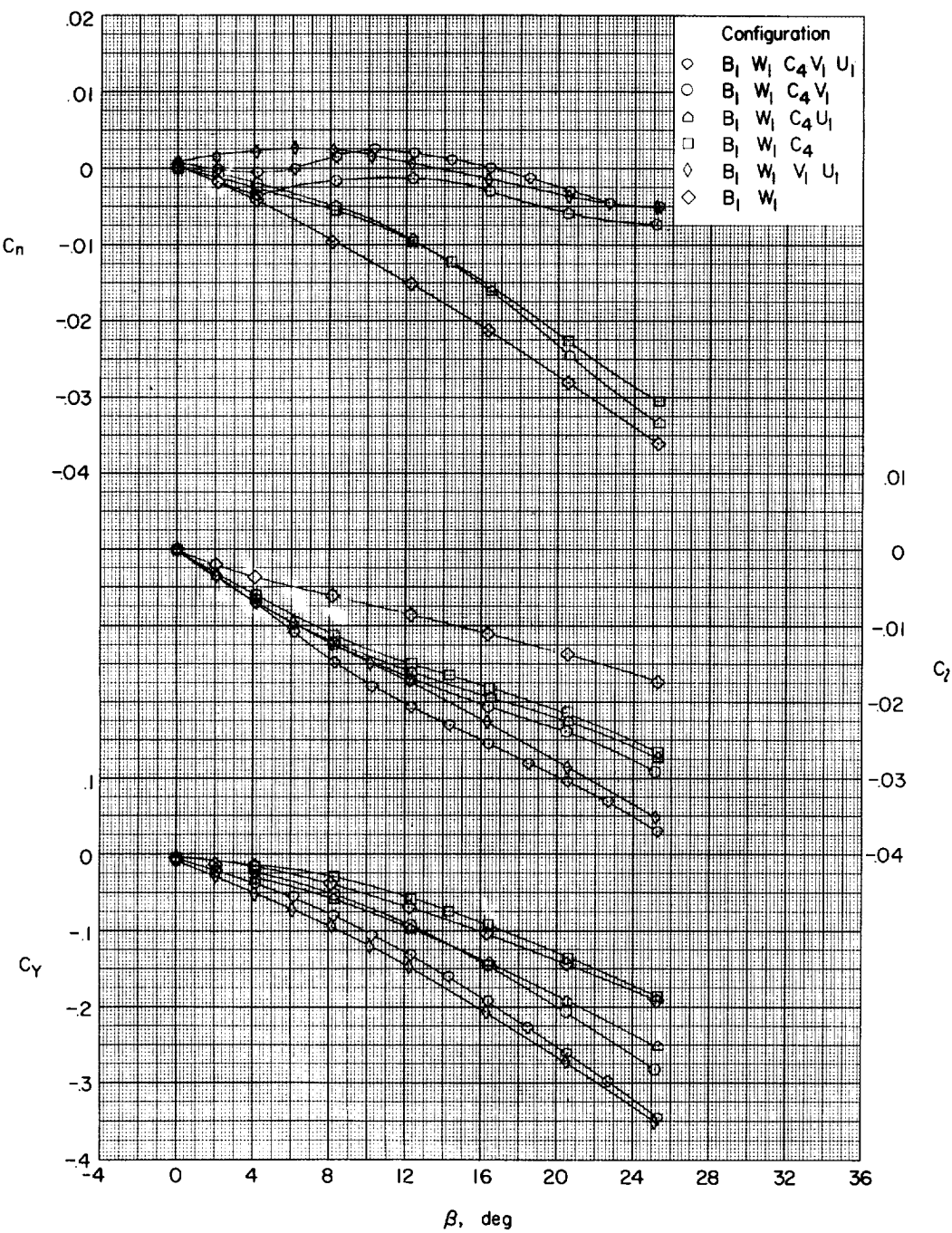
(d) α = 12.4°.

Figure 21.- Continued.
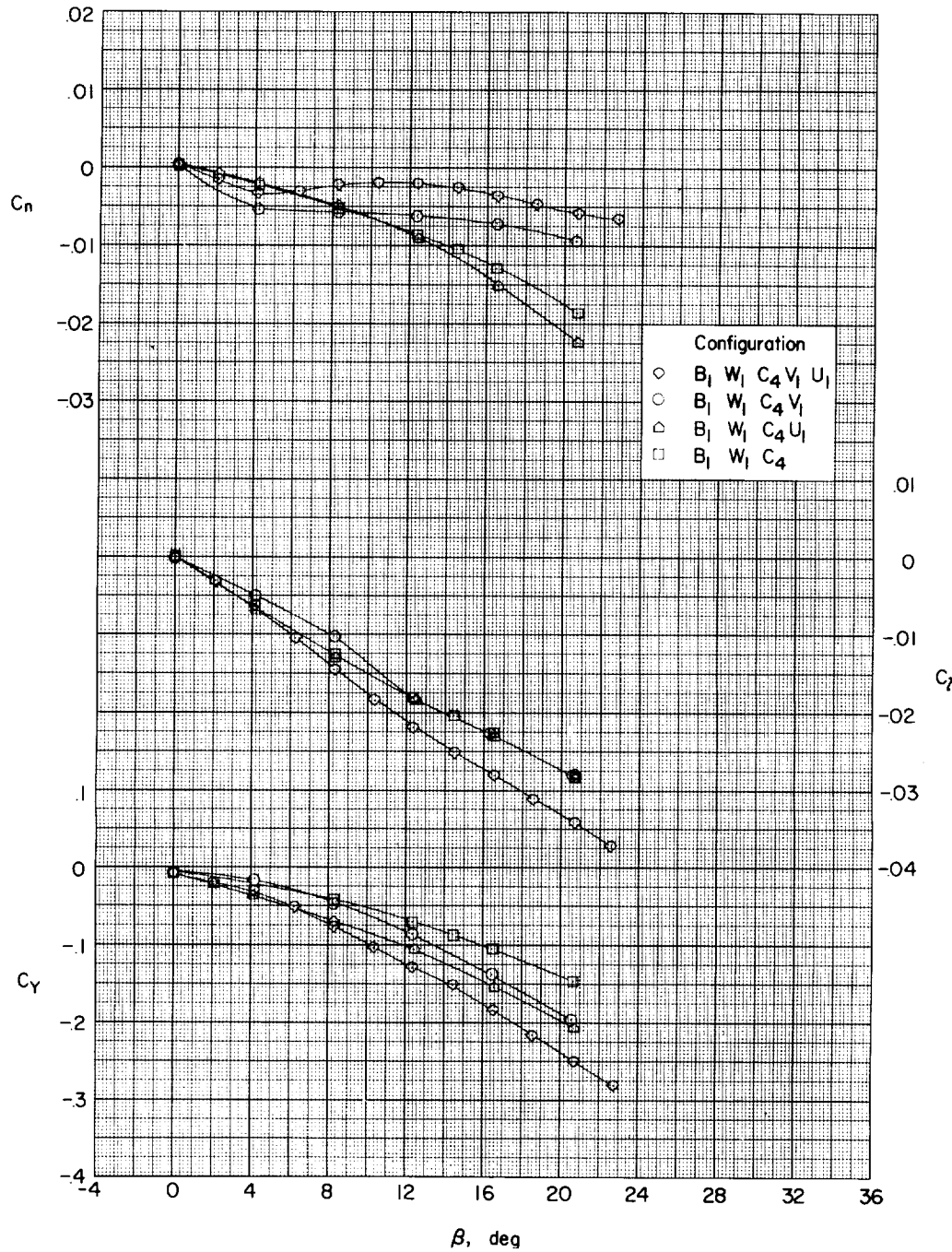
(e) $\alpha = 16.5°$.

Figure 21.- Continued.
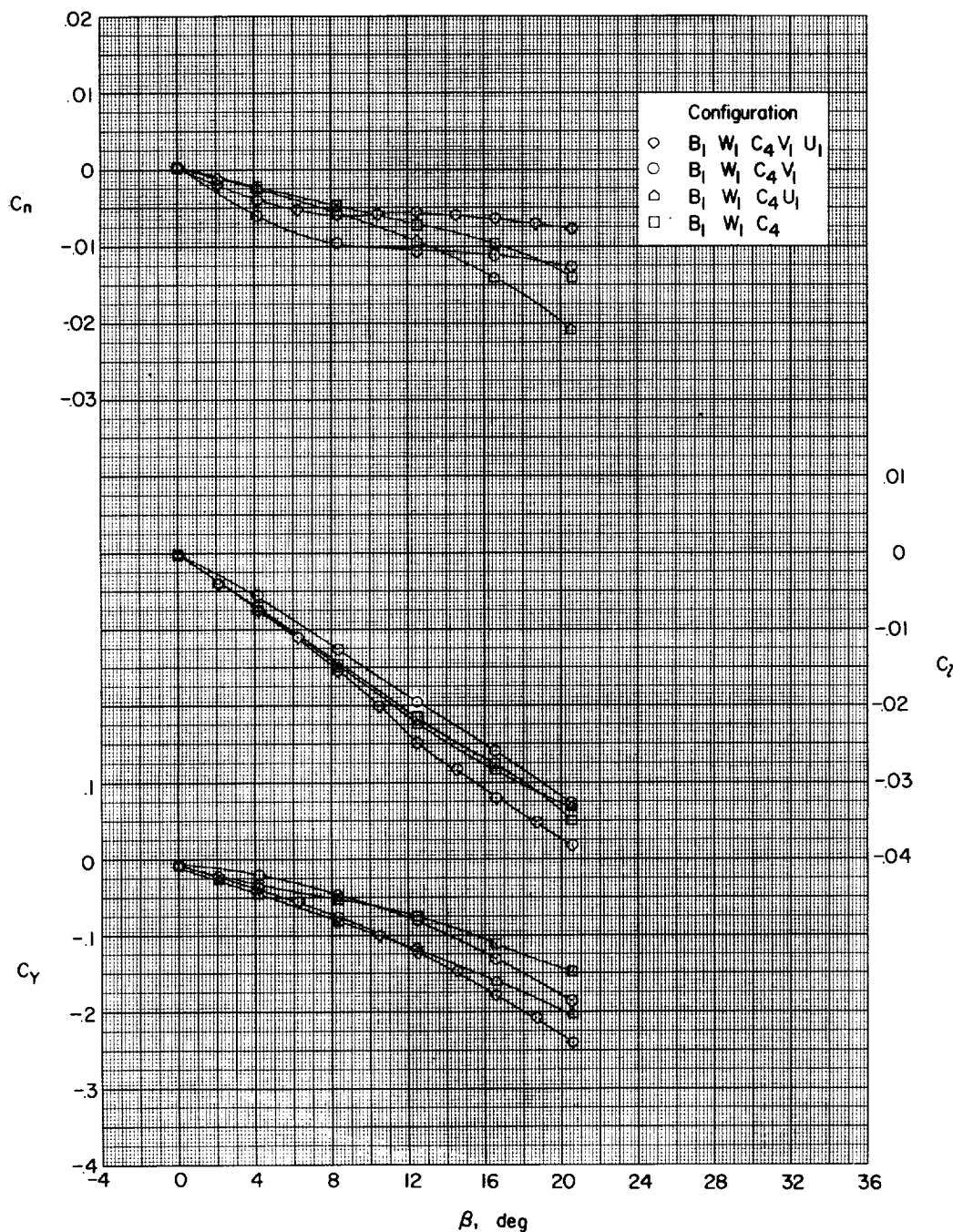
(f) $\alpha = 20.7^{\circ}$.

Figure 21.- Concluded.
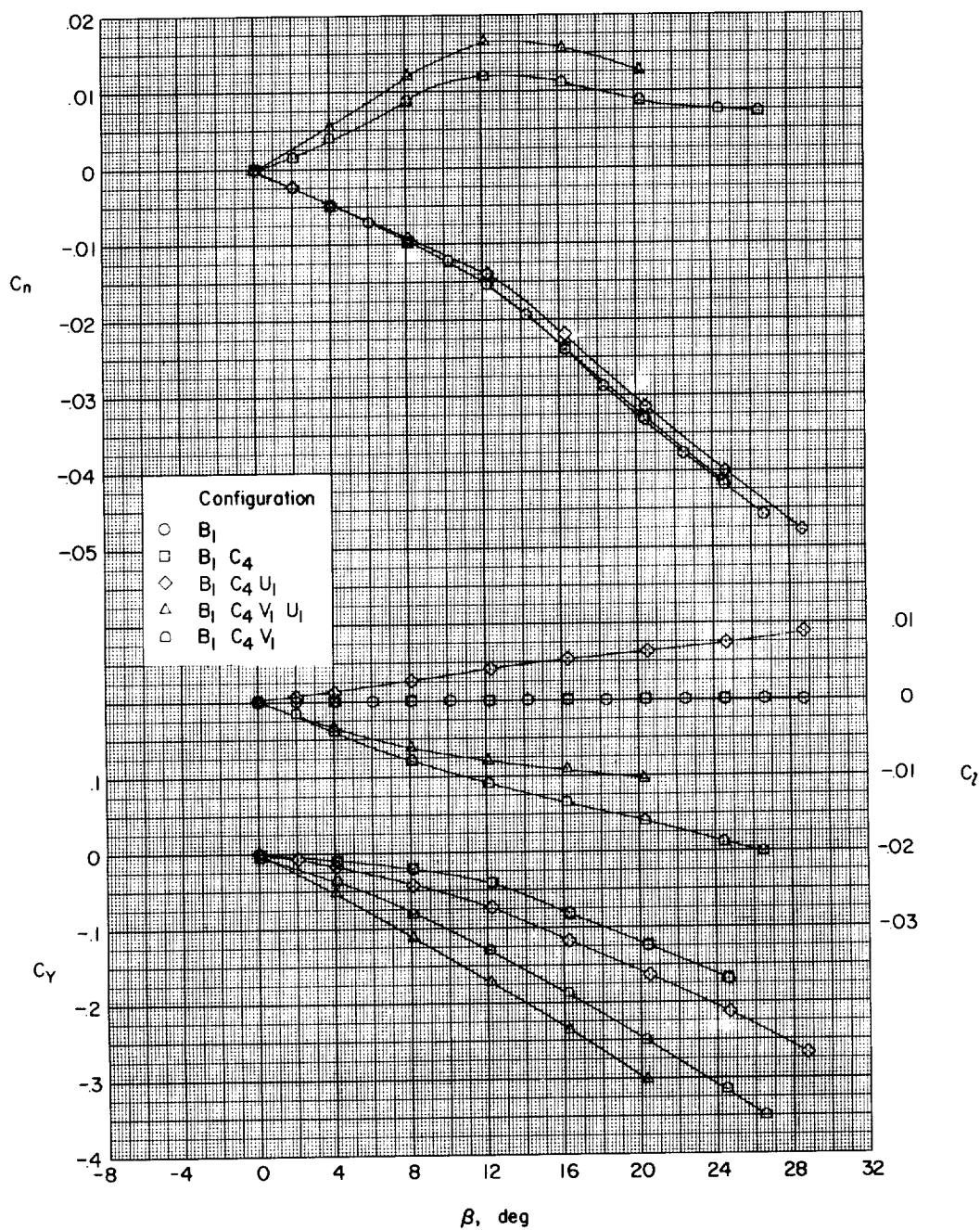
(a) $\alpha = 0°$.

Figure 22.- The aerodynamic characteristics in sideslip of the delta-wing configuration. Wing off; $M = 2.01$.
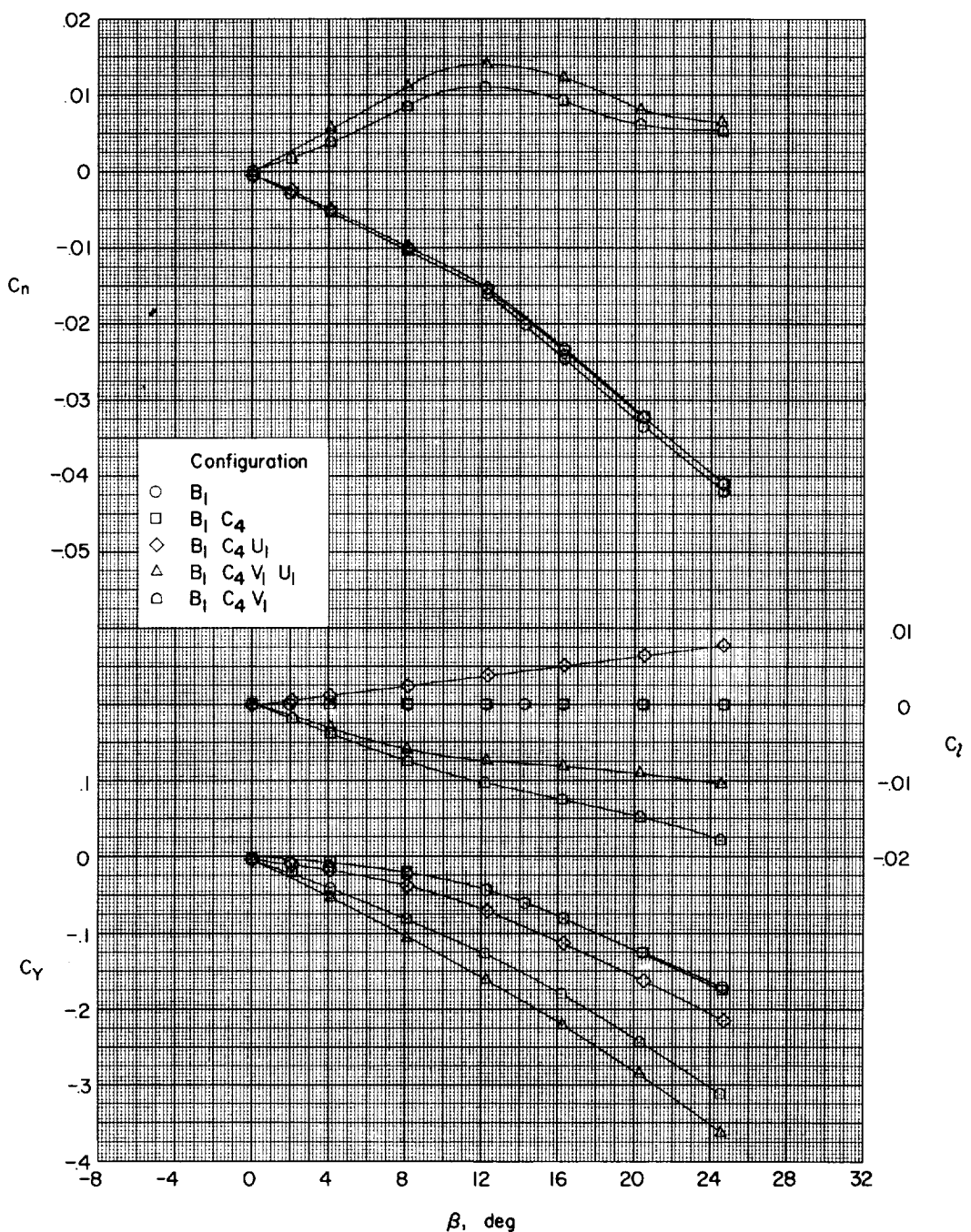
(b) α = 4.1°.

Figure 22.- Continued.
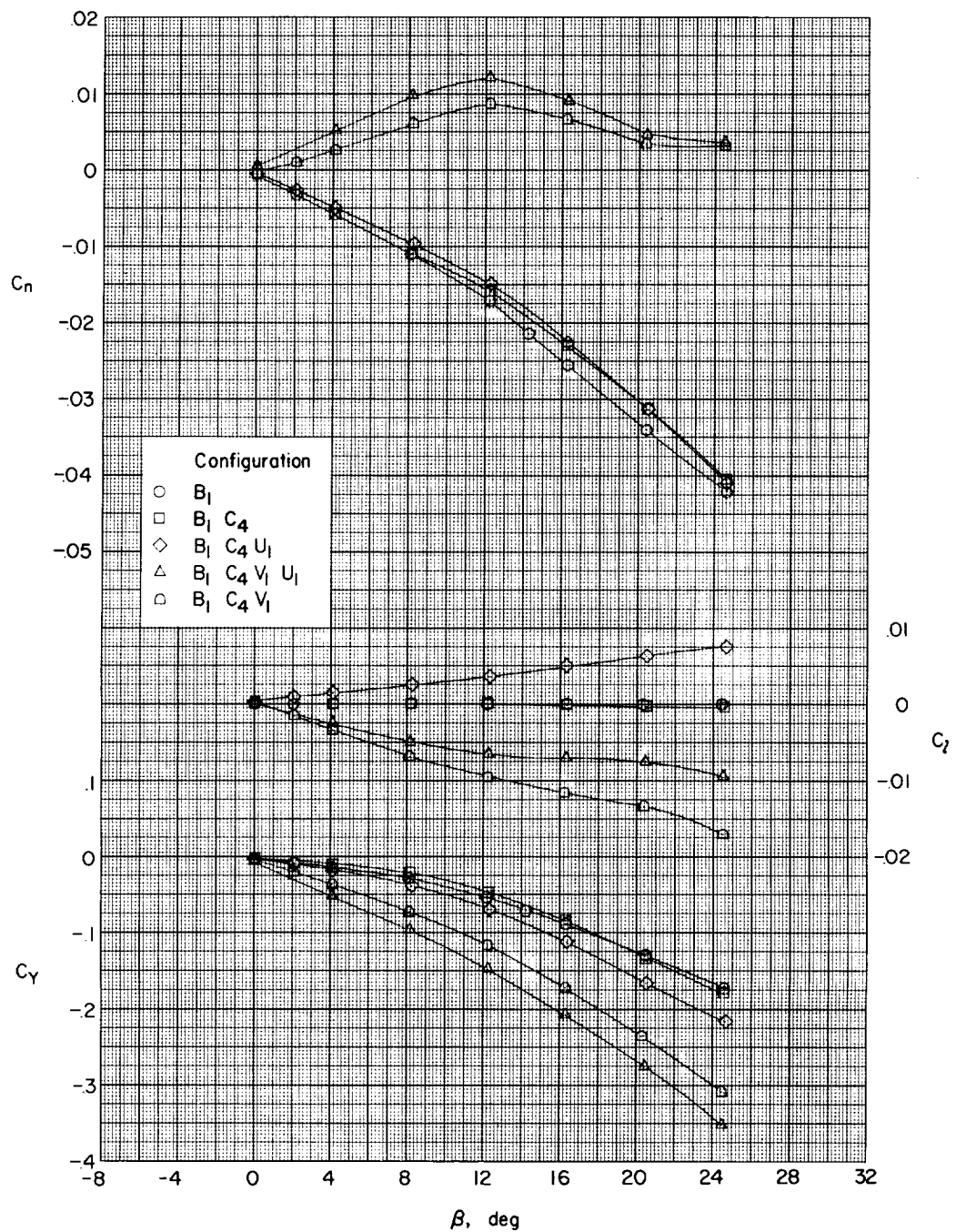
(c) $\alpha = 8.2°$.

Figure 22.- Continued.
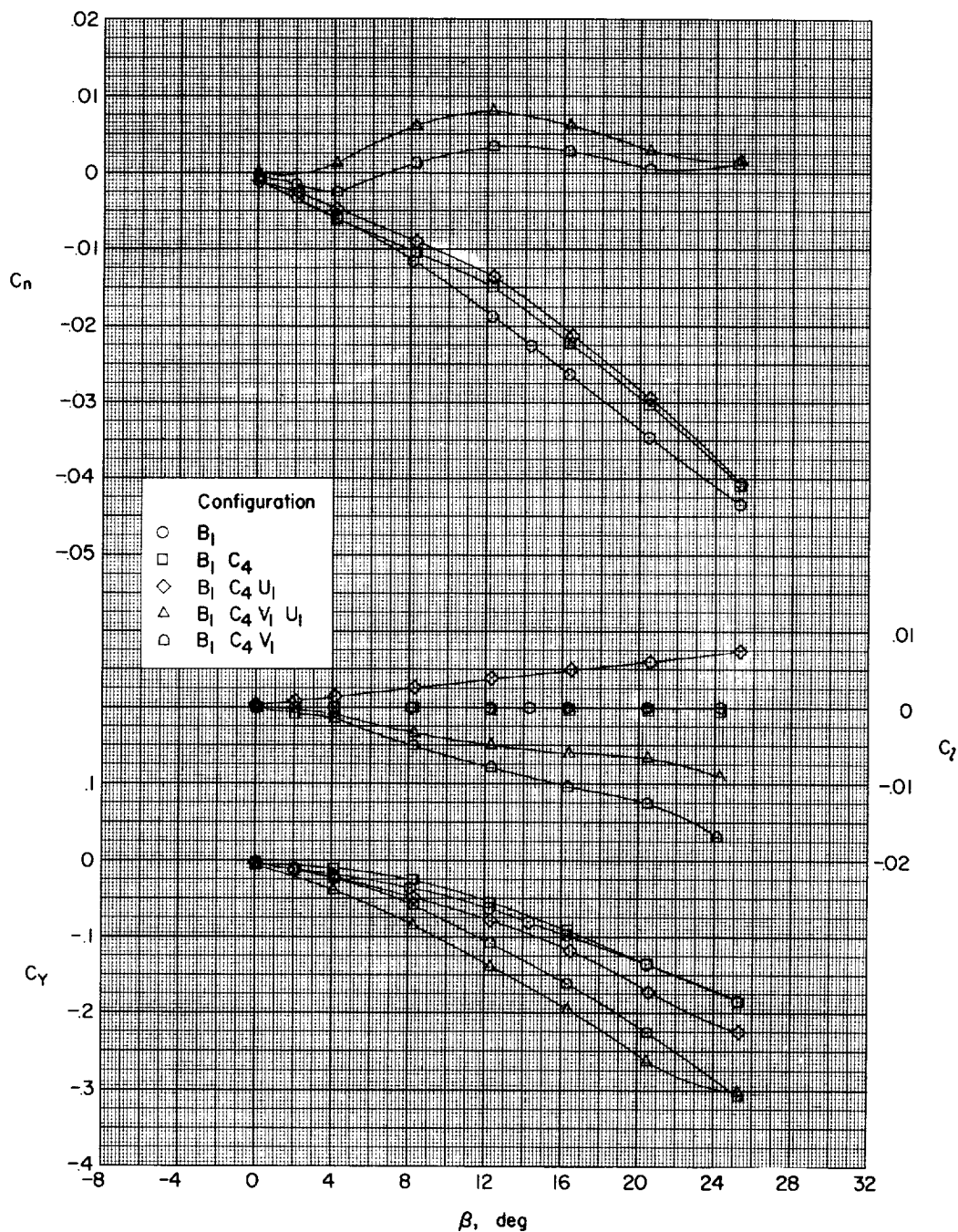
(d) $\alpha = 12.3^\circ$.

Figure 22.- Continued.
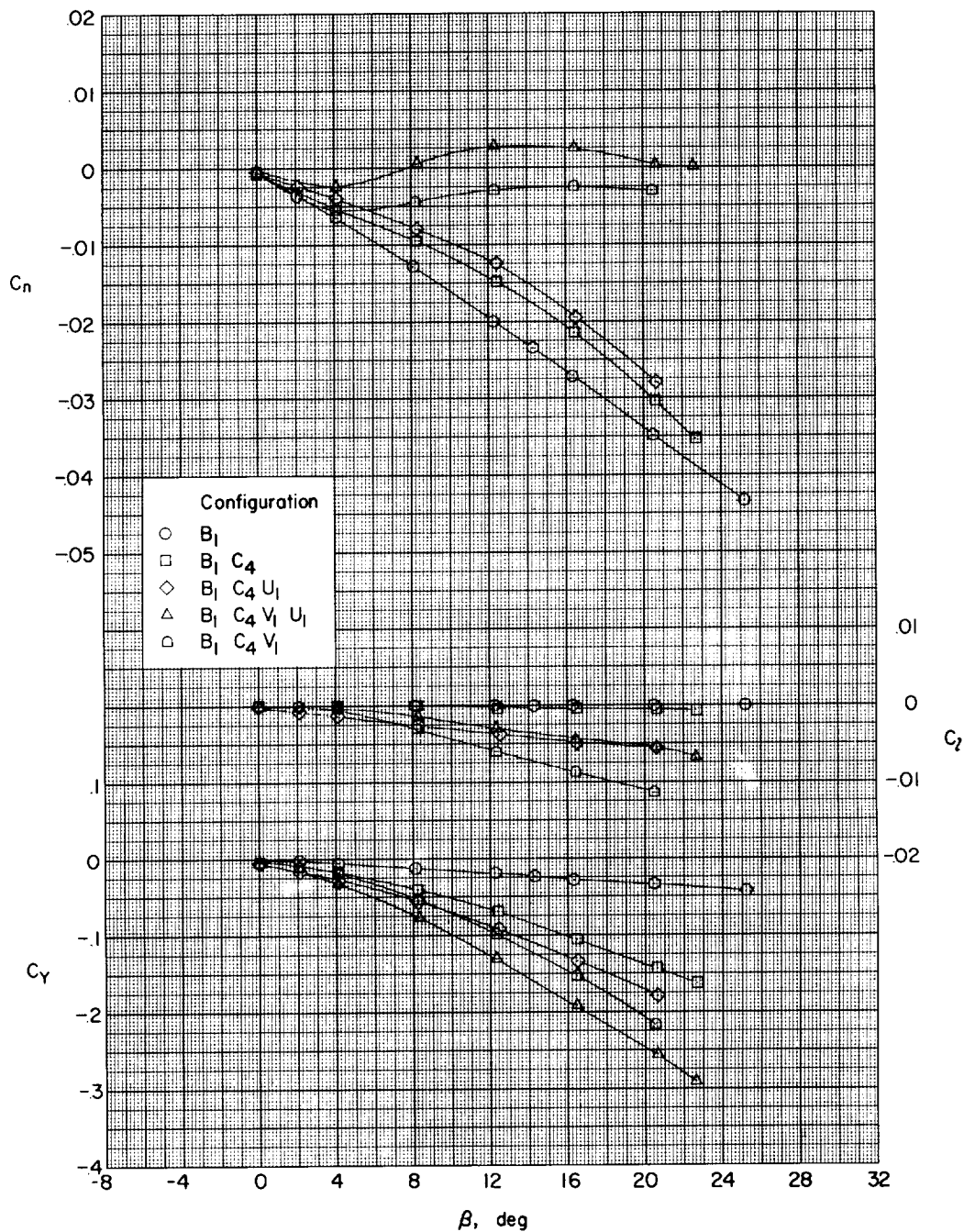
(e) $\alpha = 16.4°$.

Figure 22.- Continued.
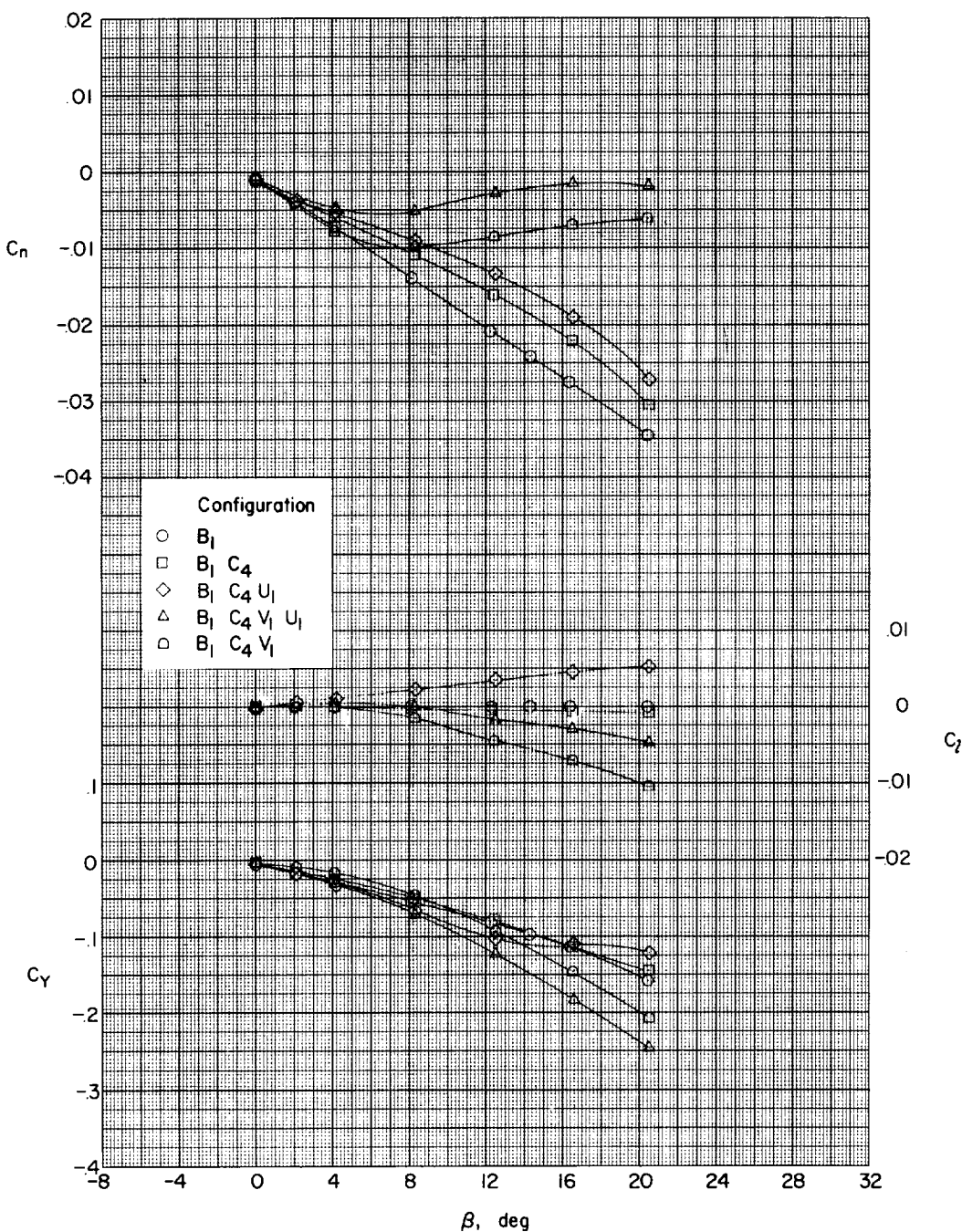
(f) α = 20.8°.

Figure 22.- Concluded.
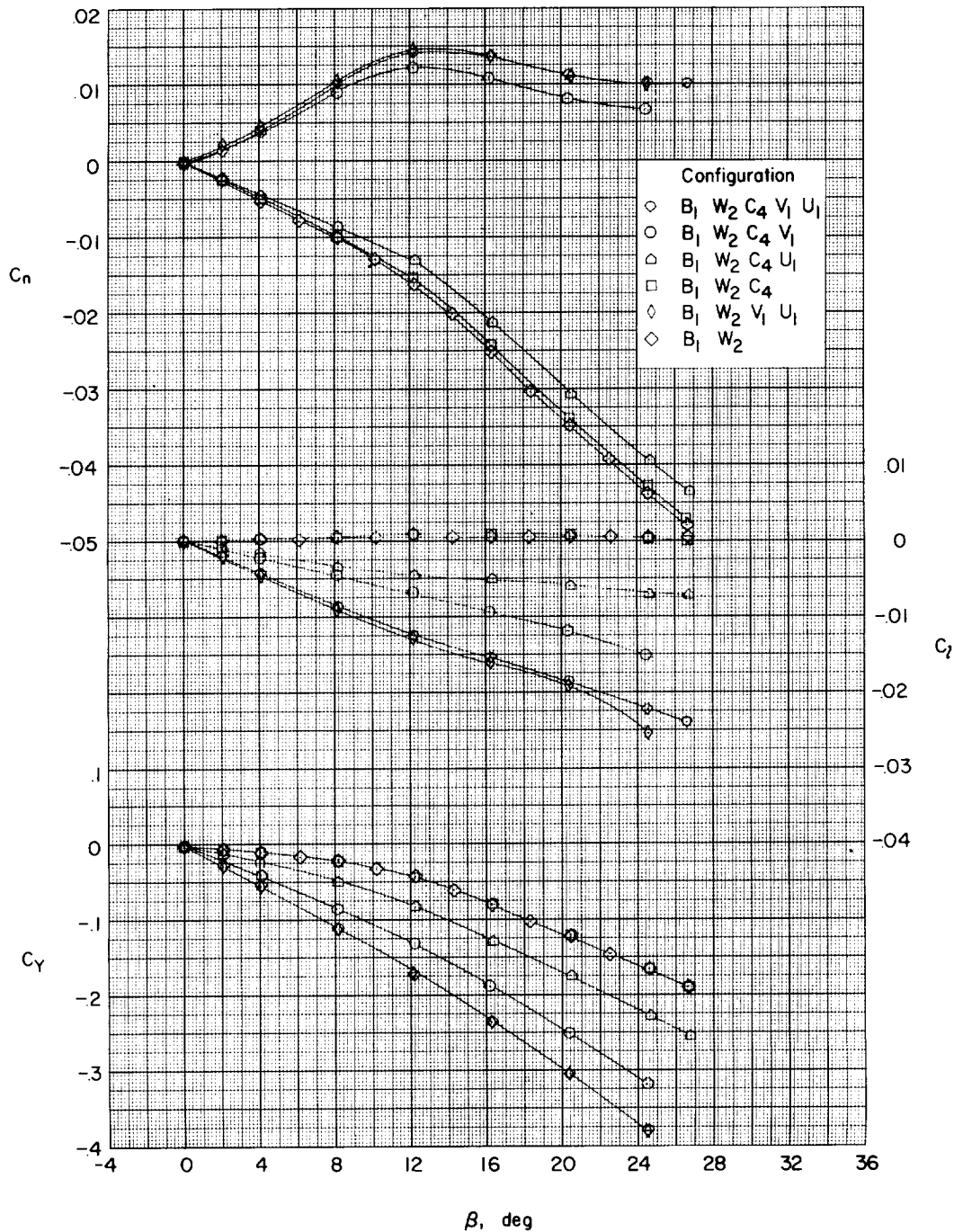
(a) $\alpha = 0^{\circ}$.

Figure 23.- The aerodynamic characteristics in sideslip of the delta-wing configuration. Wing on; M = 2.01.
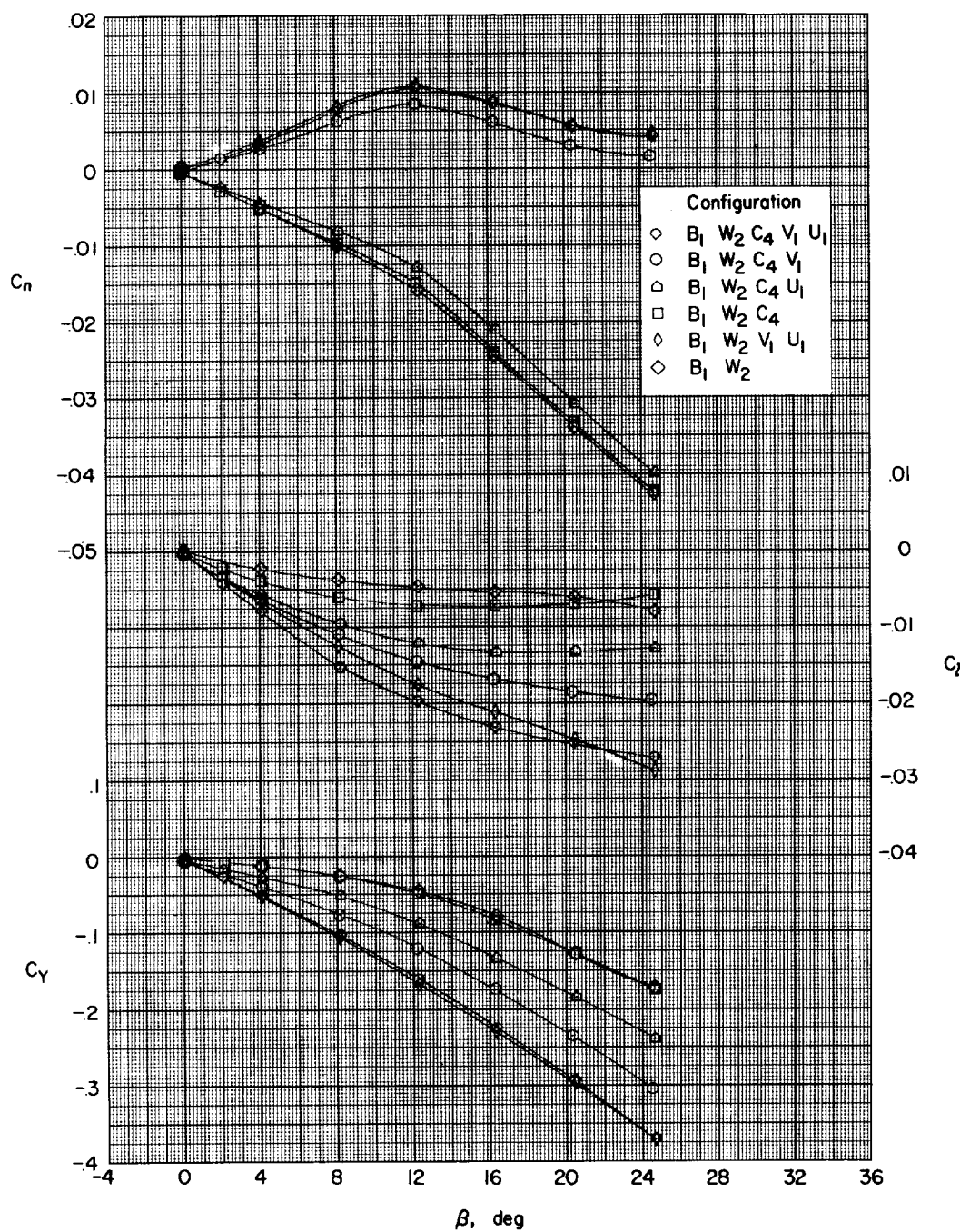
(b) α = 4.1°.

Figure 23.- Continued.
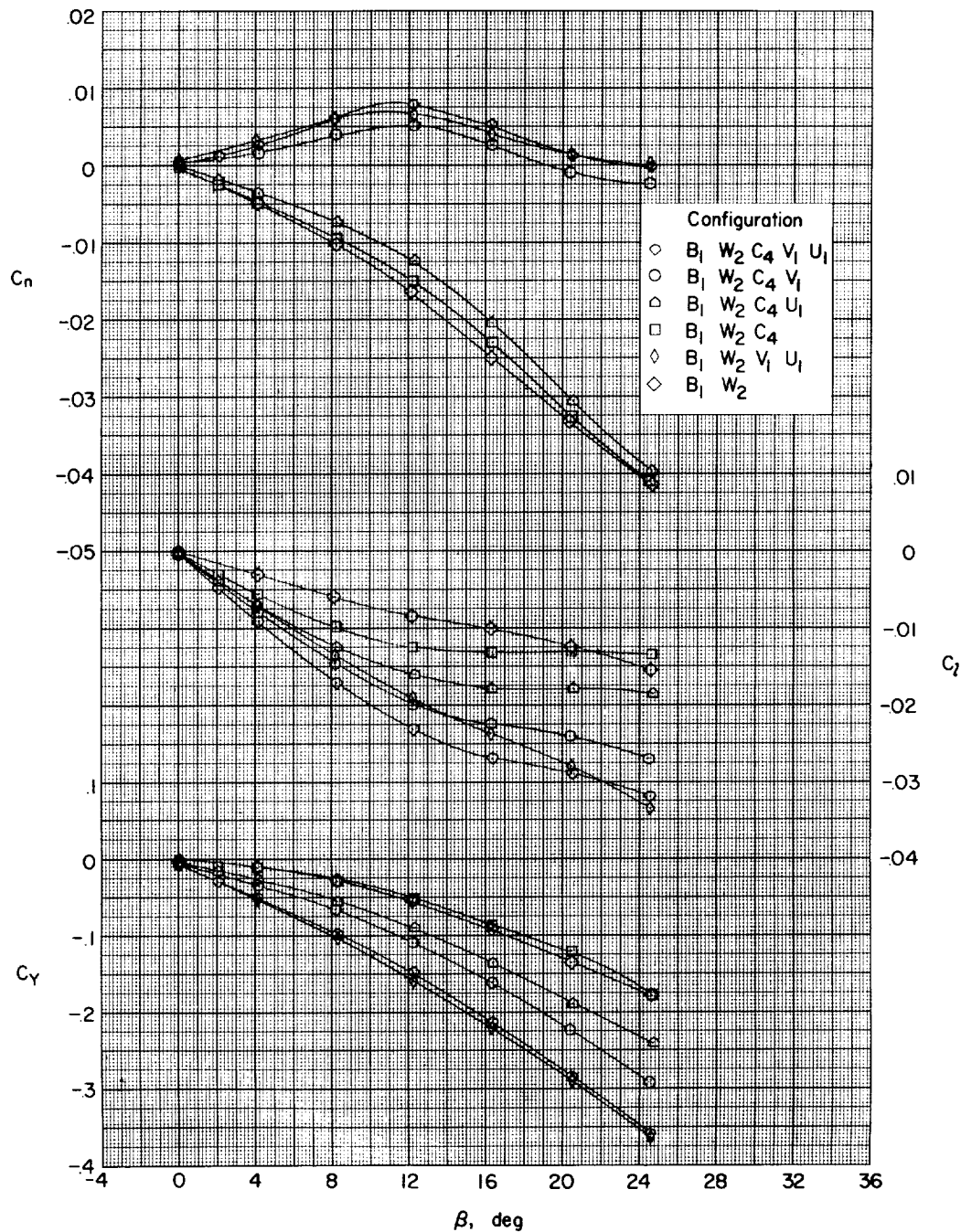
(c) $\alpha = 8.2^\circ$.

Figure 23.- Continued.
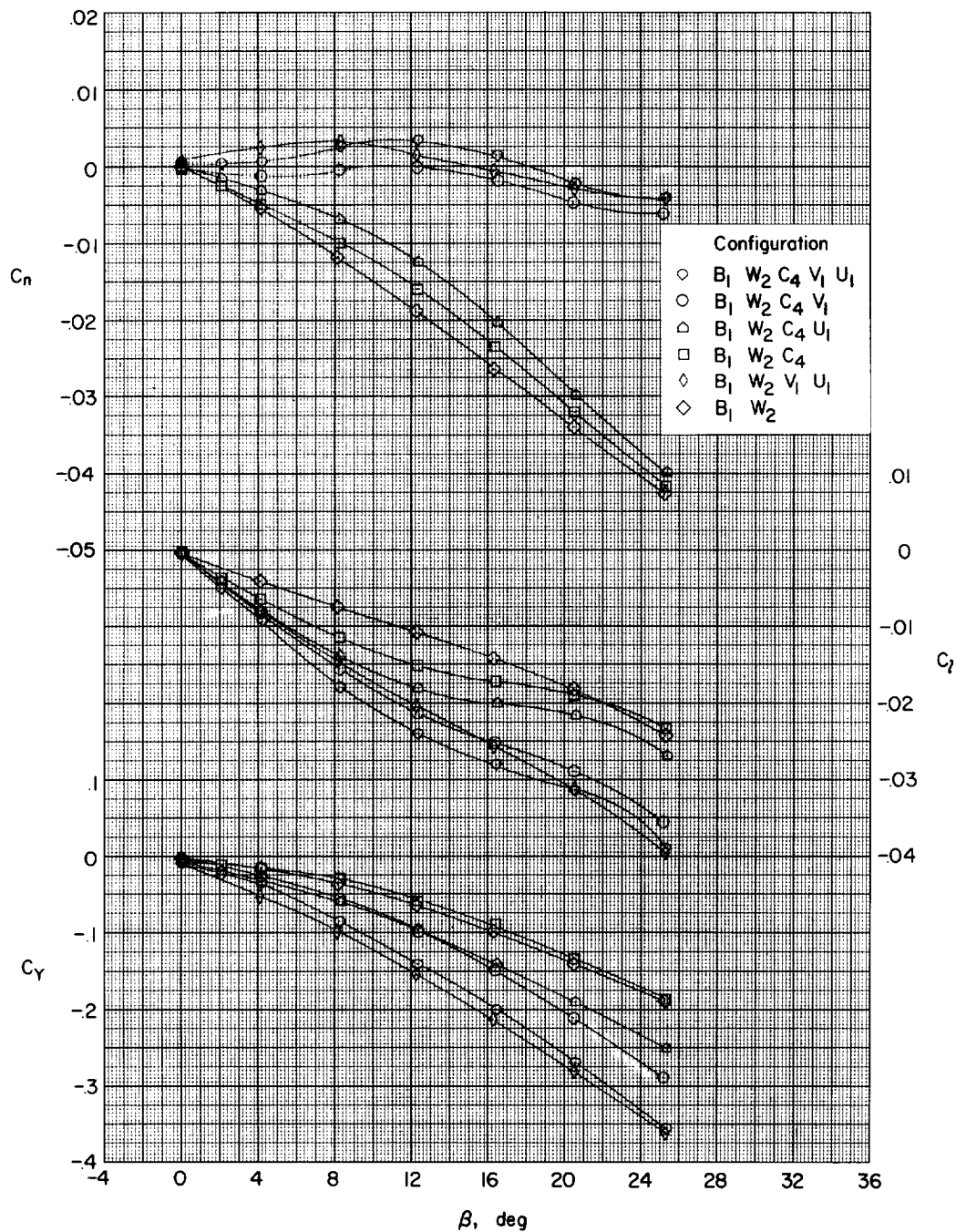
(d) $\alpha = 12.3°$.

Figure 23.- Continued.
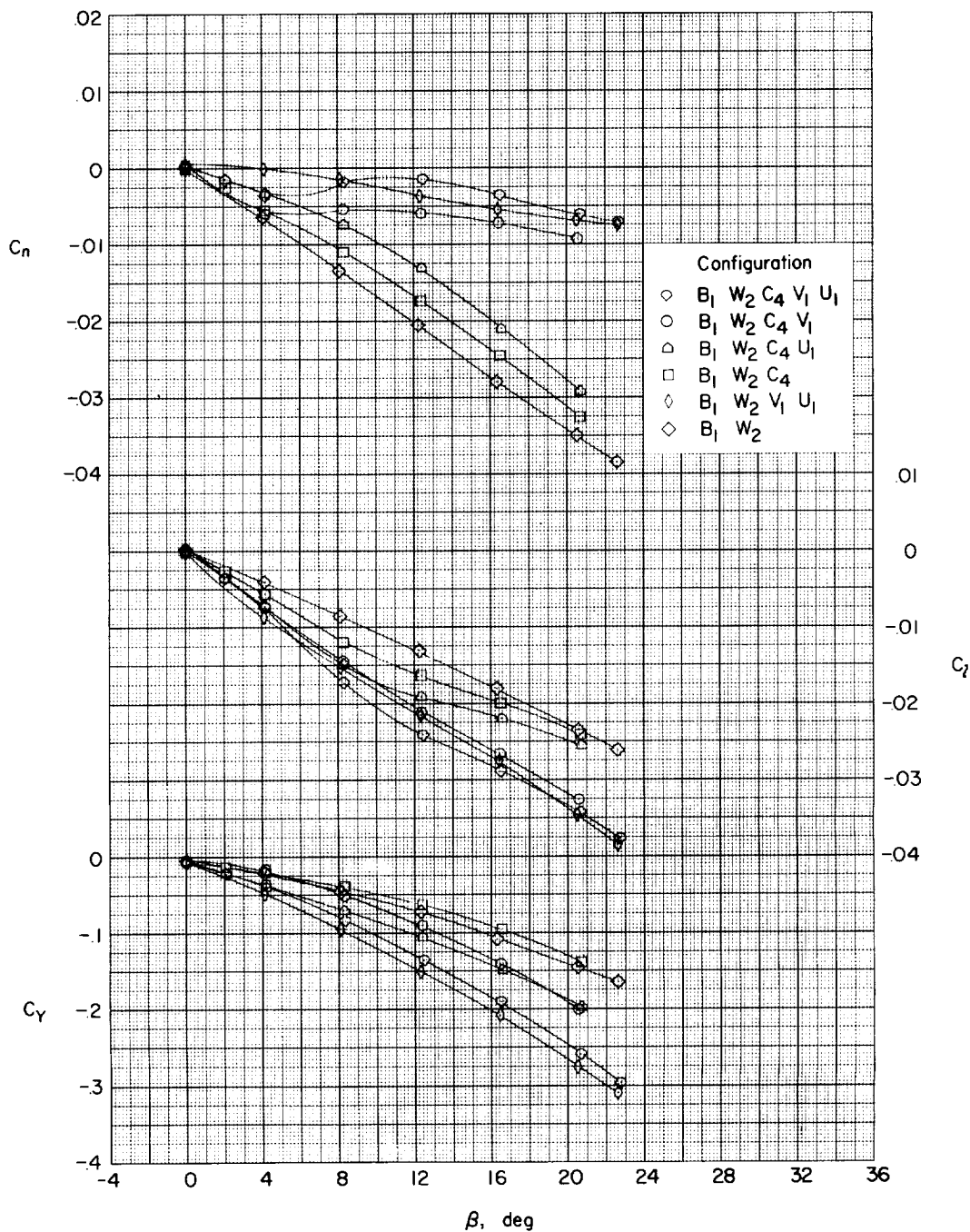
(e) α = 16.4°.

Figure 23.- Continued.
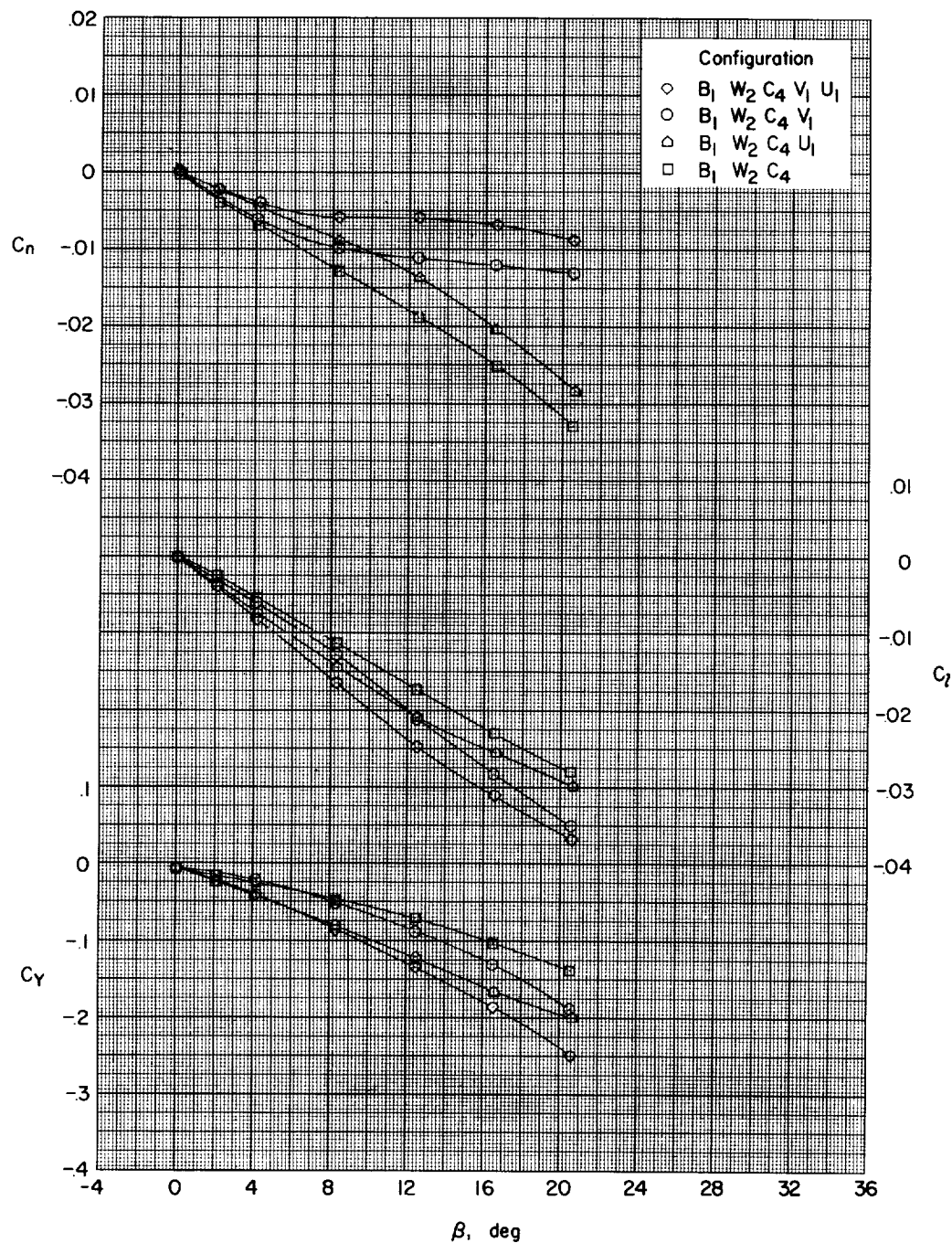
(f) $\alpha = 20.7^\circ$.

Figure 23.- Continued.
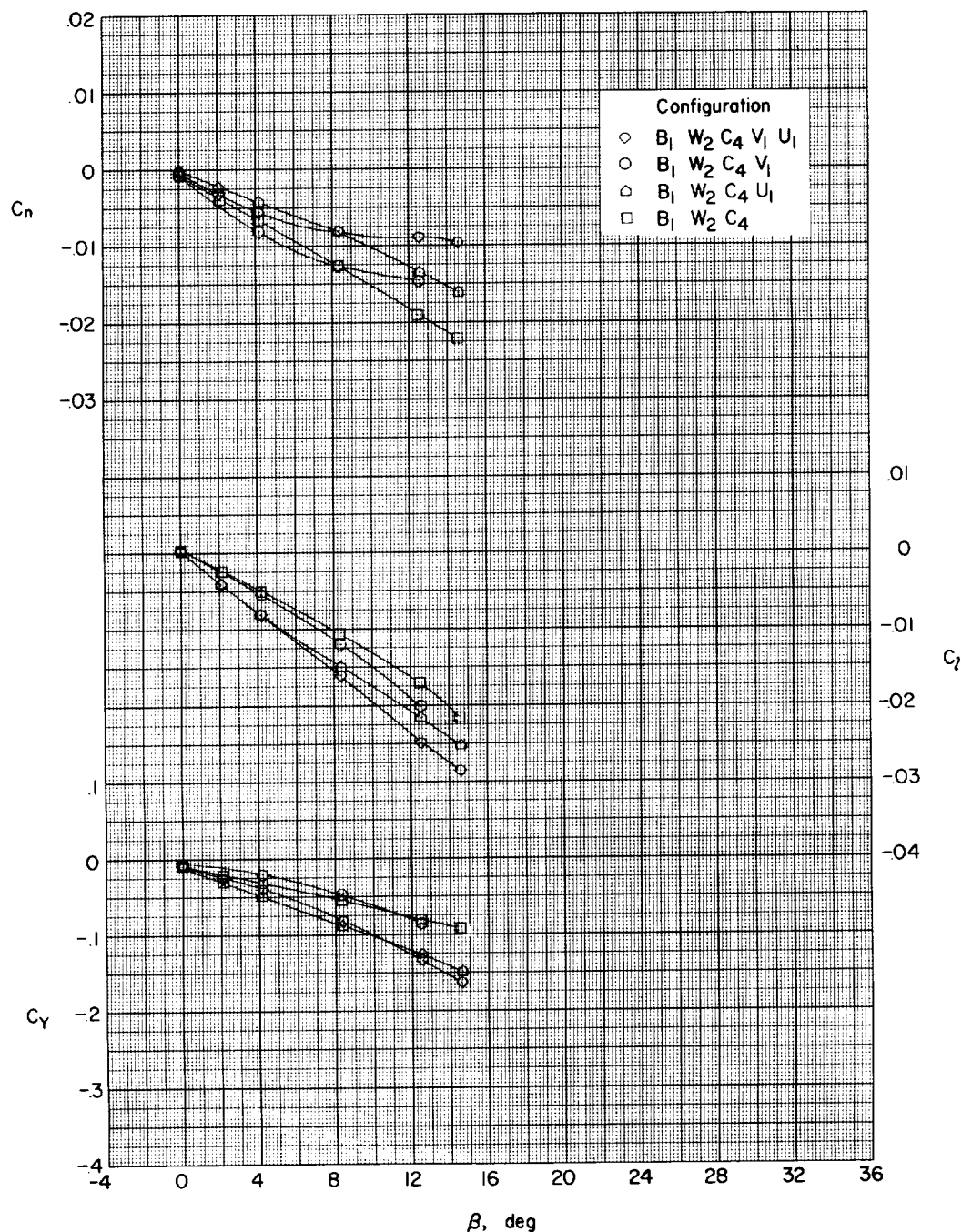
(g) $\alpha = 24.8^{\circ}$.

Figure 23.- Concluded.
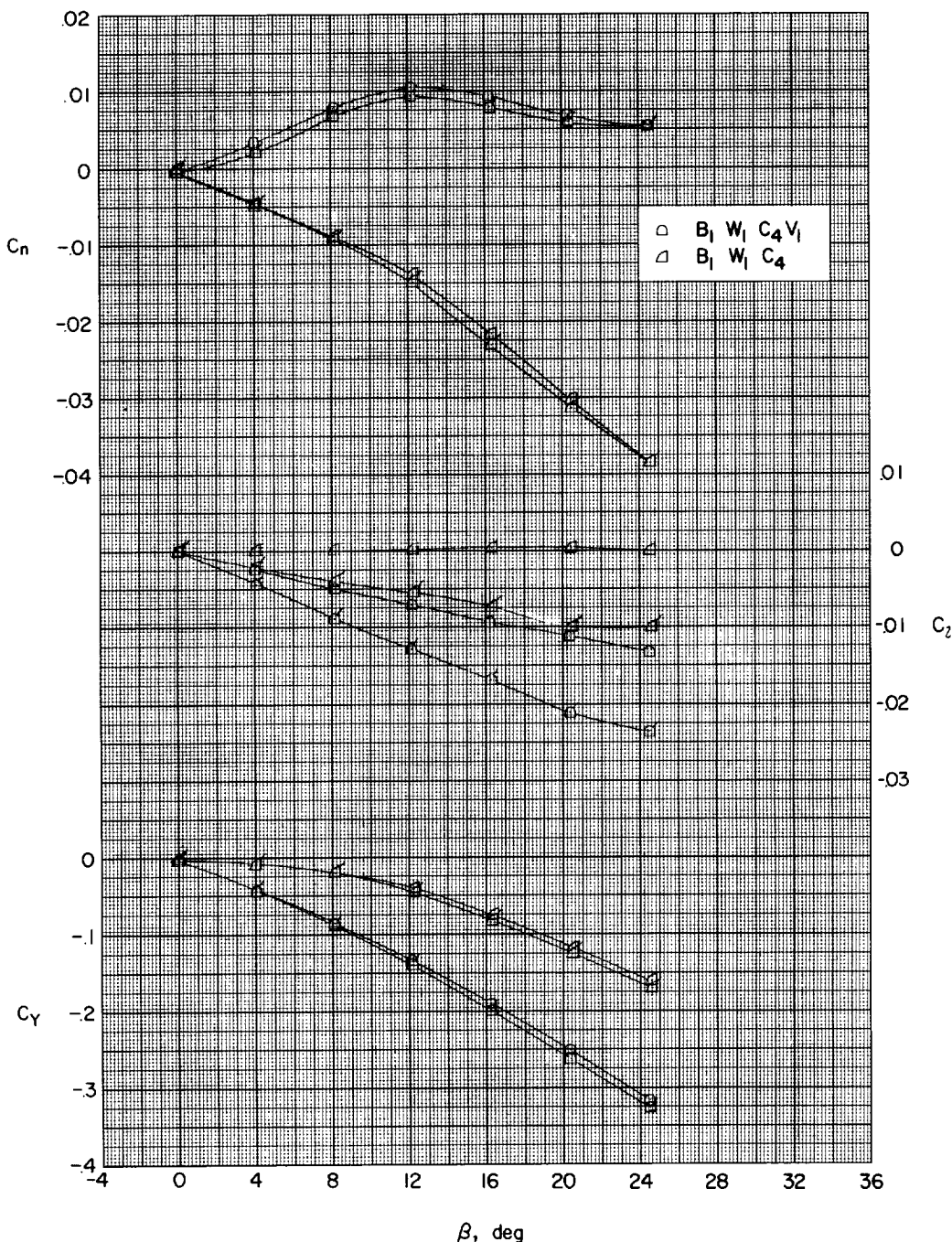
(a) α = 0°.

Figure 24.- The effect of canard deflection on the aerodynamic characteristics in sideslip of the trapezoidal-wing configuration. Flagged symbols are for $\delta_c = 15°$ and $M = 2.01$.
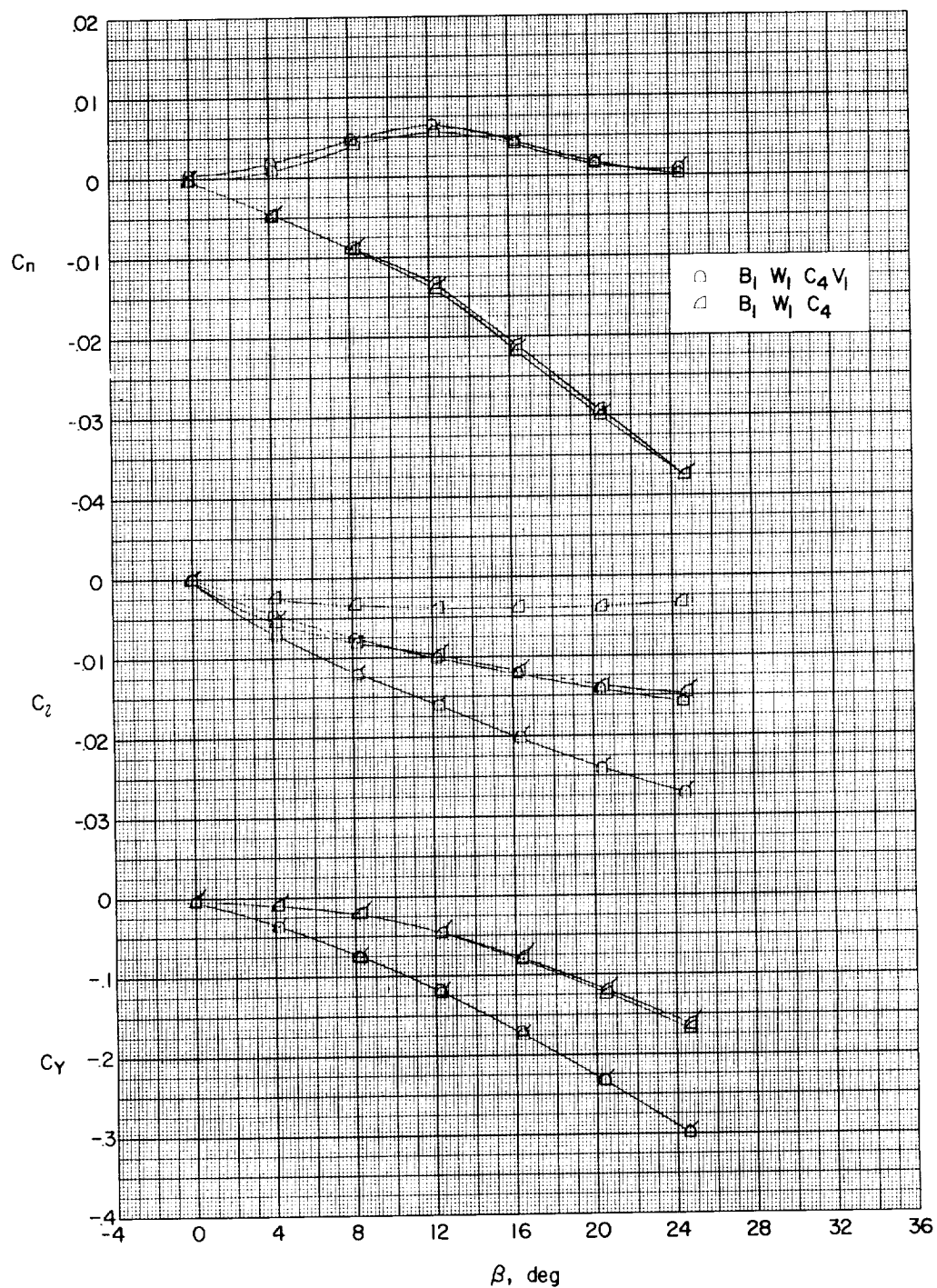
(b) α = 4.1°.

Figure 24.- Continued.
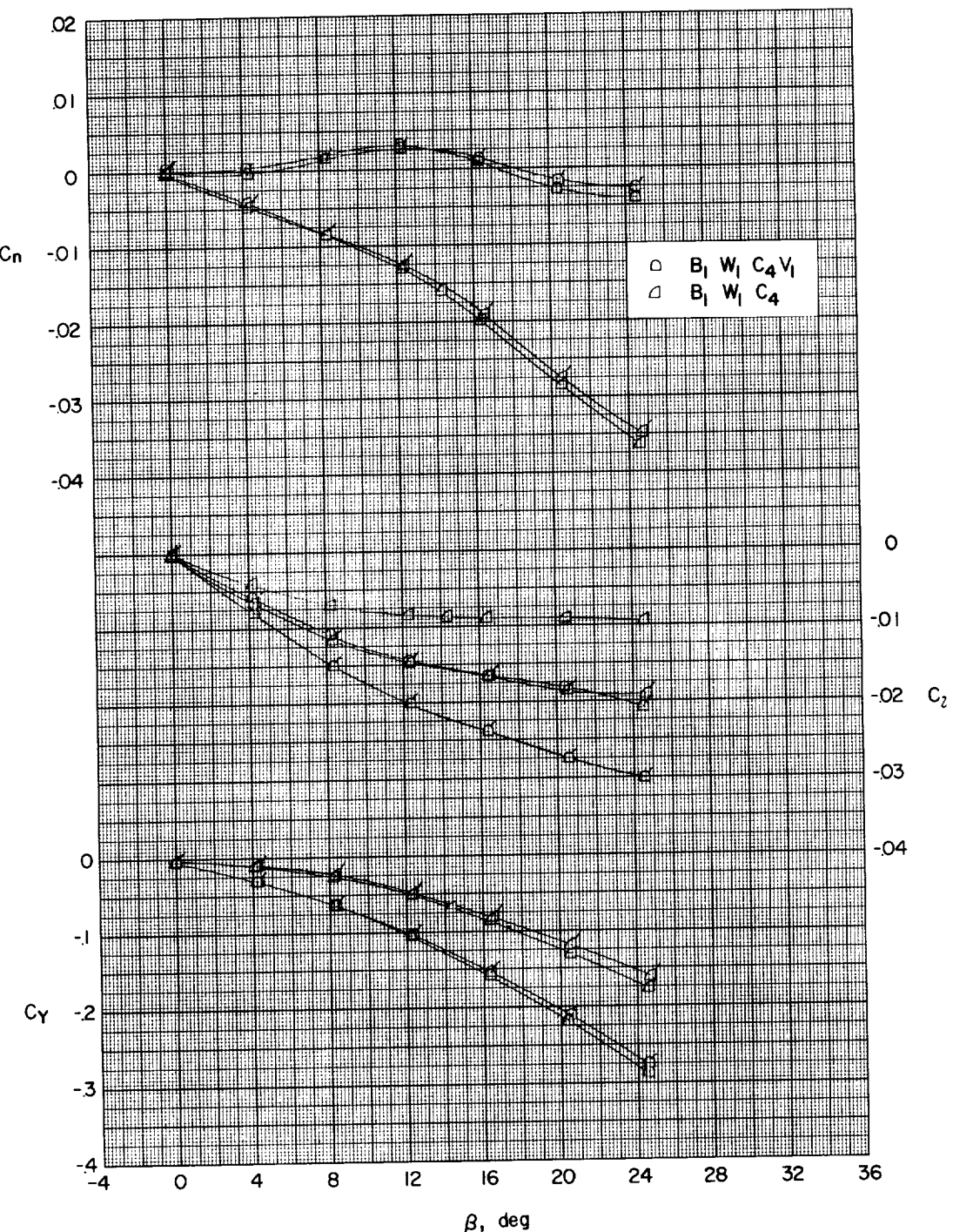
(c) $\alpha = 8.2^\circ$.

Figure 24.- Concluded.
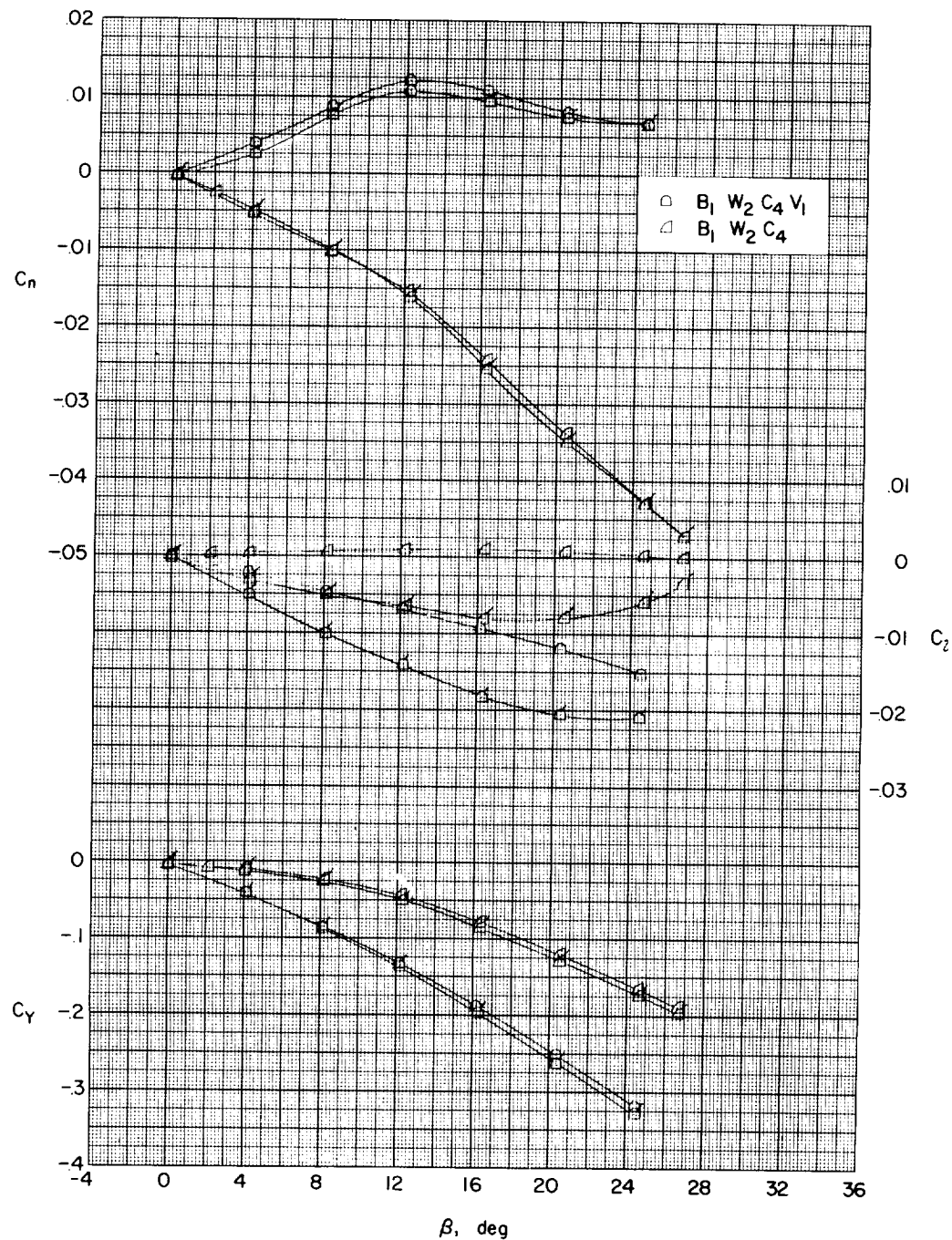
(a) $\alpha = 0^\circ$.

Figure 25.- The effect of canard deflection on the aerodynamic characteristics in sideslip on the delta-wing configuration. Flagged symbols are for $\delta_c = 15^\circ$ and $M = 2.01$.
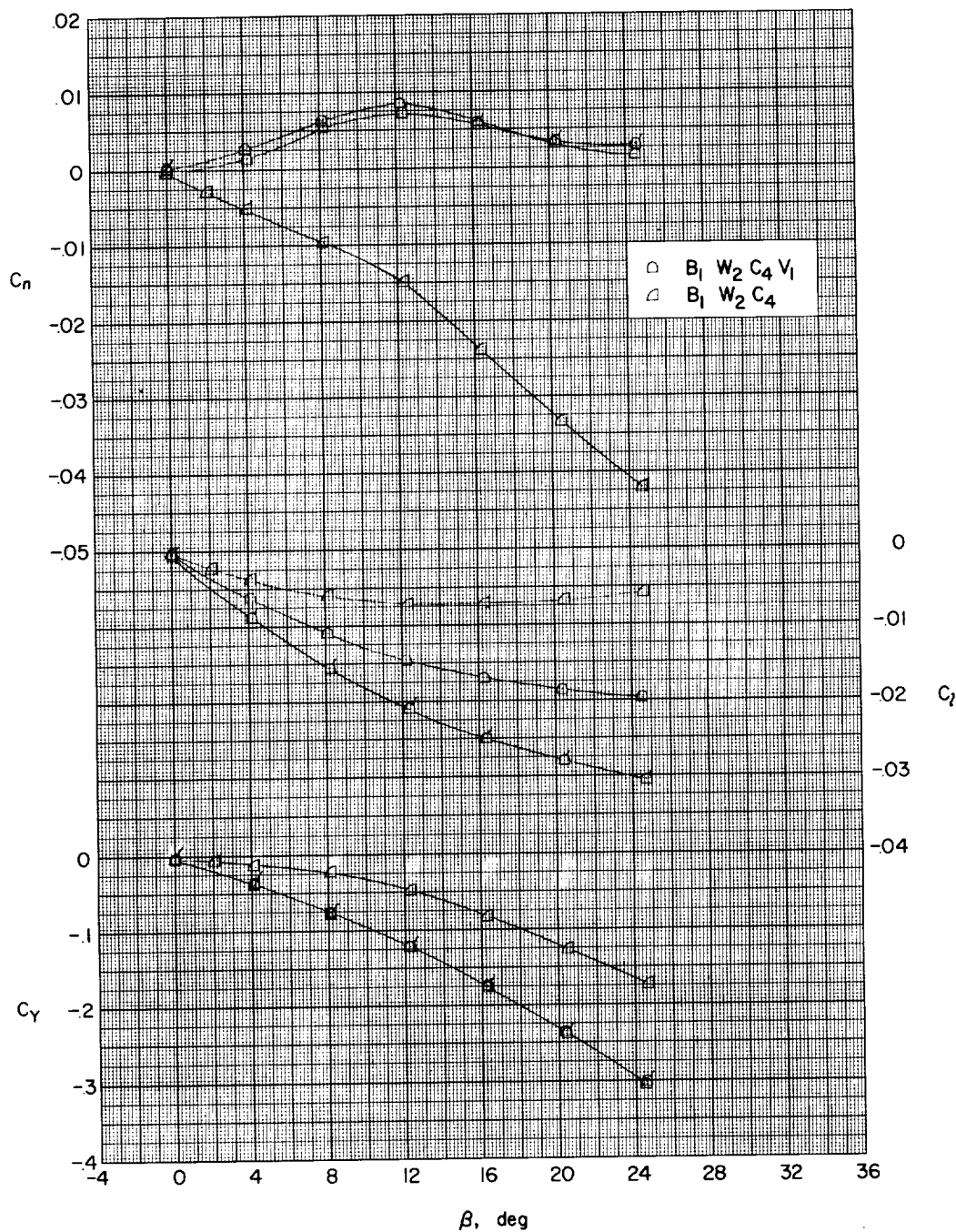
(b) $\alpha = 4.1°$.

Figure 25.- Continued.
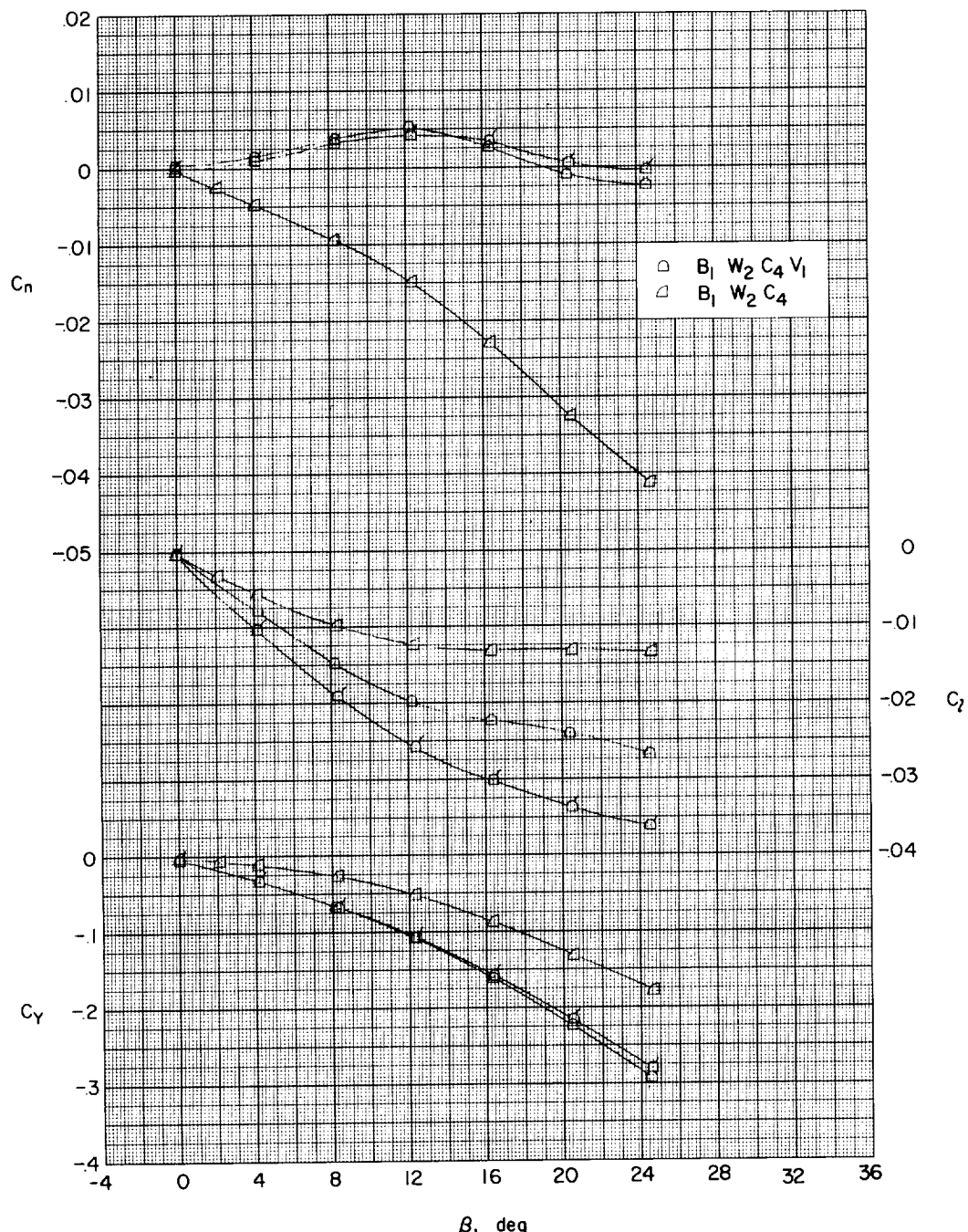
(c) $\alpha = 8.2^{\circ}$.

Figure 25.- Concluded.

102
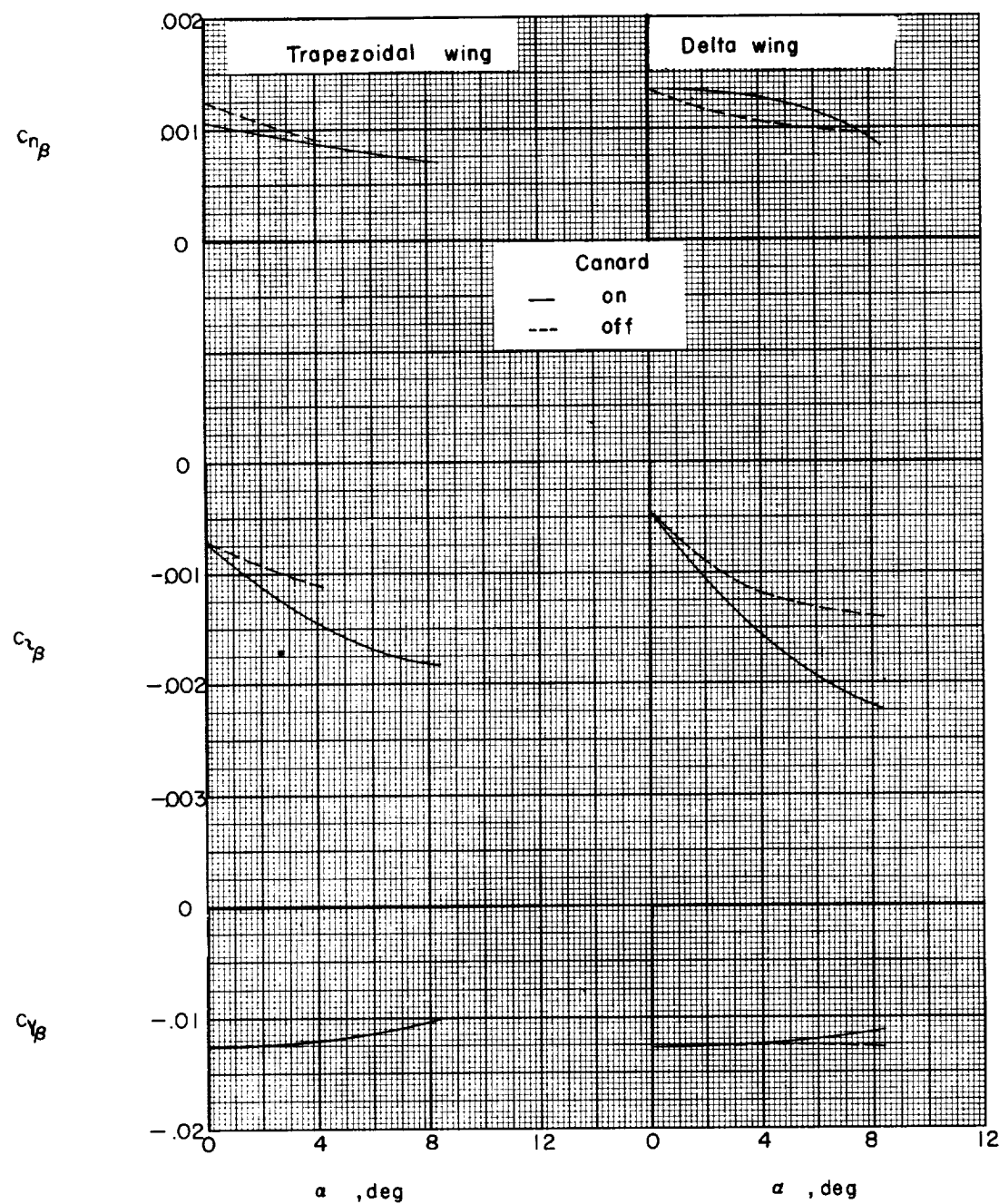
(a) M = 1.41.

Figure 26.- Variation of sideslip derivatives with angle of attack for
models with canard on and off.
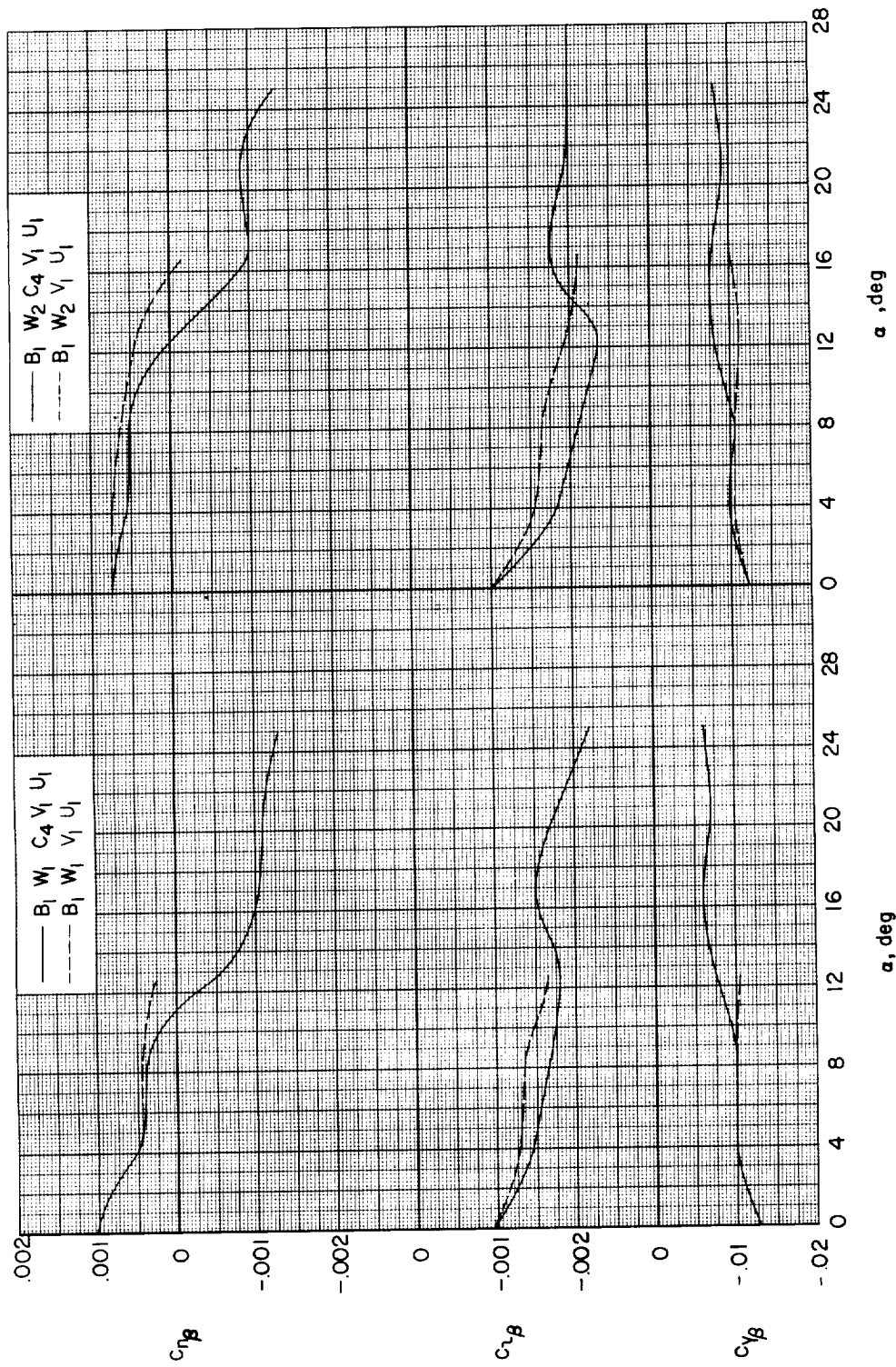
(b) M = 2.01.

Figure 26.- Concluded.
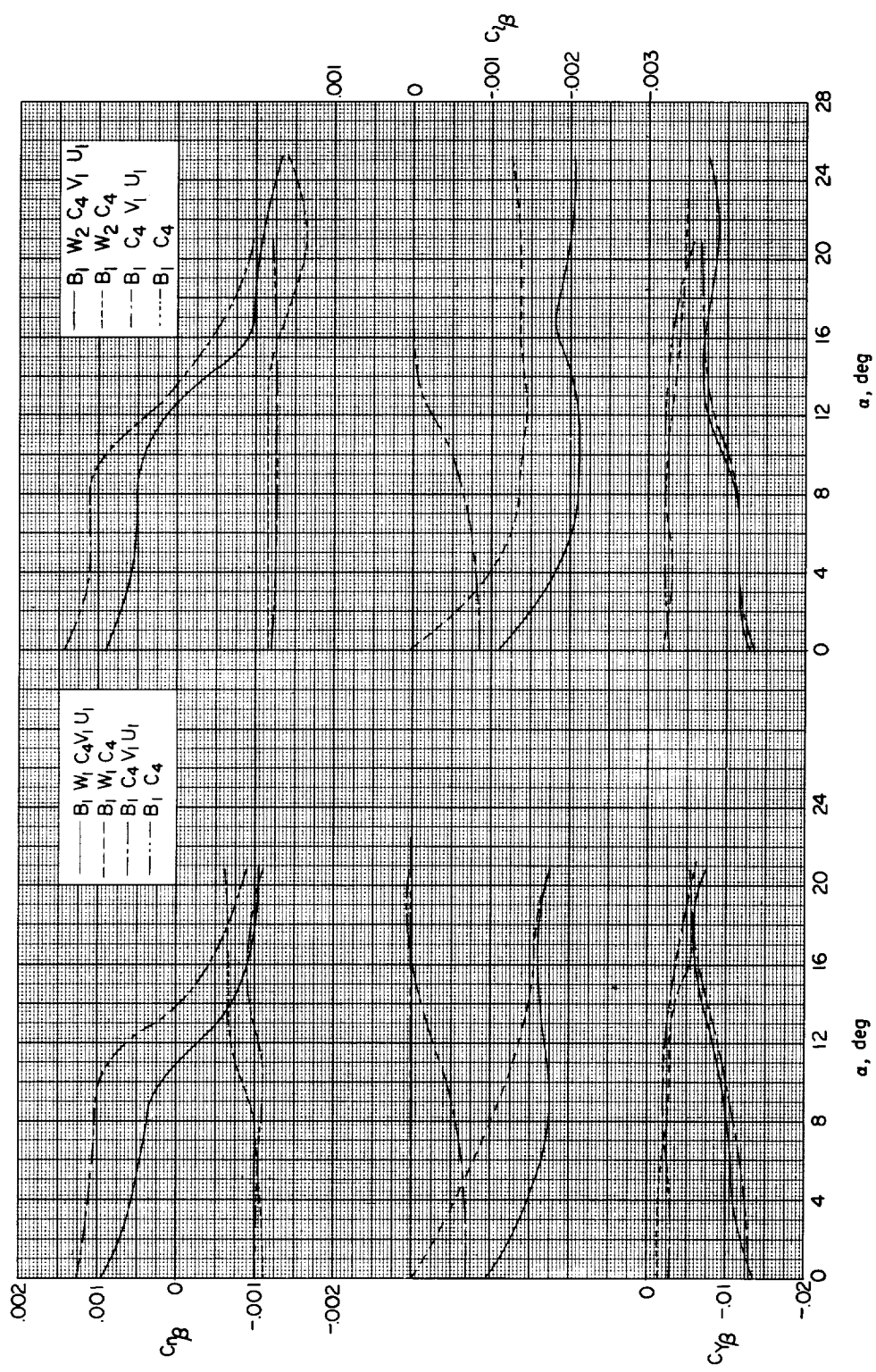
Figure 27.- Variation of sideslip derivatives with angle of attack for models with the wing on and off. $\delta_c = 0°$; M = 2.01.

NASA MEMO 10-1-58L
National Aeronautics and Space Administration.
LONGITUDINAL AND LATERAL STABILITY AND
CONTROL CHARACTERISTICS OF VARIOUS COM-
BINATIONS OF THE COMPONENT PARTS OF TWO
CANARD AIRPLANE CONFIGURATIONS AT MACH
NUMBERS OF 1.41 AND 2.01.   Cornelius Driver.
October 1958.   104p. diagrs., photos., tabs.
(NASA MEMO 10-1-58L)
                    (Title, Unclassified)
An investigation has been conducted in the Langley
4- by 4-foot supersonic pressure tunnel to determine
the aerodynamic characteristics in pitch and sideslip
of a generalized canard airplane model.   Two wings
of equal area but differing in plan form were inves-
tigated.   One had a trapezoidal plan form with an
unswept 8-percent-chord line, an aspect ratio of 3,
and a taper ratio of 0.143; the other had a 60° delta
plan form with an aspect ratio of 2.31.   The model
was equipped with a trapezoidal canard surface with
an area 12 percent of the wing area, a low-aspect-
ratio vertical tail, and twin ventral fins.   The models
Copies obtainable from NASA, Washington   (over)

1. Airplanes - Perform-
    ance   (1.7.1.3)
2. Stability, Longitudinal -
    Static   (1.8.1.1.1)
3. Stability, Lateral -
    Static   (1.8.1.1.2)
4. Stability, Directional -
    Static   (1.8.1.1.3)
5. Control, Longitudinal
                  (1.8.2.1)
I. Driver, Cornelius
II. NASA MEMO 10-1-58L

                                    NASA

NASA MEMO 10-1-58L
National Aeronautics and Space Administration.
LONGITUDINAL AND LATERAL STABILITY AND
CONTROL CHARACTERISTICS OF VARIOUS COM-
BINATIONS OF THE COMPONENT PARTS OF TWO
CANARD AIRPLANE CONFIGURATIONS AT MACH
NUMBERS OF 1.41 AND 2.01.   Cornelius Driver.
October 1958.   104p. diagrs., photos., tabs.
(NASA MEMO 10-1-58L)
                    (Title, Unclassified)
An investigation has been conducted in the Langley
4- by 4-foot supersonic pressure tunnel to determine
the aerodynamic characteristics in pitch and sideslip
of a generalized canard airplane model.   Two wings
of equal area but differing in plan form were inves-
tigated.   One had a trapezoidal plan form with an
unswept 8-percent-chord line, an aspect ratio of 3,
and a taper ratio of 0.143; the other had a 60° delta
plan form with an aspect ratio of 2.31.   The model
was equipped with a trapezoidal canard surface with
an area 12 percent of the wing area, a low-aspect-
ratio vertical tail, and twin ventral fins.   The models
Copies obtainable from NASA, Washington   (over)

1. Airplanes - Perform-
    ance   (1.7.1.3)
2. Stability, Longitudinal -
    Static   (1.8.1.1.1)
3. Stability, Lateral -
    Static   (1.8.1.1.2)
4. Stability, Directional -
    Static   (1.8.1.1.3)
5. Control, Longitudinal
                  (1.8.2.1)
I. Driver, Cornelius
II. NASA MEMO 10-1-58L

                                    NASA

NASA MEMO 10-1-58L
National Aeronautics and Space Administration.
LONGITUDINAL AND LATERAL STABILITY AND
CONTROL CHARACTERISTICS OF VARIOUS COM-
BINATIONS OF THE COMPONENT PARTS OF TWO
CANARD AIRPLANE CONFIGURATIONS AT MACH
NUMBERS OF 1.41 AND 2.01.   Cornelius Driver.
October 1958.   104p. diagrs., photos., tabs.
(NASA MEMO 10-1-58L)
                    (Title, Unclassified)
An investigation has been conducted in the Langley
4- by 4-foot supersonic pressure tunnel to determine
the aerodynamic characteristics in pitch and sideslip
of a generalized canard airplane model.   Two wings
of equal area but differing in plan form were inves-
tigated.   One had a trapezoidal plan form with an
unswept 8-percent-chord line, an aspect ratio of 3,
and a taper ratio of 0.143; the other had a 60° delta
plan form with an aspect ratio of 2.31.   The model
was equipped with a trapezoidal canard surface with
an area 12 percent of the wing area, a low-aspect-
ratio vertical tail, and twin ventral fins.   The models
Copies obtainable from NASA, Washington   (over)

1. Airplanes - Perform-
    ance   (1.7.1.3)
2. Stability, Longitudinal -
    Static   (1.8.1.1.1)
3. Stability, Lateral -
    Static   (1.8.1.1.2)
4. Stability, Directional -
    Static   (1.8.1.1.3)
5. Control, Longitudinal
                  (1.8.2.1)
I. Driver, Cornelius
II. NASA MEMO 10-1-58L

                                    NASA

NASA MEMO 10-1-58L
National Aeronautics and Space Administration.
LONGITUDINAL AND LATERAL STABILITY AND
CONTROL CHARACTERISTICS OF VARIOUS COM-
BINATIONS OF THE COMPONENT PARTS OF TWO
CANARD AIRPLANE CONFIGURATIONS AT MACH
NUMBERS OF 1.41 AND 2.01.   Cornelius Driver.
October 1958.   104p. diagrs., photos., tabs.
(NASA MEMO 10-1-58L)
                    (Title, Unclassified)
An investigation has been conducted in the Langley
4- by 4-foot supersonic pressure tunnel to determine
the aerodynamic characteristics in pitch and sideslip
of a generalized canard airplane model.   Two wings
of equal area but differing in plan form were inves-
tigated.   One had a trapezoidal plan form with an
unswept 8-percent-chord line, an aspect ratio of 3,
and a taper ratio of 0.143; the other had a 60° delta
plan form with an aspect ratio of 2.31.   The model
was equipped with a trapezoidal canard surface with
an area 12 percent of the wing area, a low-aspect-
ratio vertical tail, and twin ventral fins.   The models
Copies obtainable from NASA, Washington   (over)

1. Airplanes - Perform-
    ance   (1.7.1.3)
2. Stability, Longitudinal -
    Static   (1.8.1.1.1)
3. Stability, Lateral -
    Static   (1.8.1.1.2)
4. Stability, Directional -
    Static   (1.8.1.1.3)
5. Control, Longitudinal
                  (1.8.2.1)
I. Driver, Cornelius
II. NASA MEMO 10-1-58L

                                    NASA

NASA MEMO 10-1-58L

were tested through an angle-of-attack range from -4° to 28° with canard deflections of 0°, 5°, 10°, and 15°. Sideslip tests were made to angles of sideslip of about 24° at angles of attack from 0° to 28° and with canard deflections of 0° and 15°.

Copies obtainable from NASA, Washington

NASA

NASA MEMO 10-1-58L

were tested through an angle-of-attack range from -4° to 28° with canard deflections of 0°, 5°, 10°, and 15°. Sideslip tests were made to angles of sideslip of about 24° at angles of attack from 0° to 28° and with canard deflections of 0° and 15°.

Copies obtainable from NASA, Washington

NASA